

Identifying Critical Biological Effectors in Glioma Initiating Cells

by

Hui Wang

Department of Pharmacology and Cancer Biology
Duke University

Date: _____

Approved:

Xiao-Fan Wang, Supervisor

Qi-Jing Li

Bernard Mathey-Prevot

Ann Marie Pendergast

Dissertation submitted in partial
fulfillment of the requirements for the degree
of Doctor of Philosophy in the Department of
Pharmacology and Cancer Biology in the Graduate School of
Duke University

2012

ABSTRACT

Identifying Critical Biological Effectors in Glioma Initiating Cells

by

Hui Wang

Department of Pharmacology and Cancer Biology
Duke University

Date: _____

Approved:

Xiao-Fan Wang, Supervisor

Qi-Jing Li

Bernard Mathey-Prevot

Ann Marie Pendergast

An abstract of a dissertation submitted in partial
fulfillment of the requirements for the degree
of Doctor of Philosophy in the Department of
Pharmacology and Cancer Biology in the Graduate School of
Duke University

2012

Copyright by
Hui Wang
2012

Abstract

Glioblastoma (GBM) represents the most common and lethal brain tumor in adults, with glioma initiating cells (GICs) implicated to play a critical role in its progression and recurrence. However, the molecular mechanisms underlying the distinct function of GICs and non-GICs remain largely unknown. Elucidating distinct molecular features of GICs will pave the foundation for GIC directed therapies for GBM treatment.

We first demonstrated that GICs preferentially express two interleukin 6 (IL6) receptors: IL6 receptor alpha (IL6R α) and glycoprotein 130 (gp130). Targeting IL6R α or IL6 ligand expression in GICs using short hairpin RNAs (shRNAs) significantly reduces growth and neurosphere formation capacity while increasing apoptosis. Block IL6 signaling in GICs attenuates Stat3 activation, and small molecule inhibitors of STAT3 potently induce GIC apoptosis. Targeting IL6R α or IL6 expression in GICs increases the survival of mice bearing intracranial human glioma xenografts. The promising application of anti-IL6 therapies is demonstrated by decreased subcutaneous tumor growth of human GIC-derived xenografts treated with IL6 antibody. Together, our data indicate that IL6 signaling contributes to glioma malignancy through the promotion of GIC growth and survival, and that targeting IL6 may offer benefit for glioma patients.

MicroRNAs (miRNAs) are a class of non-coding small RNA molecules which negatively regulate gene expression and are deregulated in many types of cancer. Through a candidate-based screen, we identified microRNA-33a as a master determinant whose expression controls the functional differences between GIC and non-GICs. Antagonizing miR-33a function in GICs led to reduced self-renewal and tumor progression in immune-compromised mice, whereas overexpression of miR-33a in non-GICs rendered them to display features associated with GICs. Mechanistically, miR-33a acts to confer the biological property of GICs via enhancing the activities of cAMP/PKA pathway and Notch signaling by targeting negative regulators of these two pathways. Together these findings reveal a miR-33a-centered signaling network that dictates the identity/activity of GICs and consequently serves as a therapeutic target for the treatment of GBM.

In summary, this doctoral thesis reveals two novel molecular events that characterize the distinct feature of GICs and develops preclinical strategies for the therapeutic application of GBM.

Contents

Abstract	iv
List of Tables	x
List of Figures	xi
Acknowledgements	xiv
1. Background and Overview.....	1
1.1 Glioblastoma	1
1.2 Tumor Initiating Cells and Glioma Initiating Cells.....	3
1.2.1 Discovery of Tumor Initiating Cells/Cancer Stem Cells	3
1.2.2 Definition and Terminology	5
1.2.3 Tumor Initiating Cells in GBM.....	6
1.2.4 Reversibility of Non-TICs to TICs.....	8
1.3 MicroRNAs in Cancer Biology	9
1.3.1 Discovery of microRNAs.....	9
1.3.2 MicroRNA biogenesis and function	10
1.3.3 MicroRNAs in Cancer and TICs.....	11
2. Targeting Interleukin 6 Signaling Suppresses Glioma Initiating Cell Survival and Tumor Growth.....	13
2.1 Introduction.....	13
2.2 Results	16
2.2.1 GICs Express IL6 Receptors and Ligand.....	16
2.2.2 Targeting of IL6R α in GICs Decreases Growth and Survival.....	19

2.2.3 Targeting of IL6 Ligand in GICs Decreases Growth and Survival.....	24
2.2.4 IL6 Signaling Promotes GIC Survival through Stat3 Activation	27
2.2.5 IL6 Signaling Promotes Tumor Growth and Decreases Patient Survival	30
2.2.6 IL6 Antibody Treatment Decreases the Growth of GIC-Derived Tumors	32
2.3 Material and Methods.....	35
2.3.1 Isolation of GICs and Non-GICs and Cell Culture	35
2.3.2 Immunofluorescence Staining	36
2.3.3 Quantitative Real-Time Polymerase Chain Reaction	37
2.3.4 Lentiviral Mediated shRNA Targeting	37
2.3.5 Small Molecule Inhibitors	38
2.3.6 Cell Viability Assay	38
2.3.7 Neurosphere Formation Assay.....	38
2.3.8 Annexin V Staining	39
2.3.9 Caspase 3/7 Assay	39
2.3.10 Western Blotting and Antibodies.....	39
2.3.11 Intracranial Tumor Assays and IL6 Antibody Treatment	40
2.3.12 Statistical Analysis.....	40
2.4 Discussion.....	40
3. miR-33a Confers Biological Properties of Glioma Initiating Cells via Modulation of the cAMP/PKA and Notch Signaling Pathways	44
3.1 Introduction.....	44
3.2 Results	46

3.2.1 Identification of miR-33a as a top candidate capable of affecting the neurosphere-forming activity of GICs	46
3.2.2 Inhibition of miR-33a suppressed self-renewal, proliferation and tumor-initiation of GICs	51
3.2.3 Overexpression of miR-33a rendered non-GICs to behave like GICs	55
3.2.4 PDE8A and UVRAG are direct targets of miR-33a.....	59
3.2.5 Repression of PDE8A and UVRAG expression is required for miR-33a to maintain the biological properties of GICs.....	63
3.2.6 Both PKA and Notch signaling pathways are required by miR-33a to maintain the biological properties of GICs.....	67
3.2.7 Targeting miR-33a by a LNA inhibitor suppressed tumor formation in vivo .	72
3.3 Material and Methods.....	73
3.3.1 Isolation of GICs and Non-GICs from patient specimen and mice xenografts	73
3.3.2 miRNA Profiling.....	74
3.3.3 Plasmids.....	75
3.3.4 Cell Culture	75
3.3.5 Neurosphere Formation Assay.....	76
3.3.6 Cell Viability Assay	76
3.3.7 Cell Proliferation Assay	76
3.3.8 Quantitative Real-Time PCR.....	77
3.3.9 Intracranial tumor assay.....	78
3.3.10 Isolation of RISC-associated RNA.....	79
3.3.11 Immunoblots and Antibodies.....	79

3.3.12 Luciferase Reporter Assay	80
3.3.13 Lentiviral mediated shRNA targeting.....	81
3.3.14 LNA miR-33a inhibitor treatment.....	81
3.3.15 Statistical Analysis.....	82
3.4 Discussion.....	82
3.4.1 A microRNA acting as a “master determinant” of glioma cell identity.....	82
3.4.2 The requirement of activities from two pathways to maintain the properties of GICs.....	84
3.4.3 A potential therapeutic avenue for GBM.....	85
4. Conclusions and Future Directions	87
4.1 Conclusion.....	87
4.2 Future Direction.....	88
Appendix.....	90
References	92
Biography	101

List of Tables

Table 1: Information of shRNA clones targeting IL6R α and IL6	38
Table 2: Fold change of deregulated miRNAs in GICs compared to non-GICs in two patient specimens (PS) and two xenografted glioma lines (XL).....	49
Table 3: Fold change of down-regulated genes in 11-0040 and D456MG CD133-negative cells with miR-33a overexpression compared to control.	60
Table 4: Primer sequences for qRT-PCR.....	78
Table 5: Information of shRNA clones targeting PDE8A and UVRAG	81

List of Figures

Figure 1: Kaplan–Meier survival curve of newly diagnosed GBM patients with radiotherapy alone or radiotherapy plus continuous daily Temozolomide.	2
Figure 2: Stochastic and Hierarchical model of tumorigensis.	4
Figure 3: Characteristics of Glioma Initiating Cells	7
Figure 4: Bidirectional model of Tumor Initiating Cells.....	8
Figure 5: MicroRNA biogenesis and function.	11
Figure 6: Canonical IL6 signal transduction pathway	15
Figure 7: GIC Markers co-expressed with IL6R α and gp130.....	17
Figure 8: IL6 Receptor and IL6 ligand mRNA levels indicated a potential paracrine loop between GICs and non-GICs.....	18
Figure 9: Non-GICs secreted more IL6 ligand than matched GICs.	19
Figure 10: Targeting of IL6 receptor expression reduced GIC growth due to increased apoptosis.	21
Figure 11: Targeting IL6R α /IL6 in a primary glioma specimen CCF3863 decreases GIC survival.....	22
Figure 12: Targeting IL6R α or IL6 expression reduced GIC proliferation.....	23
Figure 13: Targeting IL6R α or IL6 increased differentiation marker expression.....	24
Figure 14: Targeting of IL6 ligand expression decreased GIC growth as a result of increased apoptosis.....	26
Figure 15: Elevated Stat3 phosphorylation in GICs and induction by exogenous IL6.	27
Figure 16: Stat3 is a downstream mediator of IL6 in GICs and mediates GIC survival. ..	28
Figure 17: Targeting Stat3 activity in D456MG GICs with small molecule inhibitors decreased proliferation and increased cell death.	30

Figure 18: Targeting of either IL6R α or IL6 suppressed tumor growth and increased the survival of mice bearing intracranial xenografts.....	31
Figure 19: Higher IL6R α and IL6 mRNA levels in GBM patients correlate with poor patient survival.....	32
Figure 20: Systemic treatment with an anti-IL6 antibody inhibited the growth of human glioma xenografts in vivo.	34
Figure 21: Venn Graph analysis of the up- and down-regulated miRNAs.	48
Figure 22: Identification of miR-33a as among those differentially expressed miRNAs between GICs and non-GICs.....	50
Figure 23: Antagonism of miR-33a by miR-33a sponge indicates miR-33a is required for self-renewal and proliferation in GICs.	52
Figure 24: Antagonism of miR-33a by Zip-33a indicates miR-33a is required for self-renewal and proliferation in GICs.....	53
Figure 25: Antagonism of miR-33a by miR-33a sponge indicates miR-33a is required for tumor progression in GICs.	54
Figure 26: Antagonism of miR-33a by Zip-33a indicates miR-33a is required for tumor progression in GICs.	55
Figure 27: miR-33a level after primary miR-33a over-expression.....	56
Figure 28: Overexpression of miR-33a in non-GICs promotes self-renewal and tumor progression.....	58
Figure 29: PDE8A and UVRAG are direct targets of miR-33a in glioma cells.	62
Figure 30: Predicted binding sites of miR-33a in the 3'UTR of PDE8A and UVRAG.....	63
Figure 31: Overexpression of PDE8A and UVRAG compromised self-renewal and tumor formation capabilities of GICs.....	64
Figure 32: Repression of PDE8A and UVRAG expression is required for the function of miR-33a in glioma cells.	66
Figure 33: PDE8A regulates GIC self-renewal through the PKA pathway.	69

Figure 34: UVRAG regulates GIC self-renewal through Notch pathway.....71

Figure 35: Treatment with a miR-33a LNA inhibitor suppressed tumor growth in vivo.73

Acknowledgements

First of all, I would like to thank my supervisor, Xiao-Fan Wang, for his tremendous support and help in my development of scientific career. He always trusted me and gave me enough freedom to pursue scientific questions; he trained me in a way that not merely focused on bench work but also other critical skills to survive in academic field including scientific writing and presentation. He not only mentored me in professional development but also gave me and my husband a lot of help and guidance in the daily life. I feel very lucky to complete my graduate training in Xiao-Fan's lab since I cannot expect a better supervisor than Xiao-Fan.

I also thank my former mentor, Jeremy Rich, who gave me opportunity to work in his lab after my first-year rotation. I learned basic knowledge and techniques of cancer biology from him and also from former members of Rich lab, especially Anita Hjelmeland, Qiulian Wu, Zhizhong Li, Christine Eyler, Justin Lathia and Jialiang Wang.

I thank all members of Wang Lab who created the most inspiring and interactive working environment to work in, including Yong Yu, Tao Sun, Xin Xu, Jing Hu, Yun Zhang, Qinghong Wang, Peter Alexander, Jeffery Markowitz, Pengyuan Yang, Shanglei Ning, Lifeng Yuan and Mengyang Chong. Former members of Wang lab including Xing Guo, Chaoyu Ma, Steve Schilling, and Junjie Feng also helped me a lot during my rotation in Wang Lab.

I thank my committee members, Qi-Jing Li, Ann Marie Pendergast, Bernard Mathey-Prevot and former committee members Mark Dewhirst, Robert Wechsler-Reya for their invaluable suggestions on my thesis project. I thank Mike Cook and Bin Li for assistance with flow cytometry, our collaborators in Preston Robert Tisch Brain Tumor Center including Roger McLendon, Allan Friedman, Stephen Keir, Darell Bigner, Diana Satterfield, Ben Wiener and Lisa Ehinger for assistance with collecting xenograft tumors from nude mice and fresh GBM patient specimens. Without their help I could not complete my study.

I thank my parents, Chunsheng Wang and Jianhua li and my dear friends. Their unconditional love and support gave me courage and confidence to peruse my career in science. In difficult times, they always believed me and encouraged me to look at the bright side of life. Last but definitely not least, I want to express my deep appreciation to my beloved husband, Yanhua Rao. He has always believed me, encouraged me, supported me, and inspired me. I cannot imagine a better soul mate other than Yanhua and cannot imagine a life without him.

1. Background and Overview

As one of the major threats to human health, tumors have been studied for several decades. Modern biologists consider that tumors arise from a variety of specialized normal cells through accumulation of genetic mutations, which could take several years or even several decades to develop. Brain tumors could arise from a variety of cells in the brain, which also share these common features of tumors such as bearing aberrant gene mutations and progressive development.

1.1 Glioblastoma

Glioblastoma (GBM) is the most lethal primary brain tumor in adults, with an average survival of slightly more than one year after initial diagnosis (CBTRUS, 2005). World Health Organization (WHO) classify adult brain tumor grade from I to IV, with I being the most benign tumor and IV being the most aggressive one. GBM is classified as grade IV brain tumor which consists of poorly differentiated neoplastic cells and hyperplastic blood vessels (Furnari et al., 2007). Primary GBM can invade brain tissues but rarely metastasize outside the nervous system. Diagnosis of GBM usually depend on the initial symptoms of affected brain region, including headaches, seizures, nausea and vomiting, and then are confirmed by Magnetic Resonance Imaging (MRI) and pathological analysis (Furnari et al., 2007). Incidence of primary GBM is low, only two to three cases per 100,000 people in the United States and Europe (CBTRUS, 2005).

However, due to the malignant nature of this disease, around 13,000 patients died in 2009 even after treatment in the United States (Kohler et al., 2011).

Currently, treatment of GBM is a combination of surgery, radiotherapy and chemotherapy (Chamberlain, 2006; Kim and Glantz, 2006). After maximum safe extent of surgery which removes up to 99% of bulk tumor, patient usually receive a total radiation dose of 60–65 Gy to reach optimal effect. Temozolomide (TMZ) is the most commonly used chemotherapeutic drug for gliomas, which could prolong median patient survival by two months (Figure 1) (Stupp et al., 2005).

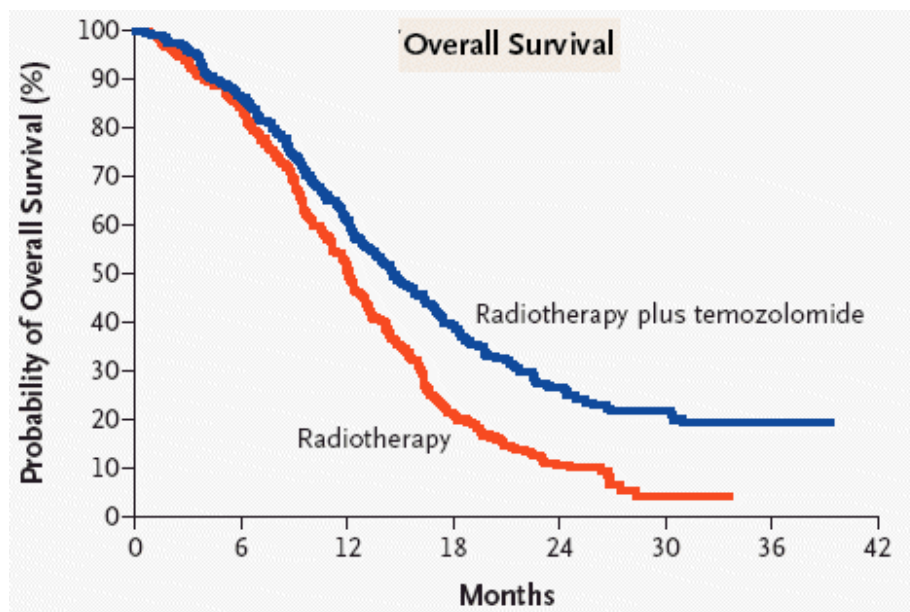


Figure 1: Kaplan–Meier survival curve of newly diagnosed GBM patients with radiotherapy alone or radiotherapy plus continuous daily Temozolomide.
(Adapted from (Stupp et al., 2005))

In 2009, the U.S. Food and Drug Administration (FDA) approved Avastin, which is a humanized antibody of VEGF, for the treatment of recurrent GBM (Cohen et al.,

2009). And treatment for primary GBM is in phase III clinical trial. Research found that Avastin could improve response and survival in patients with recurrent GBM, and reduce edema and diminish blood-brain-barrier leakage in radiation induced necrosis (Cohen et al., 2009).

However, all these treatments of GBM remain largely palliative because resistance to radiotherapy and chemotherapy are common in GBM patients.

1.2 Tumor Initiating Cells and Glioma Initiating Cells

1.2.1 Discovery of Tumor Initiating Cells/Cancer Stem Cells

The concept of Tumor Initiating Cells/Cancer Stem Cells is not a new idea. Several decades ago people have noticed that many tumors contain heterogeneous cancer cells (Fidler and Hart, 1982; Fidler and Kripke, 1977), and some tumor cells could “differentiate” into non-tumorigenic tumor cells, which was described as model b in Figure 2 (Dick, 2008; Reya et al., 2001; Shackleton et al., 2009). Back to 1960s, people already found some germ lineage cancers can differentiate into progeny that exhibit limited proliferation potential, although they still bearing the oncogenic mutations of their progenitors (Kleinsmith and Pierce, 1964).

compromised mice, but these cells may not necessarily be enriched by the same cell surface markers.

1.2.2 Definition and Terminology

Tumor Initiating Cells/Cancer Stem Cells are defined strictly by functional characteristics. Two criteria need to be fulfilled: (1) self-renewal, which means that at least one daughter cell retains the capacity for self-renewal as well as the ability to generate secondary tumors that phenotypically resemble the parental tumor in xenograft transplantation; (2) ability to generate secondary tumors resembling the parental tumor in xenograft transplantation assays.

Currently there is no uniform term to name this tumor subpopulation. The following terms are commonly used: Tumor Initiating Cells, Cancer Stem Cells, Tumor Propagating Cells, or Stem-like Tumor Cells. Each name bears limitations and insufficiencies. For example, "Cancer Stem Cells" raises confusion because they are not a real kind of "stem cells", although this subpopulation of cells usually expresses certain markers of adult stem cells and shares the property of prolonged self-renewal with normal adult stem cells. So based on the functional definition of this subpopulation, I personally prefer the term "Tumor Initiating Cells". In the following chapter, I will use "Tumor Initiating Cells (TICs)" and in GBM "Glioma Initiating Cells, (GICs)" instead of "Glioma Stem Cells (GSCs)".

In summary, regardless of the terminology employed, the capacity for self-renewal and potent tumor formation are the definitive characteristics of this tumor subpopulation.

1.2.3 Tumor Initiating Cells in GBM

In 2004, Peter Dicks and his colleagues firstly reported that TICs in glioblastoma could be enriched by CD133, here termed as Glioma Initiating Cells (GICs) (Singh et al., 2004). Besides definitional characteristics of self-renewal and ability to initiate tumor formation in immune-compromised mice, these GICs share properties with normal neural stem cells: they form neurosphere-like spheroids, express neural stem cell markers, and differentiate into multiple cell types including neurons, astrocytes, and oligodendrocytes (Bao et al., 2006a; Mizrak et al., 2008; Yuan et al., 2004). Most importantly, GICs are highly resistant to radio- and chemotherapy compared to non-GICs, which potentially explained why current treatments of GBM remain largely palliative. Figure 3 summarized the key characteristics of Glioma Initiating Cells.

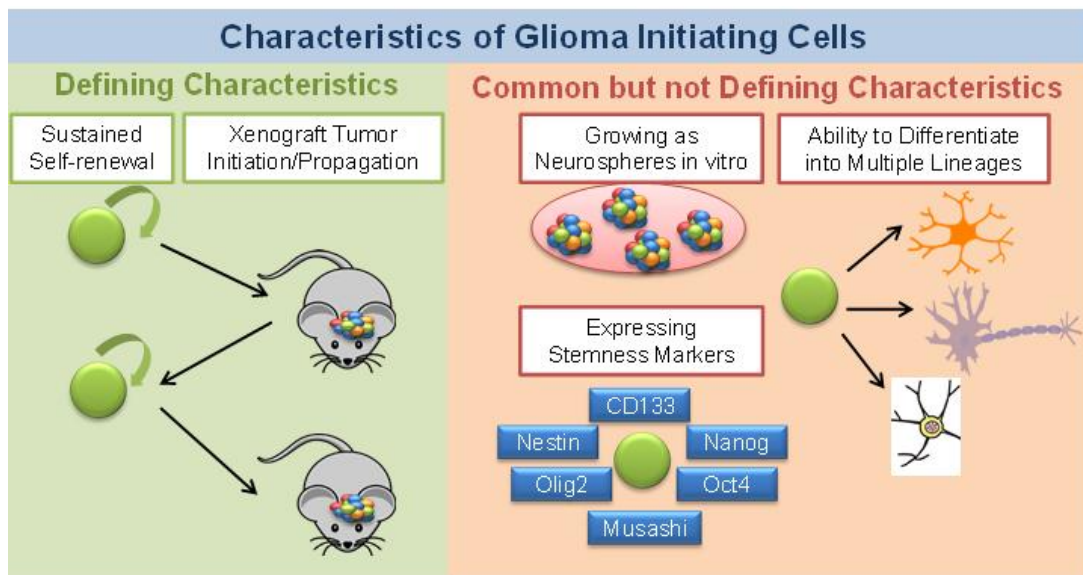


Figure 3: Characteristics of Glioma Initiating Cells

How to enrich GICs also received controversy after CD133 was firstly used as a molecular marker (Bao et al., 2006a). CD133-negative GICs were identified by several groups, and also using defined medium to enrich GICs was demonstrated by several groups to successfully enrich GICs without the limitation of cell surface markers (Chen et al., 2010). These discrepancies may arise from differences among patients, methodological differences or tumor selection bias (Magee et al., 2012). In the first part of my study in Chapter 2, I only used CD133 as markers to enrich GICs since at that time CD133-negative GICs has not been reported; and GICs from all xenograft lines utilized in my study have been demonstrated to be enriched by CD133. In the second part of my study in Chapter 3, I used defined serum-free medium to enrich GICs from patient specimens in order to avoid the limitation of cell surface markers.

1.2.4 Reversibility of Non-TICs to TICs

The idea that non-tumorigenic cancer cells could revert to having tumorigenic capacity is plausible, since differentiated fibroblast cells could be reprogrammed to pluripotent stem cells after introducing four master regulators of stem cells (Takahashi et al., 2007). Recent studies also suggested this possibility: immortalized human mammary epithelial cells (HMECs) could undergo Epithelial-Mesenchymal Transition (EMT) and obtained the phenotype of breast TICs after sustained expression of the transcription factors Snail or Twist (Mani et al., 2008; Morel et al., 2008; Scheel et al., 2011); under chronic hypoxia conditions or sustained HIF2a overexpression, CD133-negative glioma cells could re-express CD133 and also presented properties of GICs, including expression of several stemness markers and enhanced tumorigenic ability in vivo (Heddleston et al., 2009). So the model of Tumor Initiating Cells should be a bidirectional model rather than a single-direction model (Figure 4).

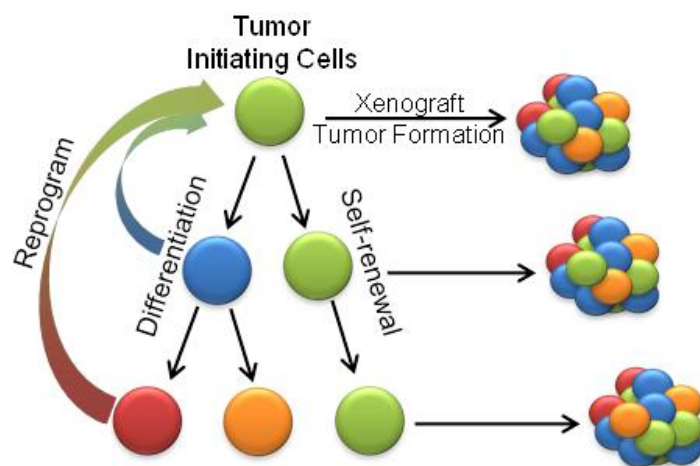


Figure 4: Bidirectional model of Tumor Initiating Cells

Given the possibility that non-tumorigenic cancer cells could be reprogrammed to a tumorigenic state at certain circumstances, it would be a new challenge in this field to target these cells effectively and to prohibit this reversion.

1.3 MicroRNAs in Cancer Biology

1.3.1 Discovery of microRNAs

In 1993, Ambros and his colleagues discovered a 22-nucleotide RNA, which contained sequences complementary to multiple sequences in the 3' UTR of the *lin-14* mRNA, could inhibit the translation of the *lin-14* mRNA into the protein in *C. elegans* (Lee et al., 1993). At that time, people thought this repressive regulation of mRNA by a short RNA was a distinctive phenomenon in *C. elegans*. In 2000, let-7 was discovered as a second member of this type of short RNA, which repressed several genes expression during development in *C. elegans* (Reinhart et al., 2000). Following this discovery, microRNAs are found in many other eukaryotic cells including plants and metazoans.

MicroRNAs (miRNAs) are a class of non-coding small RNA molecules, typically about 18-22 nucleotides in the mature form (Bushati and Cohen, 2007). MicroRNAs negatively regulate gene expression at the post-transcriptional level by promoting mRNA degradation and/or inhibiting mRNA translation. In human genome, over one thousand microRNAs may target about one-third genes of the whole genome, which in theory could be involved in almost every aspect of biological processes (Baek et al., 2008).

1.3.2 MicroRNA biogenesis and function

miRNAs are produced from either their own genes or introns of other genes (Bushati and Cohen, 2007; Meltzer, 2005). The primary transcripts (pri-miRNA) are first cropped into the approximately 70-nucleotide hairpin intermediates called precursor-miRNA (pre-miRNA) by the microprocessor complex including Drosha and DGCR8 in the nucleus. The RNA helicases p68 and p72 are also part of the large microprocessor complex and may help the processing of a subset of pri-miRNAs. Pre-miRNA hairpins are exported from the nucleus to cytoplasm by nucleocytoplasmic shuttle complex Exportin-5. In cytoplasm, the pre-miRNA hairpin is cleaved by the RNase III enzyme Dicer in a cytoplasmic microprocessor complex including Dicer/TRBP/PACT, yielding an miRNA:miRNA* duplex. Although either strand of the duplex could potentially act as a functional miRNA, usually only one strand is incorporated into the RNA-induced silencing complex (RISC). In rare cases, both strands of the miRNA:miRNA* duplex are incorporated and function as mature miRNA that target different mRNA populations. In an active RNA-induced silencing complex (RISC), members of the Argonaute (Ago) protein family bind the mature miRNA and match it with a target mRNA. Then either mRNA is directly cleaved by Ago, or translational repression is achieved by recruiting additional proteins (Figure 5) (Meltzer, 2005).

1.3.3 MicroRNAs in Cancer and TICs

In recent years, a large number of miRNAs have been found to be deregulated in many types of cancer: some function as tumor promoters/onco-mirs and others as tumor suppressors (Farazi et al., 2011). For example, among the most extensively studied miRNAs, the miR-17-92 clusters and miR-21 are reported to function as onco-mirs in a variety of tumors through multiple mechanisms (Jazbutyte and Thum, 2010; Mendell, 2008; Poliseno et al., 2010).

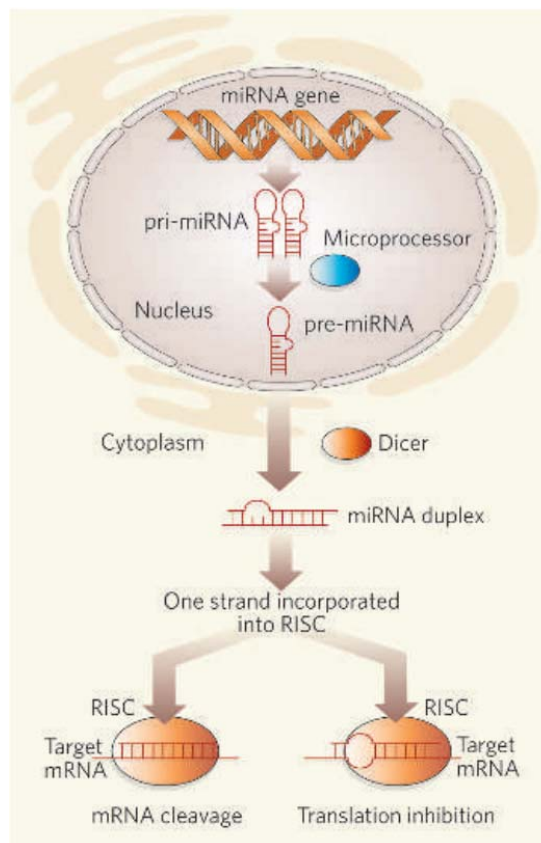


Figure 5: MicroRNA biogenesis and function.

(Adapted from (Meltzer, 2005))

Recently, a rising number of studies have focused on miRNAs that play critical role in TIC self-renewal and differentiation. For example, miR-495 was up-regulated in breast tumor initiating cells and promoted oncogenesis and hypoxia resistance via repression of E-cadherin and REDD1 (Hwang-Verslues et al., 2011). Ma and his colleagues found that miR-130b promoted liver tumor-initiating cell growth and self-renewal within cells containing CD133 by targeting the tumor protein 53-induced nuclear protein 1 (TP53INP1) (Ma et al., 2010b).

In the context of GBM, particularly GICs, several miRNAs, for example miR-124 and miR-137, displayed higher expression levels in non-GICs and overexpression of these miRNAs induced differentiation of GICs (Silber et al., 2008). However, little is known about miRNAs that may play critical roles in defining the functions of GICs, with only recent reports on the role of miR-9 and miR-138 in GIC proliferation and anti-apoptosis (Chan et al., 2012; Schraivogel et al., 2011).

2. Targeting Interleukin 6 Signaling Suppresses Glioma Initiating Cell Survival and Tumor Growth

This chapter is based on a research article I published as first author in the journal *Stem Cells*.

Wang H, Lathia JD, Wu Q, Wang J, Li Z, Heddleston JM, Eyler CE, Elderbroom J, Gallagher J, Schuschu J, MacSwords J, Cao Y, McLendon RE, Wang XF, Hjelmeland AB, Rich JN. Targeting Interleukin 6 Signaling Suppresses Glioma Stem Cell Survival and Tumor Growth. *Stem Cells*. 2009 Oct; 27(10): 2393-404.

Permission to reproduce this article was granted by John Wiley & Sons, Inc.

2.1 Introduction

As I introduced in Chapter 1, glioblastoma (GBM; WHO grade IV) is the most common and aggressive primary brain tumor in adults. Despite advances in cancer therapy, GBMs are incurable with an average survival of slightly more than 1 year past the initial diagnosis (CBTRUS, 2005). New GBM therapeutic strategies are desperately needed, requiring insights into the biological and molecular mechanisms driving the tumor growth. From Chapter 1, we have also known that Glioma Initiating Cells (GICs) express neural stem cell markers, self-renew, drive tumor propagation in xenograft models, and are highly resistant to radio- and chemotherapies. These facts strongly suggest that GICs are important for tumor maintenance and recurrence. In addition, GIC directed therapies may have important clinical applications.

Aberrant production and signaling of the circulated cytokine interleukin six (IL6) is tightly linked to tumor generation and poor disease outcome in many cancer types,

including GBM (Choi et al., 2002; Kishimoto, 2005; Tchirkov et al., 2007; Weissenberger et al., 2004). GBM Samples contain significantly higher levels of IL6 protein compared to those of control brains (Choi et al., 2002), and higher IL6 mRNA correlates with poor GBM patient survival (Tchirkov et al., 2007). Consistent with these data, loss of IL6 signaling prevents brain tumor development in a mouse model in which expression of the src oncogene is controlled by the promoter of the astrocyte marker glial fibrillary acidic protein (GFAP) (Weissenberger et al., 2004). Although IL6 may promote the growth of astrocytes (Selmaj et al., 1990), little is known about the specific biological mechanisms through which IL6 contributes to GBM initiation or progression. In other cancers, IL6 promotes chemo-resistance, angiogenesis, and invasion (Ancrile et al., 2007; Conze et al., 2001; Ishioka et al., 1999; Sehgal and Tamm, 1991), cellular behaviors that have all been linked to tumor initiating cells. Breast cancer mammosphere survival and malignancy is promoted by IL6 (Sansone et al., 2007) , further suggesting a contribution of IL6 to tumor-initiating cells. Together, these data suggested that the role of IL6 signaling in GBM should be evaluated in the context of the GIC subpopulation.

The canonical IL6 signal transduction pathway is initiated by IL6 ligand binding to heteromeric plasma membrane receptor complexes formed from a specific IL6 binding receptor, IL6 receptor α (IL6R α , gp80), and the common signal transducing receptor glycoprotein 130 (gp130). Upon receptor activation, intracellular signaling is propagated by Janus kinase tyrosine kinase family members (JAKs), leading to the

activation of transcription factors of the signal transducers and activators of transcription (STAT) family, particularly STAT3 (Kishimoto, 2005) (Figure 6). STAT3 activation, as indicated by phosphorylation at tyrosine 705, is present in glioma patient samples and increases with tumor grade (Rahaman et al., 2002; Wang et al., 2004; Weissenberger et al., 2004). IL6 signals promote STAT3 activation in GBM cells in vitro, and targeting of either STAT3 or IL6 decreases GBM cell survival (Konnikova et al., 2003; Rahaman et al., 2002; Su et al., 2008) . Additional reports also link STAT3 to stem cell biology as STAT3 is required to maintain the propagation and pluripotency of normal embryonic stem cells and neural stem cells (Hodge et al., 2005; Matsuda et al., 1999; Niwa et al., 1998). Together, these data led us to hypothesize that IL6 may activate STAT3 in GICs to contribute to GBM progression.

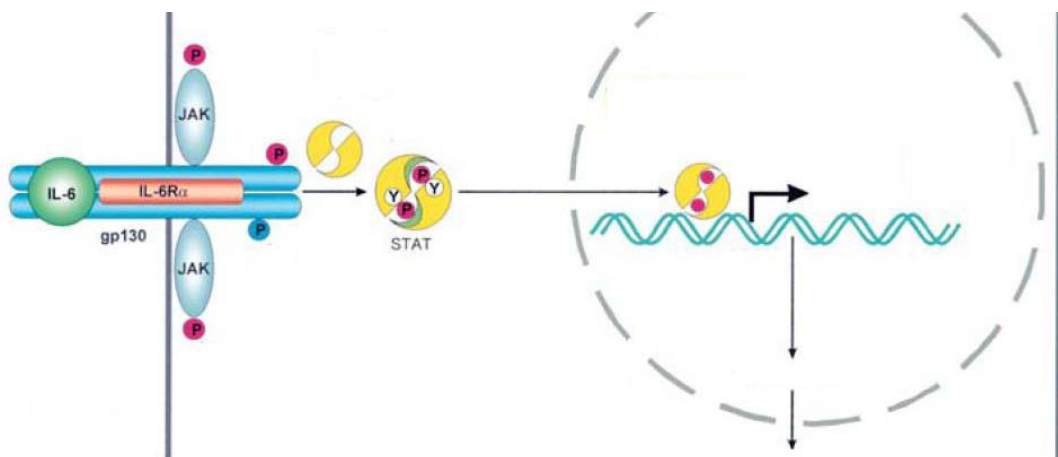


Figure 6: Canonical IL6 signal transduction pathway
(Adapted from (Heinrich et al., 2003))

2.2 Results

2.2.1 GICs Express IL6 Receptors and Ligand

To evaluate the potential contribution of IL6 signals to glioma biology in the context of the recently identified tumor subpopulations, we measured IL6 receptor expression in freshly isolated GICs and non-GICs derived from mice xenografts using CD133 as molecular marker. Enrichment or depletion of GICs by CD133 was validated using functional assays, including propagation of tumors with characteristics of the parental sample and stem cell marker expression. GICs expressed elevated levels of IL6R α and gp130 in comparison to non-GICs (Figure 7A). Isolated GICs cultured short term as neurospheres also showed co-expression of IL6R α or gp130 with CD133 (Figure 7B). We extended these studies to direct immunofluorescent staining of frozen sections of human glioma surgical biopsies that demonstrated co-localization of IL6 receptors (IL6R α and gp130) and GIC marker CD133 (Figure 7C).

Consistent with these protein expression data, quantitative real-time polymerase chain reaction (qRT-PCR) revealed that GICs expressed higher IL6R α , gp130, and Olig2 mRNA levels than matched non-GICs in four different glioblastoma samples and one primary human specimen (Figure 8A-8C). Although we detected IL6 in GICs, IL6 mRNA levels were higher in non-GICs than matched GICs in three out of four glioblastoma samples (Figure 8D).

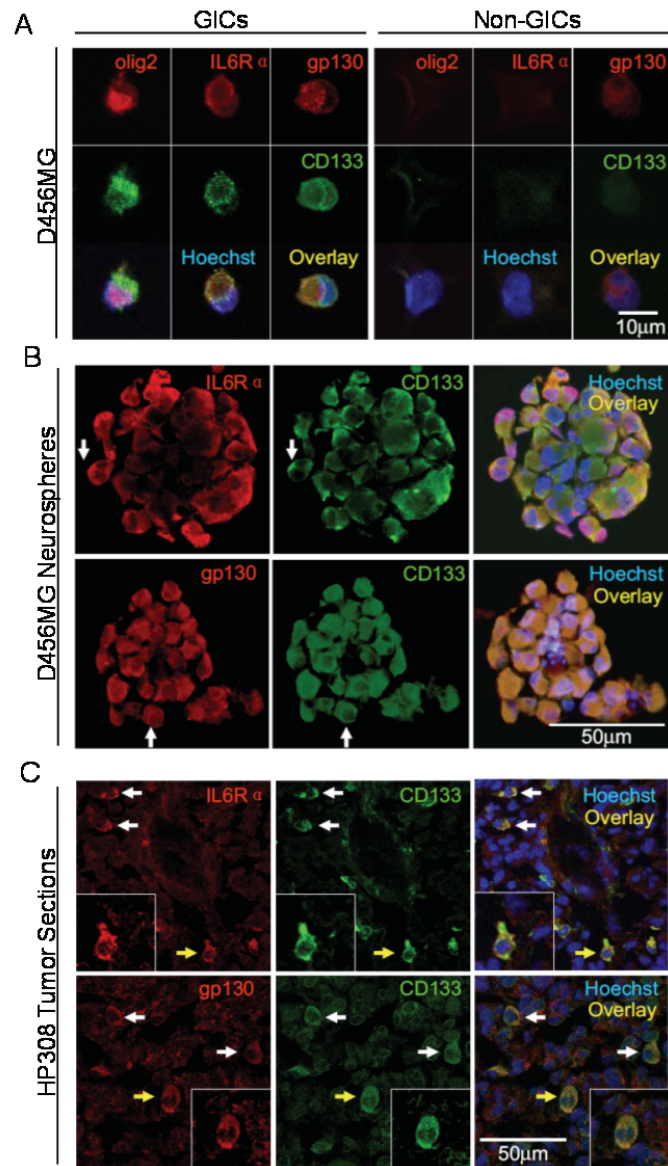


Figure 7: GIC Markers co-expressed with IL6R α and gp130.

(A) The GIC marker CD133 co-localized with IL6R α and gp130 in GICs, but not non-GICs. (B) The GIC marker CD133 co-localized with IL6R α and gp130 in neurospheres cultured in vitro from D456MG GICs. Examples of areas with co-staining are highlighted with white arrows. (C) The GIC marker CD133 co-localized with IL6R α and gp130 in the freshly frozen human glioma surgical biopsy specimen HP308 as demonstrated by immunofluorescent staining. Examples of cells with costaining are highlighted with white arrows, and the cell magnified in the inset is highlighted with a yellow arrow. Nuclei in all images were counterstained with Hoechst 33342.

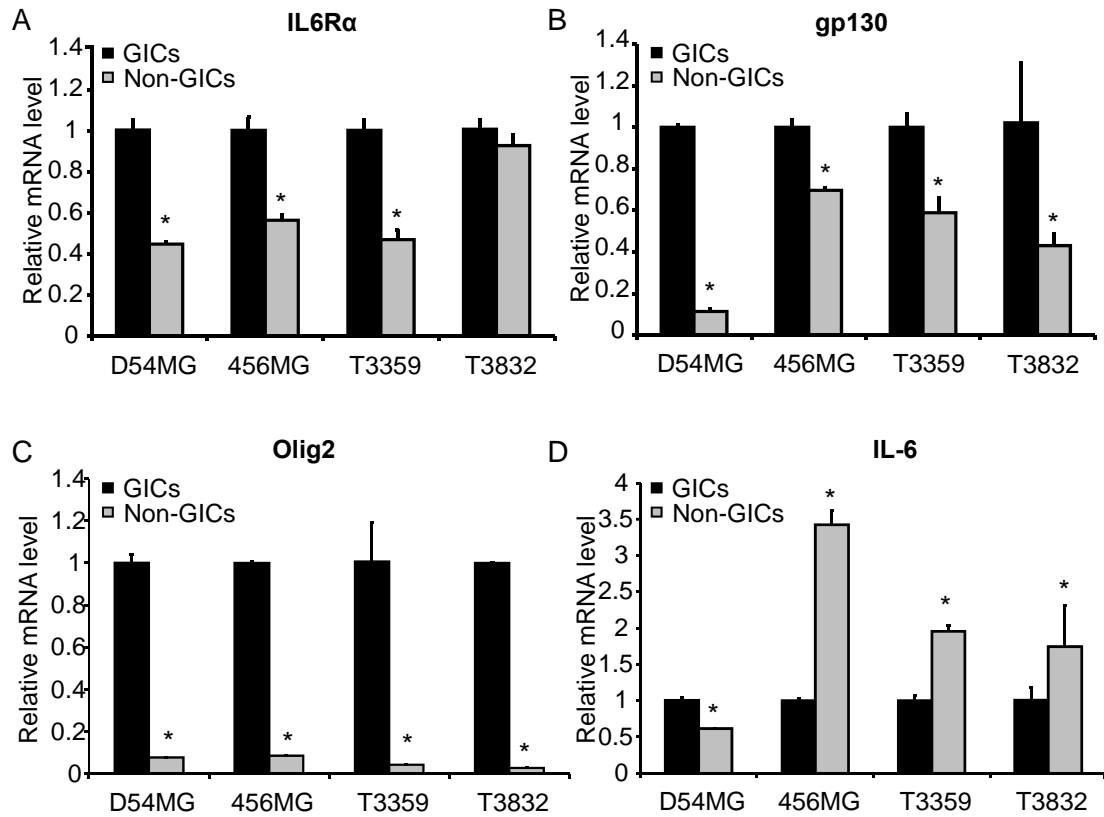


Figure 8: IL6 Receptor and IL6 ligand mRNA levels indicated a potential paracrine loop between GICs and non-GICs.

Quantitative RT-PCR was used to determine the relative mRNA levels of IL6R α (A), gp130 (B), olig2 (C), and IL6 (D) in GICs and non-GICs isolated from the long-term glioma xenografts D456MG and D54MG as well as from T3359 and T3832 patient specimens passaged short term in immune-compromised mice. The mRNA levels of IL6R α (A) and gp130 (B) were generally higher in GICs, whereas the mRNA level of IL6 was usually higher in non-GICs. Olig2, a reported marker for GICs, had consistently higher mRNA levels in isolated GIC populations. (*, $p < 0.05$ with comparison of non-GICs to matched GICs)

Consistent with these data, secreted IL6 ligand levels were also higher in non-GICs as detected by an enzyme-linked immunosorbent assay (ELISA) (Figure 9). These data suggest the existence of both autocrine IL6 signaling in GICs and paracrine

signaling between non-GICs and GICs. Taken together, these data demonstrated that the expression of IL6 receptors was elevated on GICs in comparison to non-GICs.

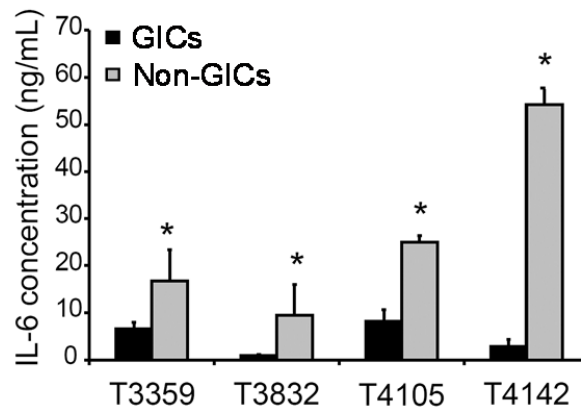


Figure 9: Non-GICs secreted more IL6 ligand than matched GICs.

ELISA was employed to determine the relative protein levels of IL6 ligand in GICs and non-GICs isolated from T3359, T3832, T4105 and T4121 patient specimens passaged short term in immune-compromised mice. GICs and non-GICs were plated in 24-well plates in equal cell number (2×10^5 cells per well) with fresh neural basal medium. After 48 hours, conditioned media were collected and IL6 ELISA was performed with the Human IL6 ELISA Kit. (*, $p < 0.05$ with comparison of non-GICs to matched GICs)

2.2.2 Targeting of IL6R α in GICs Decreases Growth and Survival

We assessed the functional significance of elevated IL6 receptors in GICs by targeting IL6R α using lentiviral transduced shRNA against IL6R α (Sigma Mission RNAi). Two different sequences of shRNA directed against IL6R α and a non-targeting shRNA were used for each experiment to control for potential off-target shRNA effects. Both IL6R α shRNA constructs led to an 80% reduction in IL6R α mRNA levels in GICs in comparison to the non-targeting control (Figure 10A). Loss of IL6R α expression in GICs significantly decreased cell growth over time associated with both decreased proliferation and increased cell death (Figure 10B, 10C; Figure 11A, 11B). Targeting of

IL6R α expression in GICs decreased percentage of proliferating cells as demonstrated by a reduction in the number of cells in the S-phase of the cell cycle as well as decreased thymidine incorporation (Figure 12). IL6R α -Knockdown also increased apoptosis as demonstrated by elevated Annexin V-positive cells (Figure 10C) as well as increased Caspase 3/7 activity (Figure 10D; Figure 11B). Targeting of IL6R α expression also attenuated the ability to form neurospheres (Figure 10E, 10F; Figure 11C, 11D) in cell culture. Of note, the neurospheres formed from the knockdown cells were smaller (potentially reflecting the decreased proliferation rate) and decreased in viability as shown by an inability to serially passage cells derived from neurospheres in the knockdown group (data not shown).

Because serial neurosphere formation is a key behavior of neural stem cells and GICs that has been associated with self-renewal capacity [2–8], these data suggest that loss of IL6R α impaired GIC self-renewal and maintenance in part due to decreased cellular survival. In addition, targeting of IL6R α increased the expression of the differentiation markers S100b (astrocytes) and GalC (oligodendrocytes), demonstrating loss of IL6R α also mediated signals promoted differentiation (Figure 13).

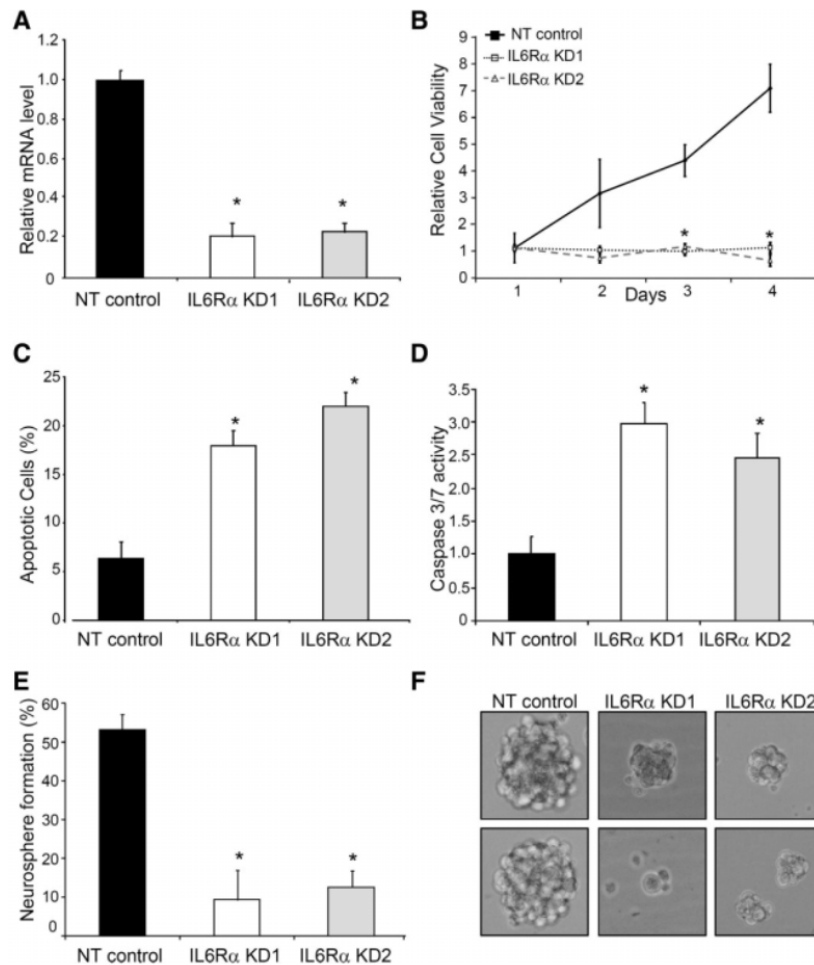


Figure 10: Targeting of IL6 receptor expression reduced GIC growth due to increased apoptosis.

(A) qRT-PCR demonstrated that IL6R α expression in GICs isolated from a D456MG human glioma xenograft was reduced via infection with lentivirus expressing two different shRNA constructs directed against IL6R α (IL6R α KD1 and IL6R α KD2) when compared with lentivirus expressing a non-targeting control shRNA (NT control). (B) Targeting of IL6R α via lentiviral shRNA significantly slowed the growth of D456MG GICs as assessed with a cell titer assay. (C and D) Targeting of IL6R α decreases the survival of D456MG GICs as demonstrated by Annexin V-FITC FACS analysis (C) and Caspase 3/7 activity (D). (E) Targeting of IL6R α expression attenuated the efficiency of D456MG GICs to form neurospheres. The percentage of wells with neurospheres is indicated when infected cells were plated with 10 cells per well in 24-well plates. (F) Representative images of neurospheres described in panel (E) are shown. (*, $p < .01$ with comparison to NT control shRNA)

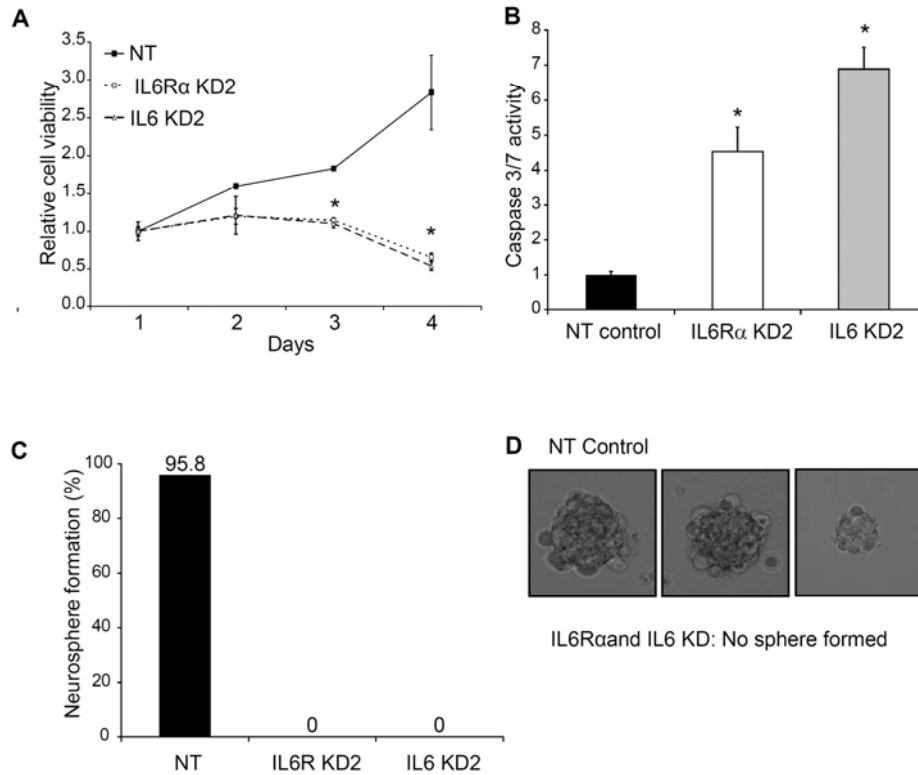


Figure 11: Targeting IL6R α /IL6 in a primary glioma specimen CCF3863 decreases GIC survival.

(A) Targeting IL6R α and IL6 via lentiviral shRNA significantly retarded the growth of CCF1863 GICs as assessed with the Cell Titer Assay. (B) Targeting IL6R α and IL6 respectively decreased the survival of CCF1863 GICs as demonstrated by Caspase 3/7 activity. (C) Targeting IL6R α and IL6 expression respectively attenuated the efficiency of CCF1863 GICs to form neurospheres. The percentage of wells with neurospheres is indicated when infected cells were plated with 50 cells per well in 24-well plates. (D) Representative images of neurospheres of non-target control. IL6R α and IL6 knockdown cells did not form neurospheres. (*, $p < 0.01$ with comparison to non-targeting shRNA)

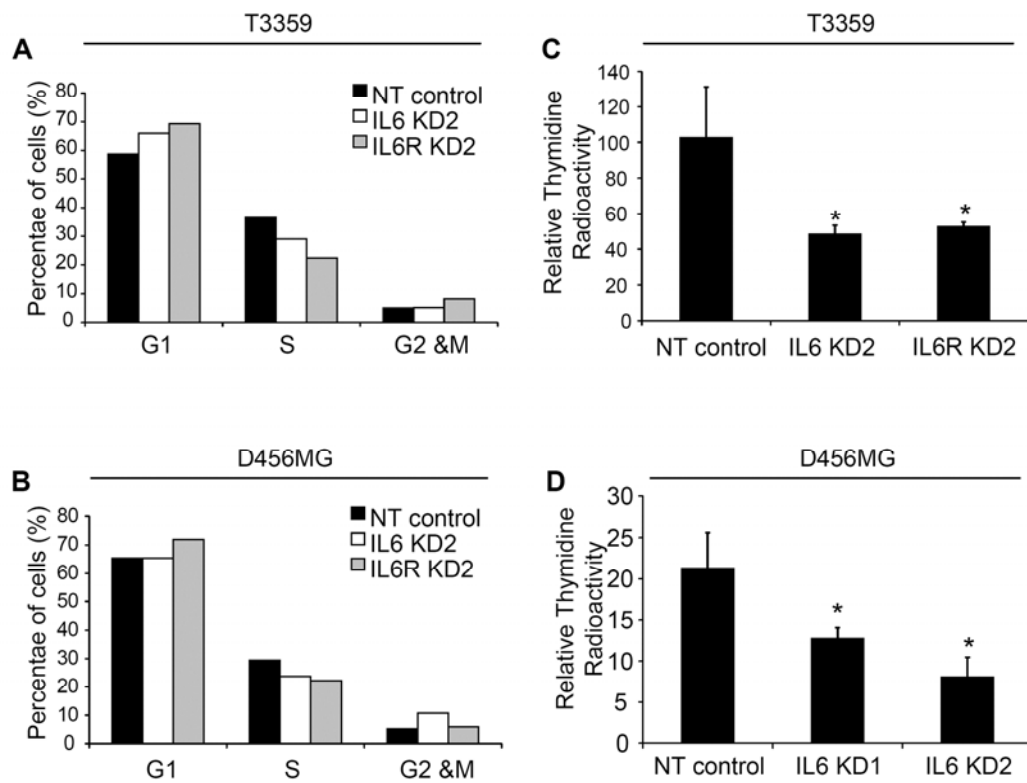


Figure 12: Targeting IL6R α or IL6 expression reduced GIC proliferation.

Targeting IL6R α or IL6 via lentiviral shRNA reduced the proportion of S-phase T3359 (A) or D456MG (B) GICs as determined by cell cycle analysis. Results were analyzed using Flowjo software. IL6R α or IL6 knockdown decreased thymidine incorporation in T3359 (C) and D456MG (D) GICs. (*, $p < 0.05$ with comparison of shRNA targeted GICs to matched non-targeting controls)

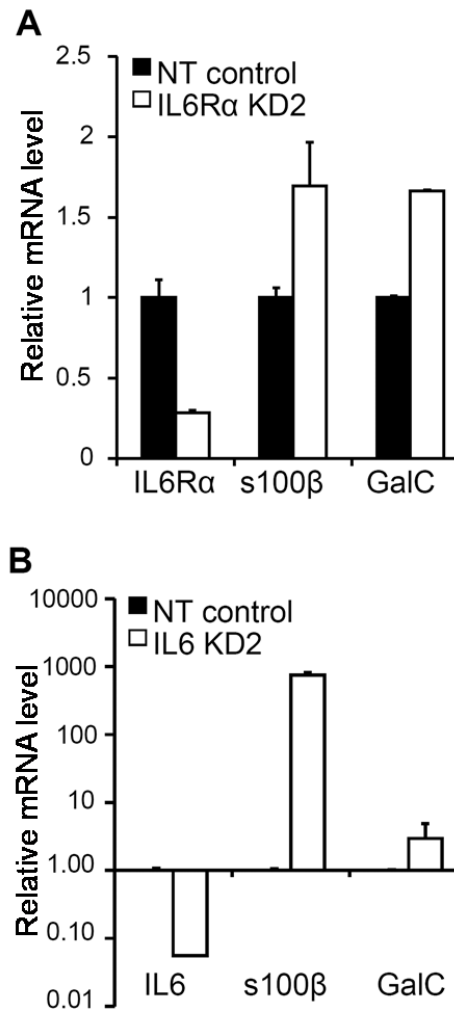


Figure 13: Targeting IL6Rα or IL6 increased differentiation marker expression. (A) After IL6Rα knockdown, qRT-PCR determined increased relative mRNA levels of the differentiation markers S100β (astrocyte lineage) and GalC (oligodendrocyte lineage). (B) Targeting IL6 also increased S100β and GalC expression.

2.2.3 Targeting of IL6 Ligand in GICs Decreases Growth and Survival

To determine if IL6 autocrine signaling in GICs contributed to the phenotype exhibited with decreased IL6Rα expression, we used a similar lentiviral shRNA-based targeting approach. Two different sequences of shRNA directed against IL6 that reduced

IL6 mRNA expression with an intermediate (IL6 KD1) and high efficiency (IL6 KD2) in GICs were identified (Figure 14A). Targeting of IL6 significantly inhibited GIC cell growth (Figure 14B; Figure 11A) with a graded effect as IL6 KD2 reduced growth more rapidly and potently than IL6 KD1 (Figure 14B), consistent with the relative knockdown efficiency. The reduced growth of IL6 knockdown cells was caused by a reduction in the percentage of proliferating cells (Figure 12) and increased apoptosis (Figure 14C, 14D; Figure 11B). Apoptosis, as demonstrated by elevated Annexin V-positive cells (Figure 14C) and increased Caspase 3/7 activity (Figure 14D), also reflected a relationship with knockdown efficiency.

Targeting IL6 in GICs significantly attenuated neurosphere formation capacity (Figure 14E, 14F; Figure 11C, 11D) and the neurospheres that developed from the knockdown cells were smaller and could not be serially passaged (data not shown). These neurosphere formation data suggest that IL6 signals regulate GIC self-renewal and maintenance, and we found that loss of IL6 also increased the expression of differentiation markers (Figure 13B). Together with the similar results derived from IL6R α targeting, these data support a pivotal role for autocrine IL6 signals in maintaining the survival of GICs.

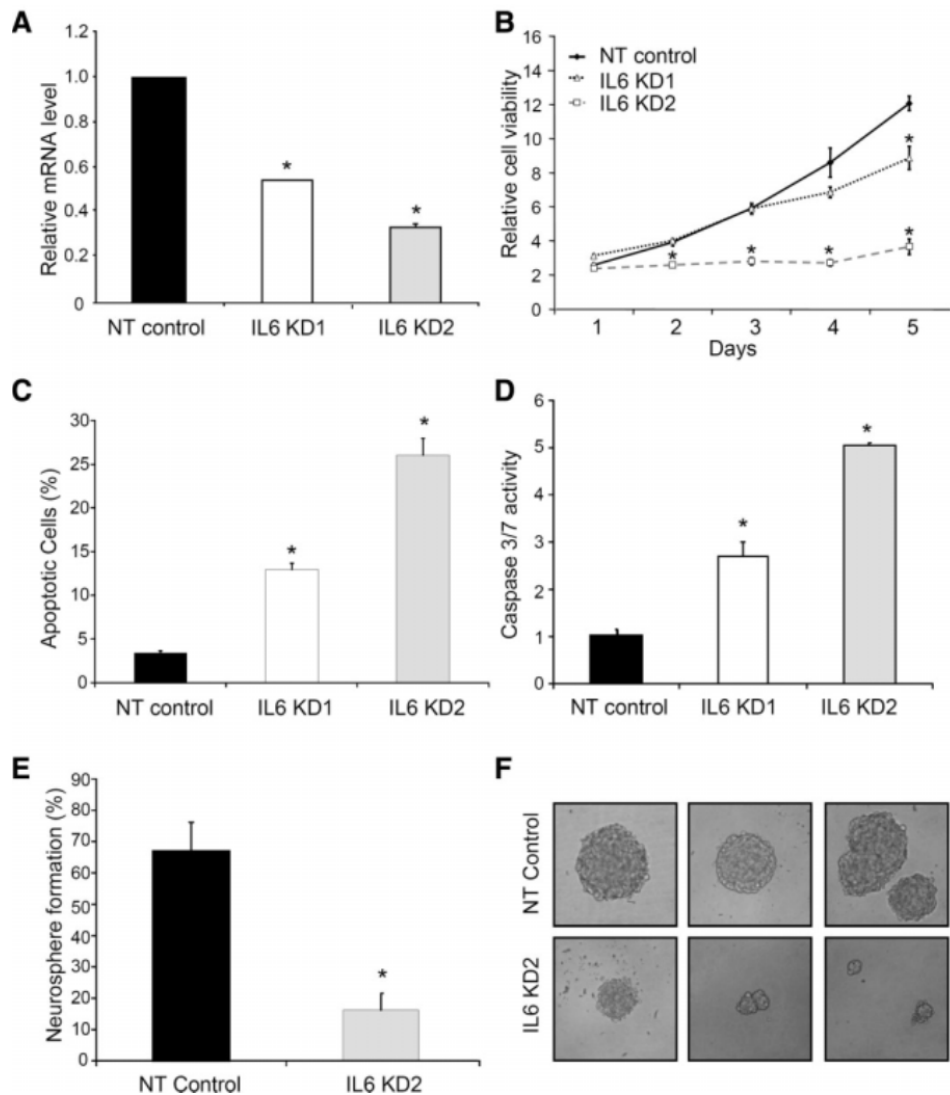


Figure 14: Targeting of IL6 ligand expression decreased GIC growth as a result of increased apoptosis.

(A) qRT-PCR demonstrated that IL6 expression in GICs isolated from D456MG xenograft was reduced via infection with lentivirus expressing IL6 shRNA constructs (IL6 KD1 and IL6 KD2) when compared with nontargeting control (NT control). (B) Targeting of IL6 via lentiviral shRNA significantly retarded the growth of D456MG GICs as assessed with a cell titer assay. (C, D) Targeting of IL6 decreases the survival of D456MG GICs as demonstrated by Annexin V-FITC analysis (C) or Caspase 3/7 activity (D). (E) Targeting of IL6 expression attenuated the efficiency of T3832 GICs to form neurospheres. (F) Representative images of neurospheres in described in panel (E) are shown. (*, $p < 0.01$ with comparison to NT control)

2.2.4 IL6 Signaling Promotes GIC Survival through Stat3 Activation

As Stat3 is a downstream mediator of IL6 signaling and has important roles in embryonic and adult stem cells as well as glioma cell lines (Konnikova et al., 2003; Matsuda et al., 1999; Niwa et al., 1998; Rahaman et al., 2002; Su et al., 2008), we explored Stat3 activation in GICs with modulation of IL6 signaling. GICs display an elevated level of basal phosphorylated Stat3 (Figure 15A) that was further induced upon the addition of exogenous IL6 (Figure 15B).

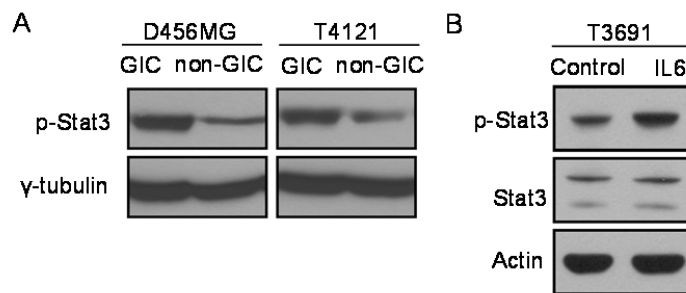


Figure 15: Elevated Stat3 phosphorylation in GICs and induction by exogenous IL6. (A) Stat3 phosphorylation at Tyr 705 is elevated in D456MG and T4121 GICs in comparison to matched non-GICs. (B) Western blotting demonstrated elevated Stat3 phosphorylation at Tyr 705 2 hours after addition of 40 ng/mL IL6 to the media of T3691 GICs.

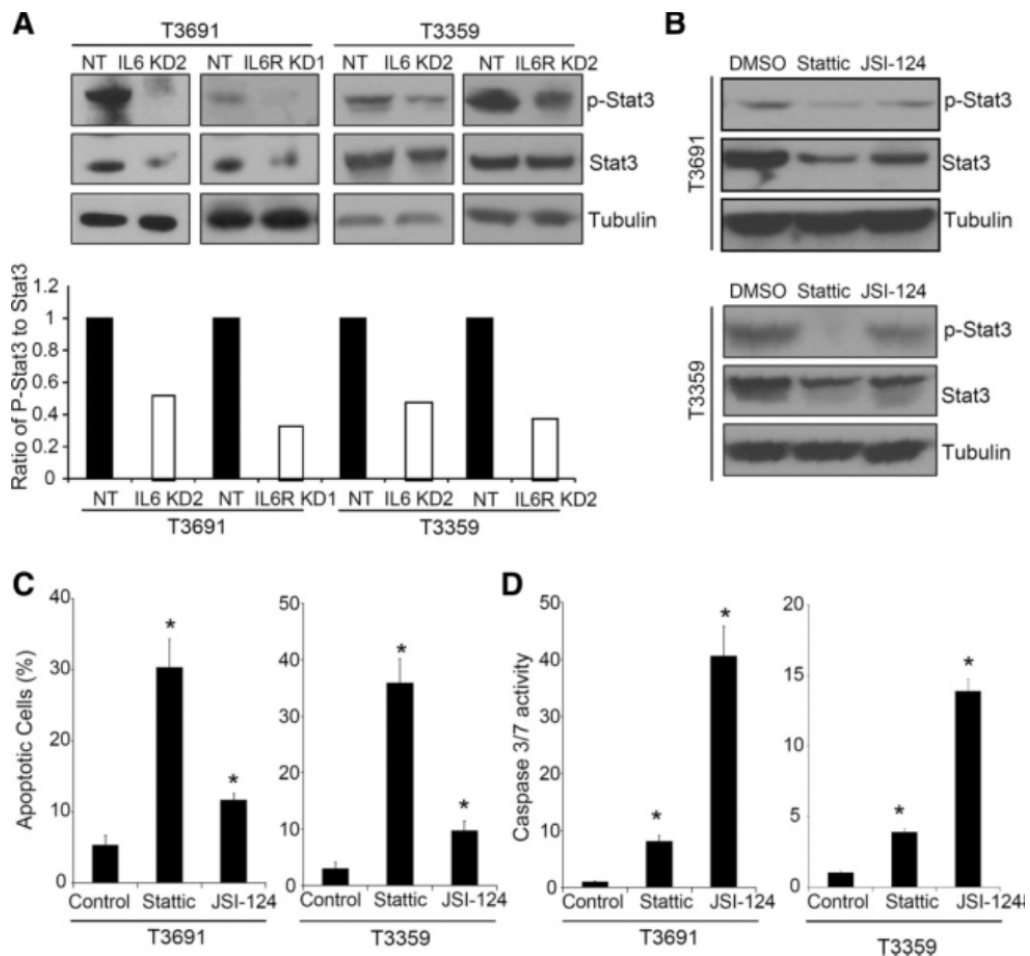


Figure 16: Stat3 is a downstream mediator of IL6 in GICs and mediates GIC survival. (A) Stat3 Phosphorylation is decreased with IL6 or IL6R α knockdown. At 48 hours after T3691 and T3359 GICs were infected with IL6 or IL6R α shRNA expressing lentivirus, levels of phosphorylated Stat3 (at Tyr705) and total Stat3 were reduced when examined with Western blot analysis. Image J software was used to quantify the relative levels of phosphorylated Stat3 to total Stat3. (B) Stat3 Inhibitors decreased the phosphorylation of Stat3 in GICs. T3691 and T3359 GSCs treated with vehicle control (DMSO) or 5 μ M Stattic or JSI-124 for 4 hours have reduced Stat3 phosphorylation assessed via Western blot analysis. (C) Stat3 Inhibitors increase the percentage of Annexin-V positive cells in GICs. T3691 and T3359 GSCs treated with 5 μ M Stattic or 5 μ M JSI-124 for 24 hours demonstrated an increased percentage of apoptotic cells as measured by FACS analysis with annexin V-FITC and PI staining compared to DMSO control. (D) Stat3 inhibitors increase Caspase 3/7 activity in GICs. T3691 and T3359 GSCs treated with 5 μ M Stattic or 5 μ M JSI-124 for 24 hours demonstrated increased activity in the Caspase 3/7 assay compared with DMSO control. (*, $p < 0.01$ with comparison to vehicle treated control)

Targeting of IL6 signaling at the level of the receptor (IL6R α) or ligand using shRNA inhibited levels of phosphorylated and total Stat3 (Figure 16A). To further interrogate the role of Stat3 in mediating the effects of IL6 on GIC survival, we used small molecule inhibitors that decrease Stat3 activity by targeting Stat3 directly (Stattic) or Janus kinase (JSI-124) (Schust et al., 2006; Su et al., 2008). Both Stat3 inhibitors reduced the activating phosphorylation of Stat3 in GICs (Figure 16B; Figure 17A). GIC Cell proliferation and survival (Figure 16C, 16D; Figure 17B–D) was dependent on Stat3 activity. Stat3 Inhibitors reduced thymidine incorporation (Figure 17B) and induced apoptosis as measured with Annexin-V staining (Figure 16C; Figure 17C) and Caspase 3/7 activity (Figure 16D; Figure 17D). Taken together, our results support an essential role for IL6-mediated Stat3 activation in GIC growth and survival.

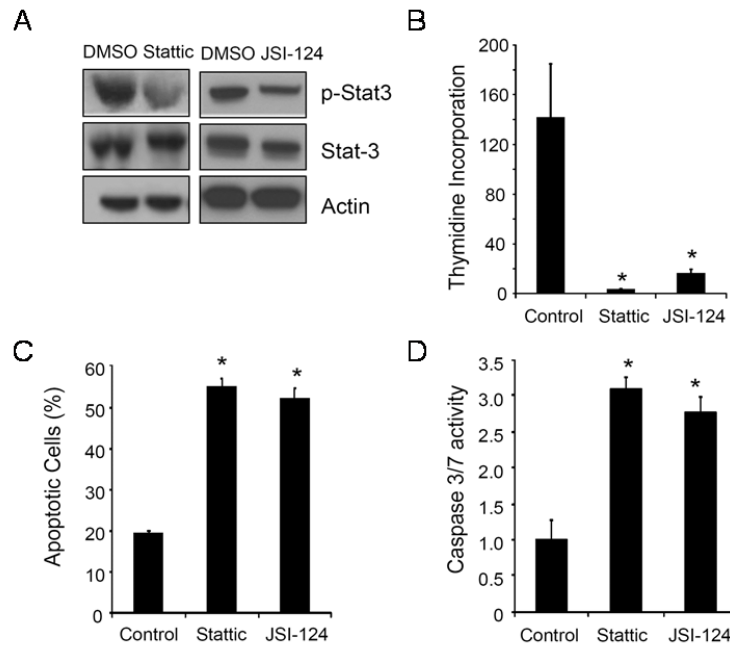


Figure 17: Targeting Stat3 activity in D456MG GICs with small molecule inhibitors decreased proliferation and increased cell death.

(A) Treatment of D456MG GICs with 5 μ M Stattic or 5 μ M JSI-124 for 4 hours have reduced Stat3 phosphorylation assessed via Western in comparison to vehicle (DMSO) treated control. (B) D456MG GICs treated with 5 μ M Stattic or 5 μ M JSI-124 for 24 hours demonstrated decreased DNA synthesis compared with vehicle control. (C) Treatment of D456MG GICs with 1 μ M Stattic or 1 μ M JSI-124 for 48 hours demonstrated an increased percentage of apoptotic cells as measured by FACS analysis with Annexin V-FITC and PI staining compared to vehicle control. (D) Treatment of D456MG GICs with 1 μ M Stattic or 1 μ M JSI-124 for 24 hours demonstrated increased activity in the Caspase 3/7 assay compared with vehicle control. (*, $p < 0.01$ with comparison to vehicle control)

2.2.5 IL6 Signaling Promotes Tumor Growth and Decreases Patient Survival

We next evaluated whether the critical effects of IL6 signals in vitro translate to in vivo survival difference by targeting IL6 receptor or ligand in intracranial tumor propagation. Targeting of IL6R α or IL6 ligand expression respectively with two different shRNA constructs in GICs prior to intracranial implantation into immune-compromised

mice significantly increased survival compared to non-targeting control (Figure 18). To determine if IL6R α or IL6 expression could also impact glioma patient survival, we utilized the National Cancer Institute's Repository for Molecular Brain Neoplasia Data (REMBRANDT) database. We found that a more than two-fold up-regulation of IL6R α mRNA correlated with a significant decrease in survival (Figure 19A). Consistent with a prior report linking IL6 to poor GBM prognosis (Tchirkov et al., 2007), we also determined that glioma patients with a more than two-fold up-regulation of IL6 mRNA have a decreased probability of survival compared with patients with reduced IL6 expression (Figure 19B).

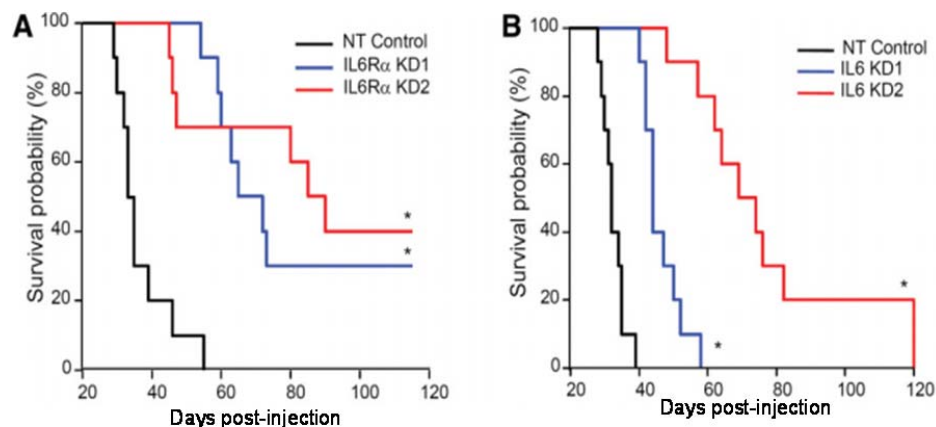


Figure 18: Targeting of either IL6R α or IL6 suppressed tumor growth and increased the survival of mice bearing intracranial xenografts.

(A) Kaplan-Meier curves demonstrate increased survival with knockdown of IL6R α in T3359 GICs. GICs infected for 24 hours with lentivirus expressing non-targeting control shRNA (NT control) or two different shRNAs directed against IL6R α (IL6R α KD1 and IL6R α KD2) were injected into the right frontal lobes of immune-compromised mice. (*, $p < 0.001$ with comparison to NT control) (B) Kaplan-Meier curves demonstrated increased survival with knockdown of IL6 (IL6 KD1 and IL6 KD2) compared to NT control shRNA in T3359 GICs injected as in panel (A). (*, $p < 0.01$ with comparison to NT control)

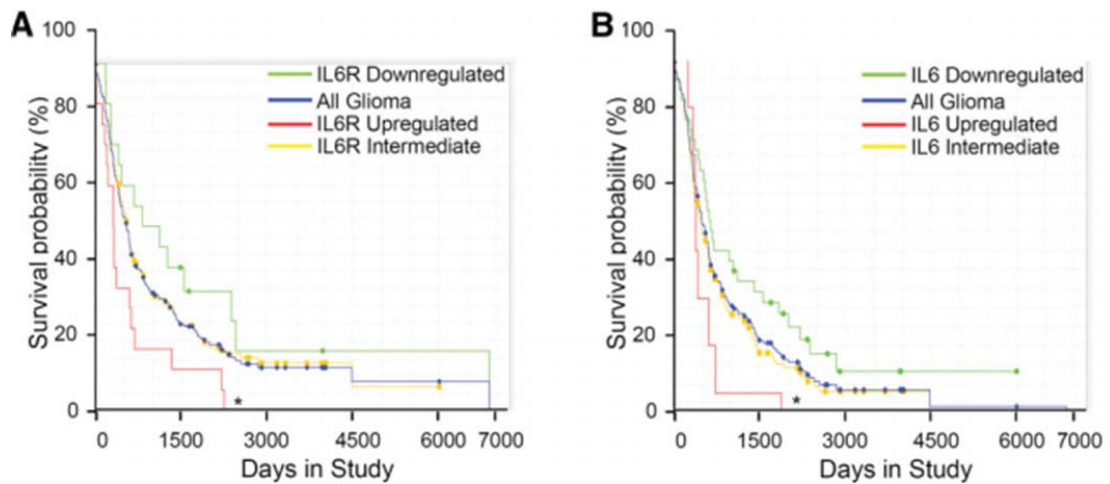


Figure 19: Higher IL6R α and IL6 mRNA levels in GBM patients correlate with poor patient survival.

(A) Clinical data from the REMBRANDT database indicates that higher IL6R α mRNA levels in gliomas correlate with poor patient survival. (*, $p=0.0076$ with comparison of survival probabilities for patients with up-regulated IL6R α expression to those with down-regulated IL6R α expression) (B) Clinical data from REMBRANDT indicates that higher IL6 mRNA levels in gliomas correlate with poor patient survival. (*, $p=0.0342$ with comparison of survival probabilities for patients with up-regulated IL6 expression to those with down-regulated IL6 expression)

These data demonstrate that IL6 signals promote the tumor-initiating capacity of GICs and strongly suggest that elevated IL6 signaling in GICs contribute to poor patient outcome.

2.2.6 IL6 Antibody Treatment Decreases the Growth of GIC-Derived Tumors

As inhibition of IL6 signals could increase tumor latency in our animal models, we performed proof-of-principle studies targeting IL6 with a humanized antibody. Although large molecules like antibodies may have limited brain penetration as a result of restriction by the neurovascular unit, the recent clinical success of Avastin, a

humanized neutralizing antibody against Vascular Endothelial Growth Factor (VEGF), suggests that systemically administered antibodies may be useful as anti-glioma therapies (Cohen et al., 2009). To evaluate the potential benefit of IL6 antibodies against gliomas in the absence of a brain-specific delivery restriction, we utilized a subcutaneous human glioma xenograft model and found that humanized IL6 antibody treatment reduced GSC tumor growth (Figure 20). After GIC implantation, treatment with IL6 antibody through intraperitoneal injection significantly reduced the volume of resulting tumors (Figure 20A). At the termination of experiments, the weight of tumors treated with IL6 antibody was significantly less than that of control (Figure 20B). Tumors treated with IL6 antibody displayed a significantly lower percentage of proliferating cells (Figure 20D, 20E) and a higher number of apoptotic cells than control tumors (Figure 20F, 20G). In contrast, the intraperitoneal administration of IL6 antibody to mice bearing intracranial GSC tumors did not improve survival (data not shown) supporting a need of intracranial delivery of the IL6 antibody for efficacy. These studies demonstrate that pharmacological targeting of IL6 signaling has the capacity to reduce the growth of glioma xenografts and may be beneficial for glioblastoma patients.

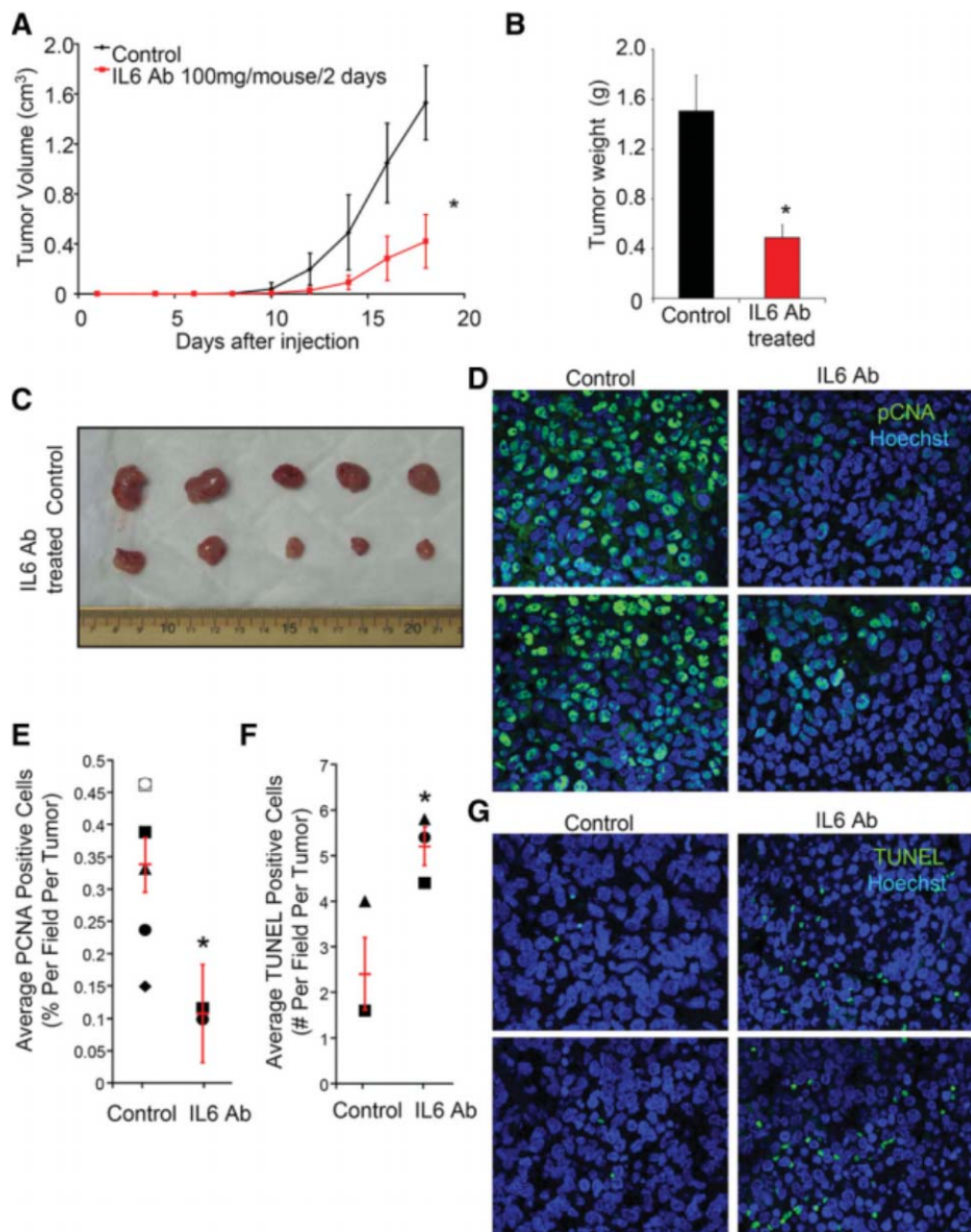


Figure 20: Systemic treatment with an anti-IL6 antibody inhibited the growth of human glioma xenografts in vivo.

(A) Subcutaneous tumor volume was significantly decreased with IL6 antibody treatment. Animals subcutaneously injected with T3359 GICs were intraperitoneally injected 24 hours later with IL6 antibody at 100 μ g every 2 days or phosphate-buffered saline as a vehicle control. (B) Total tumor burden was reduced with IL6 antibody

treatment as measured by tumor weight. (*, $p < 0.01$ with comparison to control) (C) Images of xenografts measured in panel (B). (D, E) Proliferation is decreased in human glioma xenografts treated with IL6 antibody. Representative images of sections of control and IL6 antibody-treated tumors stained with PCNA antibody (green) and Hoechst (blue) (D) were quantified based on five fields per tumor with six tumors for the control group and two tumors for the IL6 antibody-treated group. (*, $p = 0.0488$ with comparison to control) (F, G) Apoptosis is increased in human glioma xenografts treated with IL6 antibody. Representative images of sections of control and IL6 antibody-treated tumors stained with TUNEL (green) and Hoechst (blue) (G) were quantified based on five fields per tumor with three tumors per group. (*, $p = 0.036$ with comparison to control)

2.3 Material and Methods

2.3.1 Isolation of GICs and Non-GICs and Cell Culture

Similar to prior descriptions (Bao et al., 2008; Bao et al., 2006a; Li et al., 2009), matched cultures enriched or depleted for GICs were isolated from the human glioblastoma xenografts (D456MG) or fresh human surgical specimens either freshly derived (CCF1863) or immediately implanted in immune-compromised mice (T3359, T3691, T3832, T4105, T4121, and T4142), a method that has been described to preserve tumor initiating cells in glioma models (Shu et al., 2008). Patients provided informed consent under protocols approved by either the Cleveland Clinic Foundation or Duke University Institutional Review Boards. Briefly, viable tumors were disaggregated with the use of the Papain Dissociation System (Worthington Biochemical) and filtered with a 70- μm cell strainer (BD Biosciences) to remove tissue pieces according to the manufacturer's instructions. Cells were cultured in stem cell culture medium supplemented as detailed below for at least 4 hours to recover surface antigens. Cells were then labeled with an APC (allophycocyanin) or PE (phycoerythrin) conjugated

CD133 antibody (Miltenyi Biotec), and sorted by fluorescence-activated cell sorting. Alternatively, cells were separated with the use of microbead-conjugated CD133 antibodies and magnetic columns (Miltenyi Biotec).

CD133-positive cells were enriched for GICs defined through functional assays of self-renewal and tumor propagation, whereas CD133-negative cells are depleted for non-GICs. GICs were cultured in Neurobasal media supplemented with B27 without vitamin A, L-glutamine, sodium pyruvate (Invitrogen), 10 ng/ml bFGF, and 10 ng/ml EGF (R&D Systems). Non-GICs were cultured for at least 12 hours in 10% serum containing Dulbecco's modified Eagle's medium to allow cell survival. After recovery, Dulbecco's modified Eagle's medium was removed, and the cells were cultured in supplemented Neurobasal medium so experiments were performed in identical media. Non-GICs were cultured in Neurobasal media for at least 12 hours before experiments were performed. The GIC properties of the CD133-positive cells was confirmed by serial neurosphere assays, and tumor formation assays.

2.3.2 Immunofluorescence Staining

Freshly frozen human glioma surgical biopsy samples were processed in accordance with a protocol approved by the Duke University Medical Center Institutional Review Board. Slides were stained with polyclonal rabbit anti-IL6R α (Abcam) with monoclonal mouse anti-CD133 (Miltenyi) or monoclonal mouse anti-gp130 with rabbit polyclonal anti-CD133 antibodies (Abcam).

For sections of xenografts treated with IL6 antibody, slides were stained with monoclonal PCAM (Abcam). Primary antibodies were incubated for 16 hours at 4C, followed by detection with Alexa Fluor 488 goat anti-mouse (Invitrogen) and Alexa Fluor 568 goat anti-rabbit (Invitrogen) secondary antibodies. Nuclei were stained with Hoechst 33342 (Invitrogen), and slides were mounted using Fluoromount (Calbiochem).

2.3.3 Quantitative Real-Time Polymerase Chain Reaction

Total RNA was prepared using the RNeasy kit (Qiagen) and reverse transcribed into cDNA using an iScript cDNA synthesis kit (Bio-Rad). mRNA levels were measured using probes from Qiagen with SYBR Green (Qiagen) and a ABI-7900 system (Applied Biosystems).

2.3.4 Lentiviral Mediated shRNA Targeting

Lentiviral shRNA clones (Sigma Mission RNAi) targeting IL6R α , IL6, and scramble control (SHC002) were purchased from Sigma (Table1). These vectors were co-transfected with the packaging vectors psPAX2 and pCI-VSVG (Addgene) into 293FT cells by lipofectamine 2000 (Invitrogen) to produce the virus.

Table 1: Information of shRNA clones targeting IL6R α and IL6

Name of shRNA constructs	TCR number	Clone ID	Sequence
IL6R α KD1	TRCN0000058781	NM_000565.2-1800s1c1	CCGGAGCCCTTATGACATCAGCAATCTCGAGAT TGCTGATGTCATAAGGGCTTTTTTG
IL6R α KD2	TRCN0000058778	NM_000565.2-1430s1c1	CCGGGCAGGCACTTACTACTAATAACTCGAGTT ATTAGTAGTAAGTGCTGCTTTTTG
IL6 KD1	TRCN0000059205	NM_000600.1-636s1c1	CCGGCATCTCATTCTGCGCAGCTTCTCGAGAA AGCTGCGCAGAATGAGATGTTTTTG
IL6 KD2	TRCN0000059207	NM_000600.1-211s1c1	CCGGCAGAACGAATTGACAAACAAACTCGAGTT TGTTTGCAATTCGTTCTGTTTTG

2.3.5 Small Molecule Inhibitors

Stattic (6-nitrobenzo[b]thiophene-1,1-dioxide) and JSI-124 (Cucurbitacin I) were obtained from Calbiochem (EMD Chemicals).

2.3.6 Cell Viability Assay

GICs Infected with lentivirus expressing the indicated shRNAs for 48 hours were plated in 96-well plates at 1,000 cells per well. Twenty-four hours after overnight recovery, plates were examined by the cell viability assay kit (Promega) at the indicated times. Results are reported from at least triplicate samples as the mean \pm standard deviation.

2.3.7 Neurosphere Formation Assay

GICs Infected with lentivirus expressing the indicated shRNAs were plated in 24-well plates at 10 cells per well. After 7 days, the percentage of wells containing neurospheres was quantified, and neurospheres were imaged with an Olympus CK40 digital camera mounted to a light microscope.

2.3.8 Annexin V Staining

Forty-eight hours after infection, GICs were plated at 10^5 cells per well and allowed to recover for 24 hours prior to staining with an Annexin V kit (Invitrogen) and fluorescence-activated cell sorting analysis. For small molecule inhibitor studies, GICs were plated at 10^5 cells per well and allowed to recover for 24 hours prior to treatment with the indicated Stat3 inhibitors for 24 hours.

2.3.9 Caspase 3/7 Assay

GICs Infected with lentivirus expressing the indicated shRNAs for 48 hours were plated at 10^3 cells per well and assayed after 24 hours. For small molecule inhibitor studies, GICs were plated at 10^3 cells per well and allowed to recover for 24 hours prior to treatment with the indicated Stat3 inhibitors for 24 hours. A Caspase 3/7 assay kit (Promega) was used to determine caspase activity which is reported as the mean \pm standard deviation.

2.3.10 Western Blotting and Antibodies

Western blot analyses were performed as previously described [5–8]. Rabbit polyclonal antibodies for human IL6, IL6R α (Abcam), Stat3, phospho-Stat3 (Cell Signaling), γ -tubulin (Sigma) and actin (Millipore) were used according to the manufacturer's instructions.

2.3.11 Intracranial Tumor Assays and IL6 Antibody Treatment

Intracranial or subcutaneous transplantations of GICs into nude mice were performed in accordance with a protocol approved by the Duke University Institutional Animal Care and Use Committee. Briefly, 48 hours after lentiviral infection, cells were counted and the indicated number of live cells implanted into the right frontal lobes of athymic nude mice. Mice were maintained until the development of neurological symptoms.

Where indicated, animals were treated with 100 μ g anti-IL6 antibody or phosphate-buffered saline injected intraperitoneally every 2 days until the termination of experiments, at which time tumors were harvested, weighed, and examined.

2.3.12 Statistical Analysis

Results are reported as the mean \pm standard deviation. Significance was tested by one-way ANOVA using GraphPad software or MedCalc software. For in vivo studies, Kaplan-Meier curves and log-rank analysis were performed using MedCalc software.

2.4 Discussion

Together, our data demonstrate an important role for IL6 signaling in GICs. The IL6 receptors IL6R α and gp130 were elevated in GICs in comparison to non-stem glioma cells in sections of human patient specimens and isolated cell preparations. Targeting either IL6R α or IL6 in GICs significantly impaired their growth and survival in vitro, suggesting the importance of IL6 autocrine signals for GIC maintenance. IL6 Signals

were mediated through activation of Stat3, which was also critical for GIC survival. Targeting of IL6R α with shRNA or of IL6 with shRNA or antibody increased tumor latency in mice bearing human glioma xenografts, suggesting that IL6 may be a novel GIC directed therapeutic target.

Because IL6 may function as an autocrine and/or paracrine factor, we explored signaling in GIC maintenance in vitro and noted at least an autocrine role. However, cancer development is not a cell-intrinsic process driven only by a collection of genetic errors in transformed cells. Tumor growth depends on the interactions between cancer cells and surrounding stroma cells, suggesting that paracrine effects of IL6 on GICs may be critical in vivo. GICs usually compose a small population (0.5% to 5%) of bulk tumors as demonstrated with immune-histochemical staining of GBM specimens and xenografts that demonstrate sporadic localization of GICs surrounded by non-GIC glioma cells [6]. The physical location (niche) of GICs certainly suggests potential interactions with other cells. The finding that IL6 ligand (but not receptor) mRNA levels were higher in most non-GICs in comparison with matched GICs supports the hypothesis that IL6 secreted by non-GICs may support GIC maintenance. If this paradigm of elevated ligand secretion from non-GICs with higher receptor expression on GICs proves more broadly applicable, then non-GICs may prove to be a critical factor in the niche of tumor initiating cells.

The effects of IL6 activation in GBM have been largely undefined, but we now demonstrate a specific role for IL6 in GIC survival and tumorigenic capacity. Because GICs promote tumor maintenance through many biological mechanisms (invasion, angiogenesis, chemoresistance) that have also been found to be regulated by IL6, the potential for IL6 to control additional GIC-mediated behaviors exists. In particular, IL6 may regulate angiogenesis (Choi et al., 2002), and GICs have been reported to be highly pro-angiogenic (Bao et al., 2006b). We also identified IL6 as one gene among a set of genes that are specifically unregulated in GICs in comparison to non-GICs under hypoxia (Li et al., 2009), a known “angiogenic switch” (Harris, 2002). Hypoxia also induces IL6 expression in breast cancer cells grown as mammospheres, and IL-6 antibody treatment increases mammosphere cell death under hypoxic conditions (Sehgal and Tamm, 1991). Furthermore, IL6 increases VEGF transcription in GBM through Stat3 (Loeffler et al., 2005), demonstrating the potential involvement of both IL6 and Stat3 in a broad range of angiogenic behaviors. Together, these data suggest that IL6 may be additionally important for GIC survival under hypoxia and further contribute to GIC-driven angiogenesis.

Clinical and laboratory evidence demonstrates that anti-IL6 directed therapies are well tolerated in patients, indicating their potential utility for anticancer treatments (Tripathi et al., 2003). Humanized anti-IL6 and IL6R α monoclonal antibodies have been evaluated in clinical trials and the use of IL6 conjugated toxins has also been proposed

(Tripathi et al., 2003). These data, in combination with our results of IL6 antibody treatments of GBM xenografts, suggest that IL6 antibody may be useful against GBM. While treatment of GBMs is often complicated by the necessity of systemic treatments to cross the blood–brain barrier, antibody-based therapies (such as Avastin) have been administered intravenously and proven effective for GBM (Vredenburgh et al., 2007). Similarly, the ability of IL6 antibody to bind and inactivate this growth factor in the bloodstream may prove efficacious for GBM patients.

We determined that a novel molecular pathway, IL6 signaling, is linked to GIC growth and survival. The dramatic benefit of IL6R α and IL6 knockdown on the survival of mice bearing intracranial tumors and the effect of IL6 antibody against GBM xenografts strongly suggest that targeting of IL6 signals may be useful as a therapy directed by tumor initiating cells. Our studies provide evidence that inhibiting IL6 pathways should be considered for further exploitation in therapeutic development.

3. miR-33a Confers Biological Properties of Glioma Initiating Cells via Modulation of the cAMP/PKA and Notch Signaling Pathways

3.1 Introduction

Glioblastoma (GBM, WHO grade IV astrocytoma) is the most common and lethal primary brain tumor in adults, with an average survival of slightly more than one year after initial diagnosis (CBTRUS, 2005). GBMs exhibit significant heterogeneity within the tumor mass, among which a subpopulation of cells named tumor-initiating cells (TIC) or cancer stem cells possesses potent tumorigenic ability when they are implanted in immune-deficient mice (Singh et al., 2004). Those glioma initiating cells (GICs) display stem-cell-like characteristics that are normally associated with neural stem cells, including self-renewal demonstrated by their ability to form neurospheres in culture during serial dissociations and passages, expression of neural stem cells markers (e.g. cell-surface antigen CD133, transcription factor Nestin and Olig2), and potential to differentiate into multiple lineages such as neurons, astrocytes and oligodendroglia (Yuan et al., 2004). GICs have also been shown to account for resistance to radio- and chemotherapies (Bao et al., 2006a; Liu et al., 2006). These biological properties of GICs are considered to be crucial for GBM occurrence and recurrence; however, the molecular mechanisms underlying the functional differences between GICs and non-GICs within the GBM tumor mass remain largely unknown.

MicroRNAs (miRNAs) are a class of non-coding small RNA molecules, typically about 18-22 nucleotides in the mature form (Bushati and Cohen, 2007). MicroRNAs negatively regulate gene expression at the post-transcriptional level by promoting mRNA degradation and/or inhibiting mRNA translation. MicroRNAs in theory could be involved in almost every aspect of biological processes by targeting about one-third of genes in the human genome (Baek et al., 2008). In recent years, a large number of miRNAs are found to be deregulated in many types of cancer: some function as tumor promoters and others as tumor suppressors (Farazi et al., 2011). For example, among the most extensively studied miRNAs, the miR17-92 clusters and miR-21 are reported to function as onco-mirs in a variety of tumors through multiple mechanisms (Jazbutyte and Thum, 2010; Mendell, 2008; Poliseno et al., 2010). In the context of GBM, particularly GICs, little is known about miRNAs that may play critical roles in defining the functions of GICs, with only recent reports on the link between miRNAs and GBM progression (Chan et al., 2012; Schraivogel et al., 2011).

Here we report the identification of miR-33a as a master determinant that can functionally define the biological properties of GICs versus non-GICs. Specifically, antagonism of miR-33a activity in GICs led to loss of self-renewal ability measured by decreased ability to proliferate and to form neurospheres, and reduced expression of stemness markers. Furthermore, GICs with suppressed miR-33a function displayed compromised ability to generate intracranial tumors in nude mice. Importantly,

overexpression of miR-33a in non-GICs appeared to reprogram those cells into a state resembling GICs, as demonstrated by their enhanced ability to form neurospheres associated with an increased expression of stemness markers, as well as a potent augmentation in the formation of xenograft tumors, a hallmark of GICs. Mechanistically, we have identified several down-stream targets of miR-33a that could contribute to the functional effect of this microRNA on the biological activity of GICs. Among them, PDE8A is a negative regulator of the cAMP and PKA pathway that has not previously been implicated to be involved in the biology of tumor initiating cells. Another target of miR-33a, UVRAG can negatively modulate the activity of the Notch pathway. Repression of PDE8A and UVRAG by miR-33a or antagonists of the PKA or Notch pathways could potentially affect the self-renewal and stemness of the GICs. Finally, blockage of miR-33a activity by modified small RNA antagonists strongly inhibited GIC-initiated tumor progression in a subcutaneous GBM model, suggesting that the miR-33a-mediated signaling network could serve as a promising therapeutic target for the treatment of GBM.

3.2 Results

3.2.1 Identification of miR-33a as a top candidate capable of affecting the neurosphere-forming activity of GICs

To identify miRNAs that may contribute to the biological properties that distinguish GICs from non-GICs, we conducted a candidate-based screen of miRNAs that are known through previous studies to be involved in regulating stem cell biology.

We employed two established experimental procedures to enrich GICs, one with the use of cell surface marker CD133 (Bao et al., 2006; Singh et al., 2004) and the other with a specific culturing condition that could significantly enrich the population that contains both CD133-positive and CD133-negative GICs (Chen et al., 2010). Although both methods can enrich the GICs from dissociated glioma cells, it is likely that certain percentage of GICs remain in the so-called “non-GICs”. Despite of the impurity of the “non-GICs”, the two populations of glioma cells display clearly distinctive biological properties that would form the basis of our functional assays employed in this study.

For the source of glioma cells, we used two freshly isolated GBM patient specimens and three glioma lines maintained through serial passage in athymic BALB/c nu/nu mice as subcutaneous xenografts. The expression profile of the 88 miRNAs in the GICs and non-GICs isolated from those five tumor samples was determined and those miRNAs displayed more than two-fold of differences in their expression levels between the two sub-populations of cells are shown in Figure 21. Altogether, ten miRNAs were found up-regulated and four miRNAs down-regulated that are common in all five tumor samples (the fold changes of these fourteen miRNAs in two patient samples and two xenograft tumors are listed in Table 2). Among this list, several miRNAs were recently identified to exhibit differential expression profiles in CD133-positive glioma cells by a similar screen (Schraivogel et al., 2011), providing support to the reliability of our expression profiling. Interestingly, five of the ten up-regulated miRNAs belong to

the miR-17-92 cluster family that have been extensively studied and defined as onco-mirs in other cancer types.

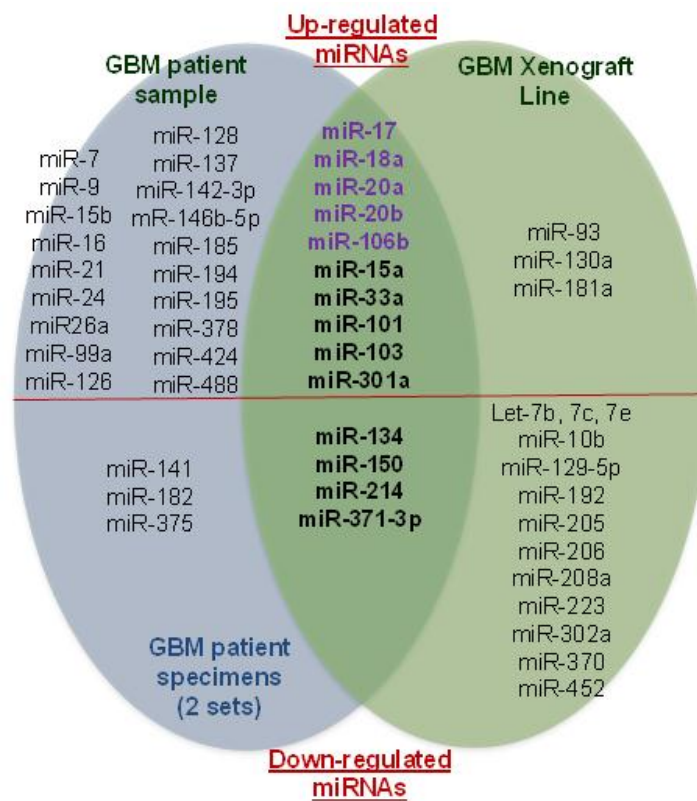


Figure 21: Venn Graph analysis of the up- and down-regulated miRNAs.

Data were collected in two GBM patient-derived sample sets, as well as in three sample sets from xenografted tumors derived from patients but maintained in nude mice in serial passages. 14 miRNAs that were commonly deregulated by more than two-fold in both patient specimens and xenografts are shown in the overlapping area.

Table 2: Fold change of deregulated miRNAs in GICs compared to non-GICs in two patient specimens (PS) and two xenografted glioma lines (XL)

Name of miRNAs	11-0296 (PS)	11-0236 (PS)	10-0228 (XL)	D456MG (XL)
hsa-miR-106b	18.25	47.50	26.35	7.31
hsa-miR-20b	2.93	28.84	18.00	2.42
hsa-miR-301a	64.45	39.12	14.62	7.25
hsa-miR-18a	3.48	33.13	3.76	7.81
hsa-miR-15a	3.39	54.95	19.43	2.71
hsa-miR-103	6.11	10.48	5.03	4.57
hsa-miR-20a	11.55	26.54	7.16	3.72
hsa-miR-101	15.78	151.17	21.11	19.35
hsa-miR-17	3.61	31.34	13.09	4.08
hsa-miR-33a	2.05	7.57	5.94	4.41
hsa-miR-134	0.015	0.418	0.005	0.210
hsa-miR-214	0.014	0.140	0.042	0.015
hsa-miR-150	0.018	0.392	0.164	0.424
hsa-miR-371-3p	0.001	0.257	0.257	0.177

To assess the potential function of these miRNAs, we overexpressed them individually in GICs and assessed whether they could have an impact on the formation of neurosphere, mainly because we were most interested in those miRNAs involved in the control of GIC properties associated with stemness. In this assay, while not exhibiting the most difference in the expression level between the two populations of glioma cells (Table 2), miR-33a emerged as the top candidate due to its potent positive effect on neurosphere formation (data not shown). Although this miRNA has never been studied in the context of cancer, previous reports indicated that miR-33a could act as an important regulator of cholesterol and fatty acid homeostasis via repression of key genes in cholesterol export, high-density lipoprotein metabolism, fatty acid oxidation, and glucose metabolism (Davalos et al., 2011; Gerin et al., 2010; Rayner et al., 2010). To further assess the expression pattern of miR-33a in GBM, we collected more than 50 fresh patient specimens from Duke Brain Tumor Center and were able to cultivate and

isolate sufficient number of cells from 16 samples to conduct validation experiments. As illustrated in Figure 22A, the expression level of miR-33a was significantly elevated in GICs compared to their corresponding non-GICs derived from the same tumor samples. In the meantime, we also examined miR-33a expression pattern in several glioma xenograft tumor lines as they would be used in the majority of the subsequent experiments. Consistent with the results generated from freshly isolated GBM specimen, miR-33a is highly expressed in the GIC population in all three lines (Figure 22B). Taken together, these results indicate that higher level of miR-33a expression could be a common molecular signature of GICs in comparison to non-GICs.

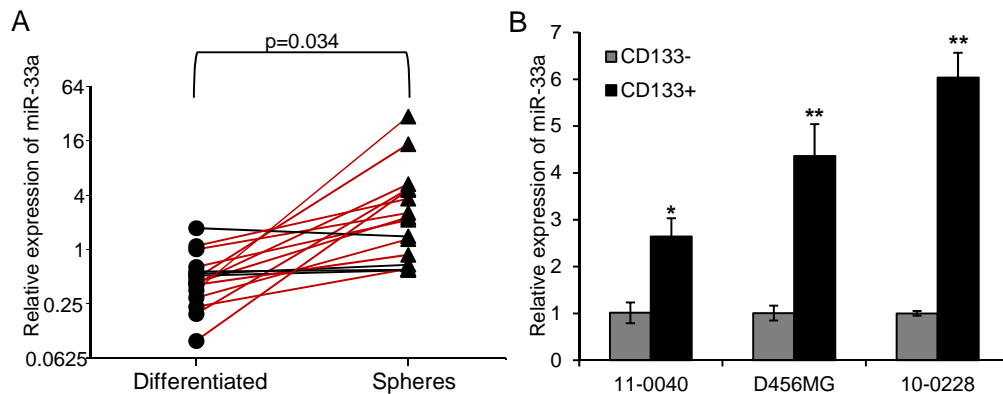


Figure 22: Identification of miR-33a as among those differentially expressed miRNAs between GICs and non-GICs.

(A) A scatter dot plot shows the expression pattern of miR-33a in GICs enriched by defined media compared to their non-GIC counterparts in 16 clinical GBM specimens, as detected by qRT-PCR. HRU6 was used as an internal control. (B) Relative expression levels of miR-33a in GICs enriched by CD133-positive selection from three xenograft tumor lines compared with their CD133-negative counterparts, as detected by qRT-PCR. HRU6 was used as an internal control. (*, $p < 0.05$, **, $p < 0.01$ compared with their non-GIC counterpart)

3.2.2 Inhibition of miR-33a suppressed self-renewal, proliferation and tumor-initiation of GICs

To determine the role of endogenous miR-33a in GICs, we employed two different methods to antagonize the function of miR-33a. First we generated a lentiviral-based sponge construct to attenuate the function of miR-33a (33a-sponge) to examine its effects in GICs. Then we verified the results using a miR-ZIP method that antagonizes miR-33a by expressing a miR-33a anti-sense RNA. Using the neurosphere formation assay, we found that attenuating the function of miR-33a in GICs led to a significant decrease in their ability to form neurospheres (Figure 23A, 23B; Figure 24A, 24B). Meanwhile, the growth rate and proliferation of miR-33a-antagonized GICs were also moderately reduced as measured by a cell titer kit and EdU incorporation assay (Figure 23C-23F; Figure 24C-24F). In addition, after withdrawing growth factors EGF and bFGF to induce differentiation of GICs, inhibition of miR-33a resulted in a dramatic decrease in the expression of stemness markers Lin28, Oct4 and Nanog (Figure 23G, 23H; Figure 24G, 24H).

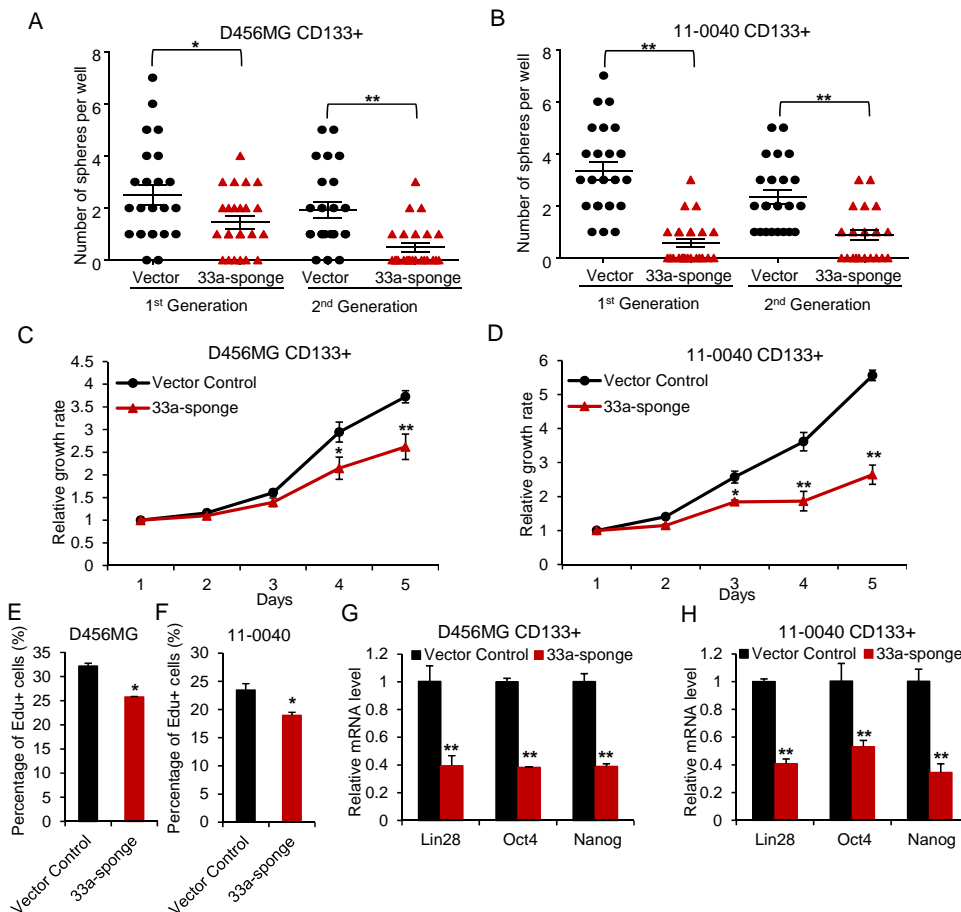


Figure 23: Antagonism of miR-33a by miR-33a sponge indicates miR-33a is required for self-renewal and proliferation in GICs.

(A, B) Neurosphere formation assays were performed for D456MG- and 11-0040-derived GICs expressing vector control or the miR-33a sponge. For D456MG GICs, 20 cells were plated per well in 24-well plates; for 11-0040 GICs, 50 cells were plated per well in 24-well plates. (C, D) Growth rate of the same GICs as in A, B was measured by cell titer assay with the dates indicated. (E, F) 10 μ M EdU was incubated with the same GICs as in A, B for two hours and incorporation rate was measured as percentage of cells labeled positive. (G, H) qRT-PCR analysis was performed to determine the expression pattern of several indicated stemness-associated genes in D456MG and 11-0040 GICs after expression of the miR-33a sponge. Beta-actin was used as an internal control. (In Figure 23A and 23B, results are reported as the mean \pm standard deviation of the mean; results from first round of neurosphere formation assays are named "1st generation" and results from second round are named "2nd generation"; * p < 0.05, ** p < 0.01 compared to control group)

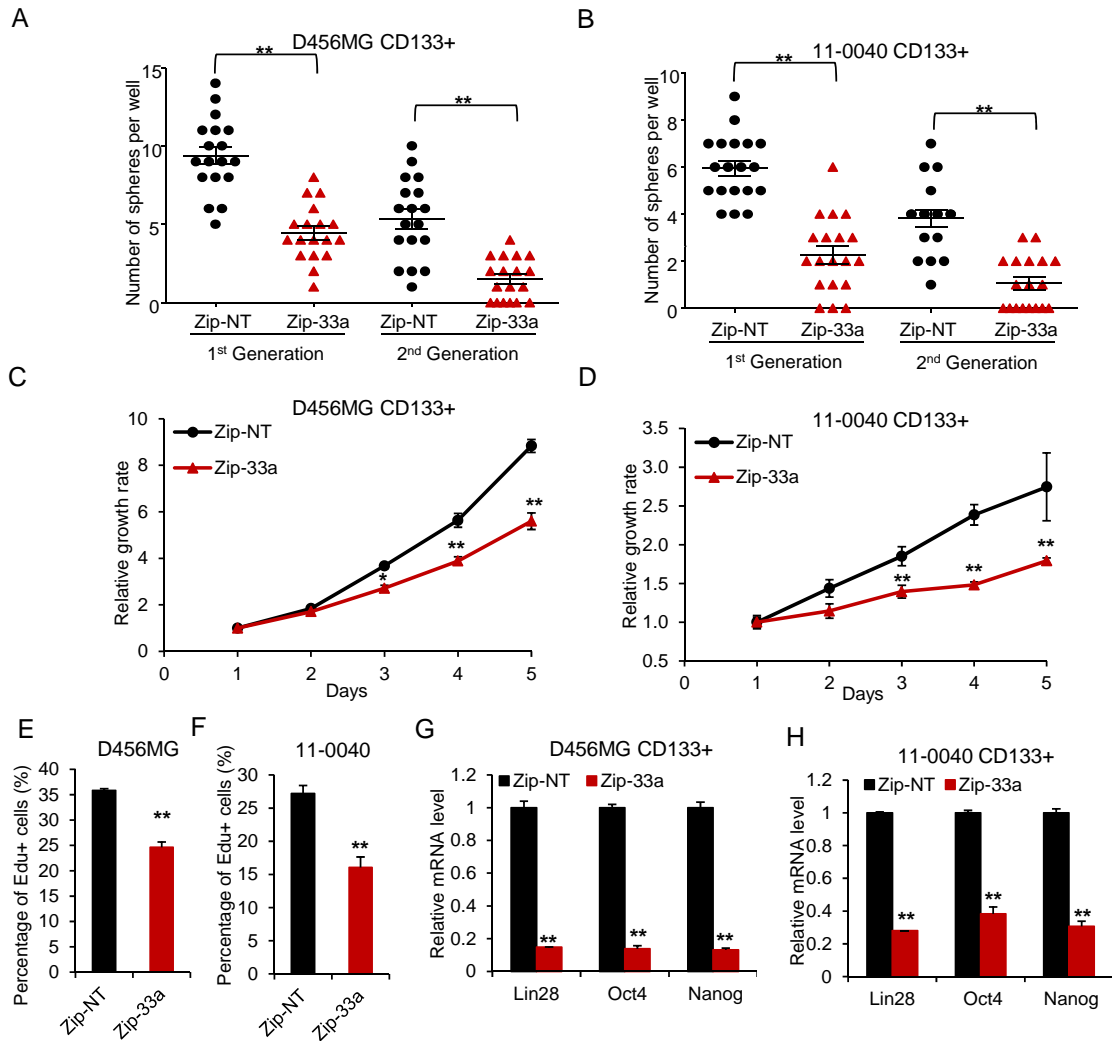


Figure 24: Antagonism of miR-33a by Zip-33a indicates miR-33a is required for self-renewal and proliferation in GICs.

(A, B) Neurosphere formation assays were performed in D456MG and 11-0040 GICs expressing Zip-NT control or Zip-33a. The same experimental procedure was used as for those in Figure 23A and 23B. (C, D) Growth rate of D456MG and 11-0040 GICs expressing Zip-NT control or Zip-33a were measured by cell titer assay. (E, F) 10 μ M EdU was incubated with cells for two hours and incorporation rate was measured in GICs expressing Zip-NT control or Zip-33a. (G, H) qRT-PCR analysis was performed to determine stemness-associated genes in D456MG and 11-0040 GICs expressing Zip-NT control or Zip-33a. Beta-actin was used as internal control. (In Figure 24A and 24B, results are reported as the mean \pm standard deviation of the mean; *, p < 0.05, **, p < 0.01 compared to control group.)

To determine the potential impact of suppressing miR-33a in vivo, we then injected these GICs into nude mice to evaluate their ability of tumor initiation and progression. Consistent with the effect on the GICs in culture, antagonizing miR-33a function significantly slowed GBM progression in mice bearing intracranial xenograft tumors as shown in Figure 25A, 25B and Figure 26A, 26B. In another experimental setting, we sacrificed the mice from both the control and miR-33a knockdown group 30 days after intracranial implantation of GICs. Histological analysis by H&E staining revealed a significantly decelerated tumor progression in miR-33a knockdown group (Figure 25C and Figure 26C). In sum, these results demonstrate that miR-33a expression was critical for the ability of GICs to maintain their stemness in culture and to generate tumors in vivo.

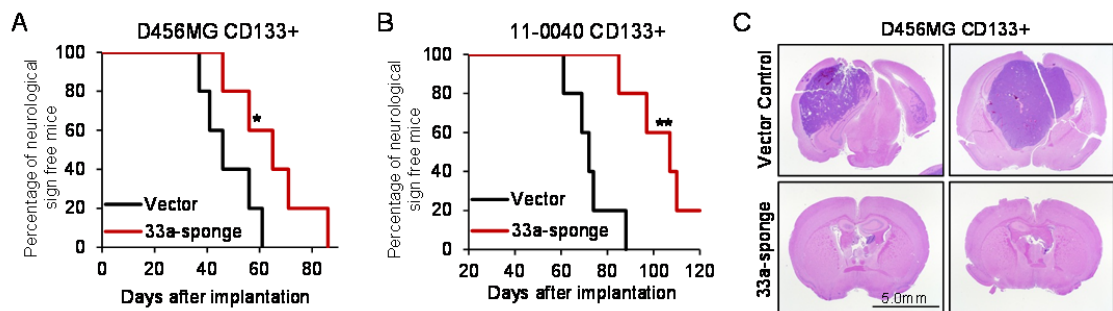


Figure 25: Antagonism of miR-33a by miR-33a sponge indicates miR-33a is required for tumor progression in GICs.

(A, B) Kaplan-Meier curves were drawn to measure the burden of tumor progression by D456MG and 11-0040 GICs expressing vector control or miR-33a sponge. 5,000 D456MG GICs and 10,000 11-0040 GICs were implanted respectively in each mouse. (C) Representative H&E staining of brain sections indicating intracranial tumors formed 30 days after inoculation of D456MG GICs expressing vector control or the miR-33a sponge. (* $p < 0.05$, ** $p < 0.01$ compared to control group.)

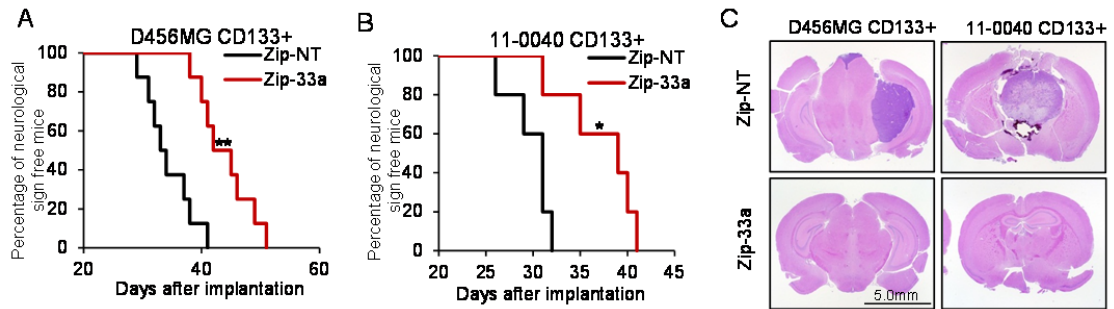


Figure 26: Antagonism of miR-33a by Zip-33a indicates miR-33a is required for tumor progression in GICs.

(A, B) Kaplan-Meier curve were shown to measure the tumor progression of D456MG and 11-0040 GICs expressing Zip-NT control or Zip-33a. The same procedure was used as described for Figure 25A and 25B. (C) Representative H&E staining of intracranial tumors of D456 MG and 11-0040 GICs expressing Zip-NT control and Zip-33a. (* $p < 0.05$, ** $p < 0.01$ compared to control group.)

3.2.3 Overexpression of miR-33a rendered non-GICs to behave like GICs

The effects of suppressing miR-33a in GICs on self-renewal and stemness prompted us to determine whether miR-33a is also sufficient to confer the stemness phenotype on non-GICs. To test this possibility, we introduced miR-33a into CD133-negative cells via a lentiviral vector that also expressed a GFP selection marker to allow isolation of transduced cells by FACS (Figure 27).

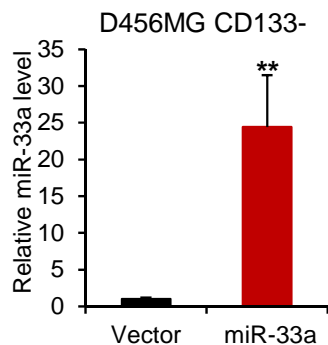


Figure 27: miR-33a level after primary miR-33a over-expression.

qRT-PCR analysis was performed to measure miR-33a level in CD133-negative D456MG cells expressing vector control and primary miR-33a. HRU6 was used as an internal control. (**p<0.01 compared to control group.)

Strikingly, miR-33a overexpressing cells displayed a significantly enhanced ability for neurosphere formation compared to control cells (Figure 28A, 28B), as well as a slight increase in growth rate (data not shown). Consistent with the increased capability for the formation of neurosphere, non-GICs overexpressing miR-33a also expressed higher levels of stemness associated genes, including Lin28, Oct4 and Nanog when the cells were grown in serum-free media (Figure 28C, 28D). Interestingly, the morphology of miR-33a-overexpressing cells was transformed to one with sphere-like cell-aggregates and less-attached to the culture dish, in sharp contrast to the control cells which displayed a dispersed morphology and attached normally to culture dish (Figure 28E). The most important criterion for the functionally defined GICs is their potent ability to initiate tumor formation in immune-compromised mice, so we next examined whether miR-33a could affect the tumor-initiating ability of the non-GICs. Indeed, the non-GICs with miR-33a overexpression formed much larger subcutaneous xenograft

tumors than the control cells (Figure 28F). Importantly, miR-33a-overexpressing cells gave rise to secondary tumors when they were serially passaged in nude mice, a hallmark for the GICs in such an experimental setting, whereas the control cells failed to do so (data not shown). Together these results indicate that non-GICs stably expressing miR-33a could display features closely resembling GICs as a consequence of reprogramming of those cells into a GIC-like state.

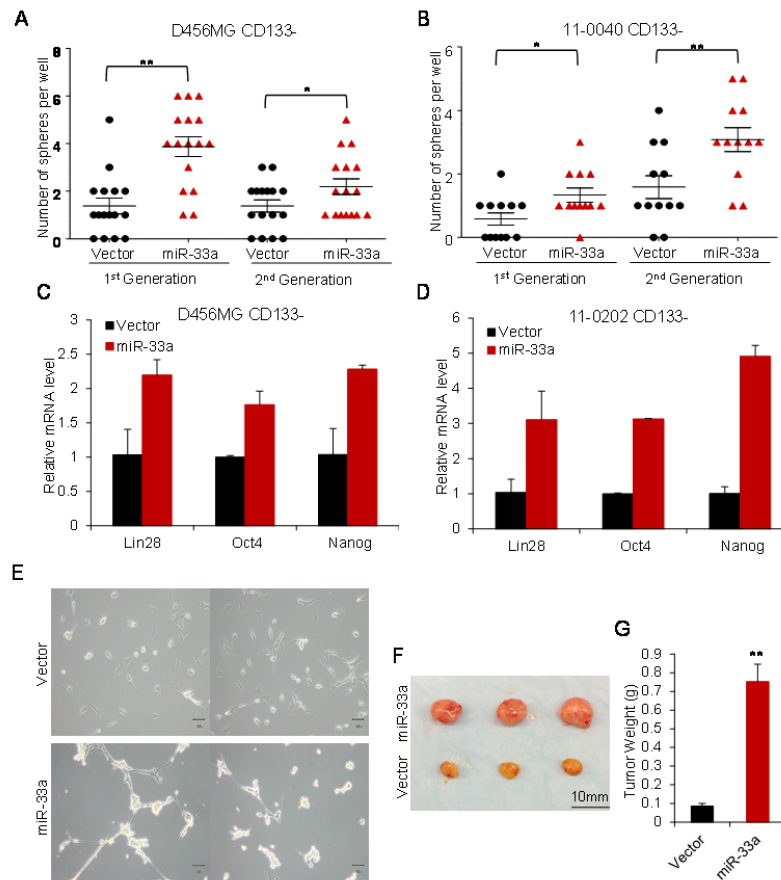


Figure 28: Overexpression of miR-33a in non-GICs promotes self-renewal and tumor progression.

(A, B) Neurosphere formation assay of CD133-negative D456MG and 11-0040 cells with miR-33a overexpression compared to vector control. 100 cells were plated per well in 24-well plates and the number of spheres was determined 7 days later. (C, D) qRT-PCR analysis was performed to determine the expression pattern of indicated stemness-associated genes in CD133-negative D456MG and 11-0202 (directly derived from patient specimen) glioma cells after miR-33a overexpression. Beta-actin was used as an internal control. (E) Representative pictures of CD133-negative D456MG cells with vector control or miR-33a overexpression. Upper panel shows pictures of cells with vector control and lower panel the pictures of cells with miR-33a overexpression. (F) Representative pictures of tumors formed by subcutaneously implanted CD133-negative D456MG cells expressing vector control or miR-33a. Tumor weights were measured and shown in (G). 10,000 CD133-negative D456MG cells were implanted into each mouse. (In Figure 28A and 28B, results are reported as the mean \pm standard deviation of the mean; * $p < 0.05$, ** $p < 0.01$ compared to control group.)

3.2.4 PDE8A and UVRAG are direct targets of miR-33a

Potent effects of miR-33a in maintaining the self-renewal of GICs and reprogramming non-GICs prompted us to explore the down-stream effectors of miR-33a. In an effort to determine the potential downstream mRNA targets regulated by miR-33a, we integrated mRNA expression profiling with bioinformatic predictions. Using microarray technology, we generated a list of down-regulated genes (0.8-fold threshold) in miR-33a-overexpressing D456MG cells. Overlapping this list with the candidate list produced by three prediction algorithms including PicTar, TargetScan and microRNA.org, we narrowed the miR-33a target candidates down to a total of 90 genes. We further verified the mRNA expression level of each candidate on this 90-gene list by qRT-PCR in non-GICs as defined by their CD133- status isolated from D456MG and 11-0040 cell lines overexpressing miR-33a. This round of screen yielded 18 putative mRNA candidates that were significantly and consistently down-regulated by miR-33a overexpression, which are listed in Table 3.

Table 3: Fold change of down-regulated genes in 11-0040 and D456MG CD133-negative cells with miR-33a overexpression compared to control.

Gene	11-0040 CD133-	D456MG CD133-
ABHD2	0.722	0.792
BACH1	0.547	0.390
CDR2	0.398	0.440
CPT1A	0.415	0.185
GALNT10	0.763	0.689
IRS1	0.953	0.556
KCNJ2	0.613	0.779
KCTD9	0.536	0.596
MAP4K5	0.566	0.436
NCAM1	0.616	0.160
PDE8A	0.785	0.501
PRDM10	0.664	0.537
SEMA6A	0.914	0.903
SERP-INF	0.904	0.841
SETD4	0.354	0.770
SNAI2	0.193	0.371
TMED5	0.707	0.975
UVRAG	0.688	0.487

To further narrow down these candidates that are most likely to be direct targets of miR-33a, we employed Ago-2 antibody to pull down RNAs associated with RNA-induced silencing complex (RISC) to identify mRNAs selectively enriched into RISC after miR-33a overexpression by qRT-PCR (Figure 29B). As an internal positive control, miR-33a incorporation into RISC was increased around 30-fold in miR-33a overexpression cells (Figure 29C). We then examined the 18 candidates and identified the mRNAs encoded by two genes, PED8A and UVRAG, with significantly elevated enrichment in miR-33a-overexpressing cells compared to the vector control group. In addition, we also measured several previously identified targets of miR-33a that were found to be regulated in the context of cholesterol homeostasis and fatty acid

metabolism, including ABCA1, ABCG1, CROT, CPT1A, PRKAA1, IRS1 and IRS2 (Davalos et al., 2011; Gerin et al., 2010; Rayner et al., 2010). Consistent with the results from our analyses on the metabolic profiling of cholesterol and fatty acid homeostasis in the glioma cells with or without overexpressing miR-33a that no significant differences were observed (data not shown), there were little or only modest increases in the level of those mRNAs incorporated into RISC as determined by this assay (Figure 29D). To determine whether the elevated levels of mRNA for PDE8A and UVRAG detected in the RISC co-IP correlated with decreased levels of their encoded protein products, we conducted Western blot analysis on cell lysates derived from both GICs and non-GICs isolated from two GBM xenograft tumor lines. As shown in Figure 29E, the protein levels of these two genes were indeed correlated directly with the status of miR-33a expression in those cells. To further explore whether these two genes represent direct targets of miR-33a, we conducted luciferase reporter assays to determine if the putative binding sites of miR-33a in the 3' UTR of PDE8A and UVRAG (Figure 30) are important for miR-33a-mediated suppression. Indeed, the luciferase reporter expression was repressed by miR-33a in a dose-dependent manner in 293T cells for both constructs (Figure 29F). Collectively, these data support the notion that PDE8A and UVRAG serve as direct targets of miR-33a in glioma cells.

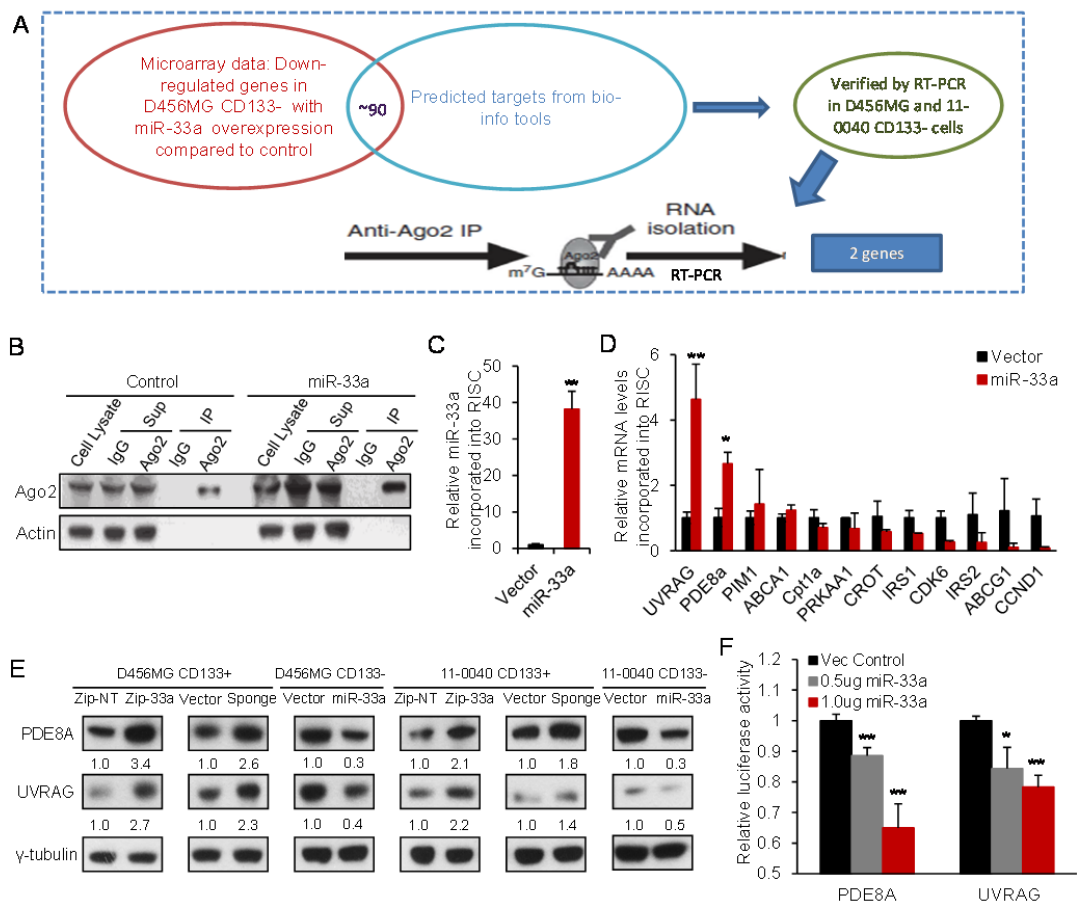


Figure 29: PDE8A and UVRAG are direct targets of miR-33a in glioma cells.

(A) An illustration of strategies to identify direct targets of miR-33a. (B) RNA-Ago2 immuno-precipitation using lysates from 11-0040 CD133-negative cells expressing the vector control or miR-33a as indicated. Beta-actin was used as the loading control. (C) qRT-PCR analysis was performed to measure miR-33a level incorporated into RISC in miR-33a overexpressing cells compared to that of the control. HRU6 was used as an internal control. (D) qRT-PCR analysis was performed to measure the level of indicated mRNAs incorporated into RISC derived from miR-33a overexpressing or vector control cells. Beta-actin was used as an internal control. (E) Immunoblots were performed to show PDE8A and UVRAG protein levels in D456MG and 11-0040 cells as indicated with repression (Zip or sponge as marked) or overexpression of miR-33a. Intensities of bands were quantified using Image J and Gamma-tubulin was used as internal control to calculate the fold-change. (F) Luciferase activity of the reporter construct containing the 3'-UTR of PDE8A or UVRAG was measured after co-transfection with control, 0.5 μ g and 1 μ g miR-33a expressing construct, respectively, in 293FT cells. (*, $p < 0.05$, **, $p < 0.01$ compared to control group.)

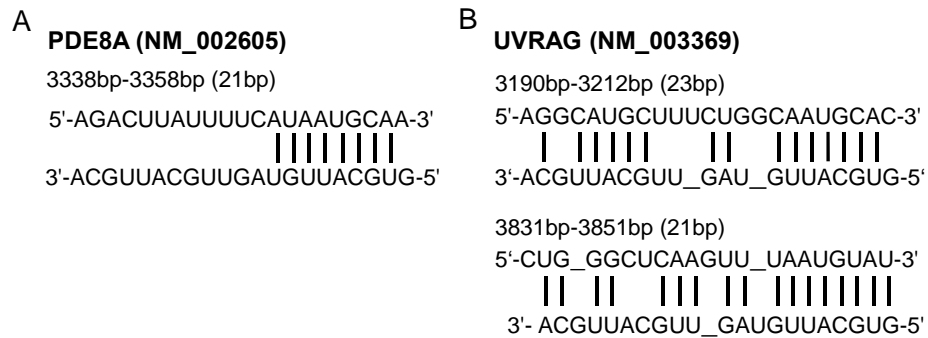


Figure 30: Predicted binding sites of miR-33a in the 3'UTR of PDE8A and UVRAG.

3.2.5 Repression of PDE8A and UVRAG expression is required for miR-33a to maintain the biological properties of GICs

Since both PDE8A and UVRAG have never been implicated to play roles in GBM progression, we first tested the effect of overexpressing these two genes in GICs, respectively (Figure 31A). Consistent with their status as targets of miR-33a, their overexpression could recapitulate phenotypes of miR-33a knockdown in GICs as demonstrated by the compromised neurosphere formation and proliferation in culture, and tumor progression in vivo (Figure 31B-31E).

Next, we used a lentiviral system to deliver short-hairpin RNA to stably knockdown the expression level of PDE8A and UVRAG individually in non-GICs (Figure 32A) and examined if either of them could enhance the ability of non-GICs to adapt a phenotype associated with GICs.

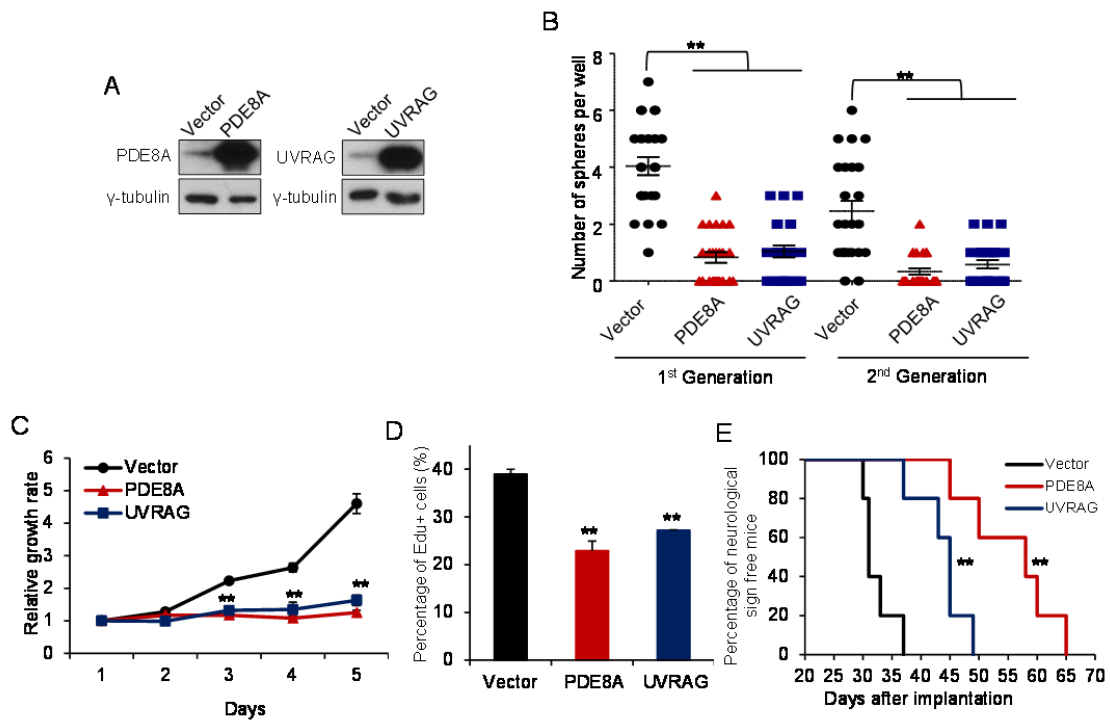


Figure 31: Overexpression of PDE8A and UVRAG compromised self-renewal and tumor formation capabilities of GICs.

(A) Immunoblots were performed to verify the ectopic expression of PDE8A and UVRAG in D456MG GICs. Gamma-tubulin was used as internal control. (B) Neurosphere formation assays were performed in D456MG GICs expressing vector control, PDE8A and UVRAG. 50 cells were plated in each well of 24-well plate, and number of spheres was counted 7 days later. (C) Growth rate of D456MG GICs expressing vector control, PDE8A and UVRAG were measured by cell titer assay. (D) 10 μ M EdU was incubated with cells for two hours and incorporation rate was measured in D456MG GICs expressing vector control, PDE8A and UVRAG. (E) Kaplan-Meier curve were shown to measure the progression of tumors derived from D456MG GICs expressing vector control, PDE8A and UVRAG. 5,000 D456MG GICs were implanted in each mouse. (In Figure 31B, results are reported as the mean \pm standard deviation of the mean; **p < 0.01 compared to control group.)

As shown in Figure 32B, 32C, reducing the expression of either PDE8A or UVRAG could significantly augment the ability of non-GICs to form neurosphere and modestly increase their growth rate. Consistent with the change in their behavior to

resemble that of the GICs, expression of several stemness markers was induced in non-GICs following the knockdown of PDE8A or UVRAG (Figure 32D).

To further determine whether the observed phenotypic properties of GICs are attributed to the suppression of PDE8A and UVRAG by miR-33a, we tested if reducing the expression of either PDE8A or UVRAG could have an impact on the ability of GICs to form neurosphere when miR-33a is repressed. Consistent with the notion that both genes act as critical effectors downstream from miR-33a, GICs with co-suppression of miR-33a and either of its targets showed enhanced neurosphere formation and self-renewal ability compared to GICs bearing a scramble control shRNA for PDE8A or UVRAG and the miR-33a-sponge (Figure 32E), indicating that miR-33a functions to control the biological property of GICs at least partially through repressing its direct targets PDE8A and UVRAG.

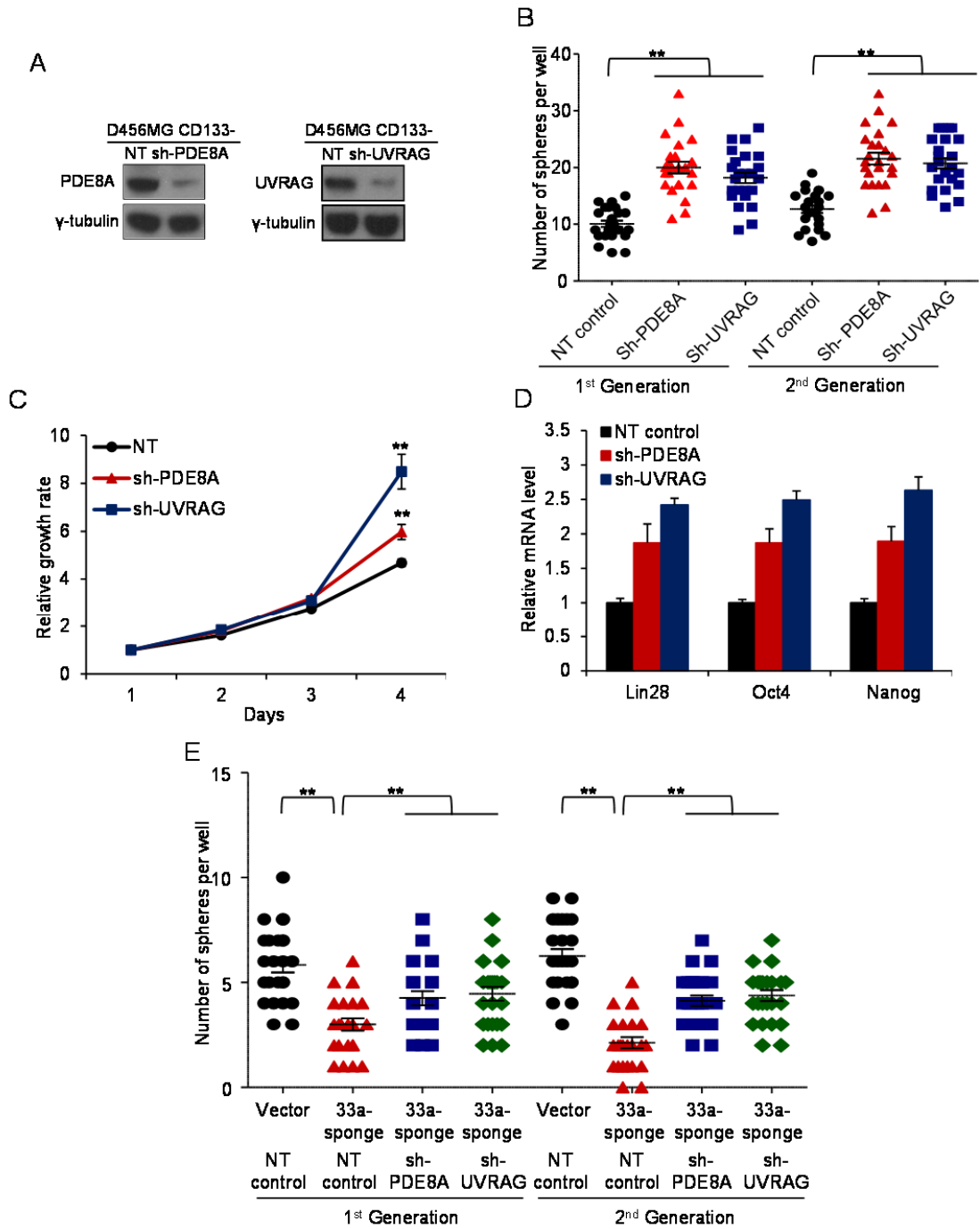


Figure 32: Repression of PDE8A and UVRAG expression is required for the function of miR-33a in glioma cells.

(A) Protein levels of PDE8A and UVRAG were measured by immunoblots in shRNA-mediated knockdown of the two genes in CD133-negative D456MG cells. Gamma-tubulin was used as internal control. (B) Neurosphere formation assays were performed in CD133-negative D456MG cells with PDE8A or UVRAG knockdown, respectively. 100 cells were plated in each well of 24-well plates at the start of the experiments, and number of spheres per well was determined 7 days later. (C) Growth rate of CD133-negative D456MG cells with PDE8A and UVRAG knockdown or vector control was measured by cell titer assay. (D) qRT-PCR analysis was performed to determine the expression levels of stemness-associated genes in CD133-negative D456MG cells with PDE8A and UVRAG knockdown or scramble control. Beta-actin was used as an internal control. (E) Neurosphere formation assays were performed in D456MG GICs expressing miR-33a sponge or vector control with stable PDE8A and UVRAG knockdown or scramble control as indicated. The assays were performed as described for B. (In Figure 32B and 32E, results are reported as the mean \pm standard deviation of the mean; * $p < 0.05$, ** $p < 0.01$ compared to control group.)

3.2.6 Both PKA and Notch signaling pathways are required by miR-33a to maintain the biological properties of GICs

Functional validation of PDE8A and UVRAG as critical effectors for miR-33a in GICs prompted us to explore how these two genes could mediate the function of miR-33a to control the biological properties of GICs. PDE8A belongs to a family of phosphohydrolyases and PDE8 subfamily, which selectively catalyze the hydrolysis of 3' cyclic phosphate bonds in adenosine monophosphate (cAMP) (Fisher et al., 1998). This enzyme could regulate the cellular level of cAMP by controlling its degradation rate. We reasoned that the level of PDE8A could directly modulate the activity of protein kinase A (PKA) pathway, which depends on cellular cAMP for its activation (Sands and Palmer, 2008; Skalhegg and Tasken, 1997). To test this possibility, we examined the functional status of a canonical downstream effector of the PKA pathway, phosphorylated CREB (p-CREB) (Sands and Palmer, 2008) in GICs overexpressing

PDE8A and observed a decreased level of p-CREB (Figure 33A). Conversely, knocking down the expression level of PDE8A in non-GICs increased the level of p-CREB (Figure 33B). Consistently, we also observed reduced level of p-CREB after miR-33a knockdown in GICs and elevated level of p-CREB after miR-33a overexpression in non-GICs (Figure 33C), which indicated that miR-33a might promote self-renewal of GIC through increasing PKA activity. Since the PKA pathway has never been implicated to play a role in stem cell biology, we further tested the functional relevance of PKA pathway in GICs by utilizing a small molecule inhibitor of PKA, KT5720 to treat GICs. As expected, 2 μ M KT5720 treatment efficiently blocked CREB phosphorylation in GICs (Figure 33D) while caused no observable acute toxicity to the cells. Importantly, KT5720 could significantly reduce neurosphere formation and growth rate, and suppress the expression of stemness markers in GICs grown in culture (Figure 33E-33G), but only slightly repressed cell proliferation (Figure 33H). Taken together, these data strongly suggest that miR-33a promotes self-renewal of GICs by repressing its direct target PDE8A to enhance the activity of the PKA pathway.

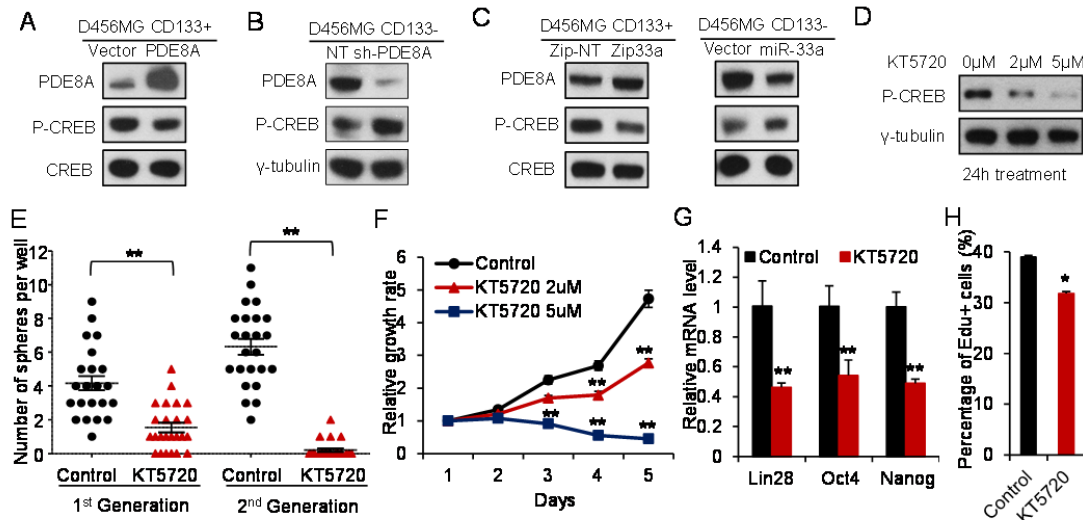


Figure 33: PDE8A regulates GIC self-renewal through the PKA pathway.

(A, B) Immunoblots were performed to show phosphorylated CREB (p-CREB) in PDE8A over-expressing and PDE8A knockdown D456MG cells. Gamma-tubulin was used as internal control. (C) Immunoblots were performed to show levels of p-CREB in D456MG cells with miR-33a reduction or overexpression, respectively. Gamma-tubulin was used as internal control. (D) Immunoblots were performed to show p-CREB levels after 24 hours treatment of 2 μ M and 5 μ M KT5720 in D456MG GICs. Gamma-tubulin was used as internal control. (E) Neurosphere formation assays were performed in D456MG GICs incubated with 2 μ M KT5720 or vehicle control. 50 cells were plated in each well of 24-well plates and the number of spheres counted 7 days later. (F) Growth rate of D456MG GICs incubated with 0 μ M, 2 μ M and 5 μ M KT5720 was measured by cell titer assay. (G) qRT-PCR analysis was performed to determine levels of stemness-associated genes in D456MG GICs after 2 μ M KT5720 treatment for 48 hours. Beta-actin was used as internal control. (H) EdU incorporation assay was performed to measure proliferation rate in GICs treated with 2 μ M KT5720 after 24 hours compared to vehicle control. (In Figure 33E, results are reported as the mean \pm standard deviation of the mean; *, $p < 0.05$; **, $p < 0.01$ compared to control group)

UVRAG (UV radiation Resistance Associated Gene), the other target of miR-33a, has been reported to regulate autophagy (Liang et al., 2007) and chromosome stability (Knaevelsrud et al., 2010; Zhao et al., 2012), and act as a tumor suppressor because allelic mutation of UVRAG was found at high frequency in human colon cancers and its

ectopic expression in a colon cancer cell line resulted in decreased proliferation and xenograft tumor formation (Liang et al., 2006). A separate report suggested that UVRAG could mediate Notch endocytosis to attenuate Notch signaling in regulating the organ rotation during development in *Drosophila* (Lee et al., 2011). Thus, the functional role of UVRAG in the context of stem cell biology is largely unknown, which prompted us to examine whether it represents a link between miR-33a and Notch signaling, since Notch has been shown previously to be critical for GIC self-renewal and resistance to radiotherapy (Wang et al., 2010). In GICs overexpressing UVRAG, we observed a decreased level of Notch intracellular domain (NICD), which is the cleaved and active domain of Notch (Figure 34A). Conversely, knocking down the expression of UVRAG led to an increased NICD level in non-GICs (Figure 34B), suggesting that UVRAG acts as an antagonist of the Notch pathway. Importantly, repressing miR-33a function also reduced NICD level in GICs, indicating suppressed activity of Notch pathway; on the other hand, overexpression of miR-33a in non-GICs promoted the activity of Notch pathway as indicated by an increase in the level of NICD (Figure 34C). Employing a different approach to antagonize Notch signaling, we added DPAT, a gamma-secretase inhibitor, to the GICs and found the self-renewal of those cells to be significantly suppressed (Figure 34D), but with only a modest effect on the growth rate of the same cells (Figure 34E). Thus, the Notch antagonist DPAT acted in the same manner as the overexpression of UVRAG, which countered the reported Notch function in supporting

GIC self-renewal. We also took advantage of the availability of these small molecule inhibitors to assess the combinational effect of simultaneously blocking PKA and Notch pathways by adding KT5720 and DAPT together to the GICs. As shown in Figure 34F, the growth of GICs was dramatically inhibited by the combined action of these two inhibitors in comparison to the addition of KT5720 or DAPT separately.

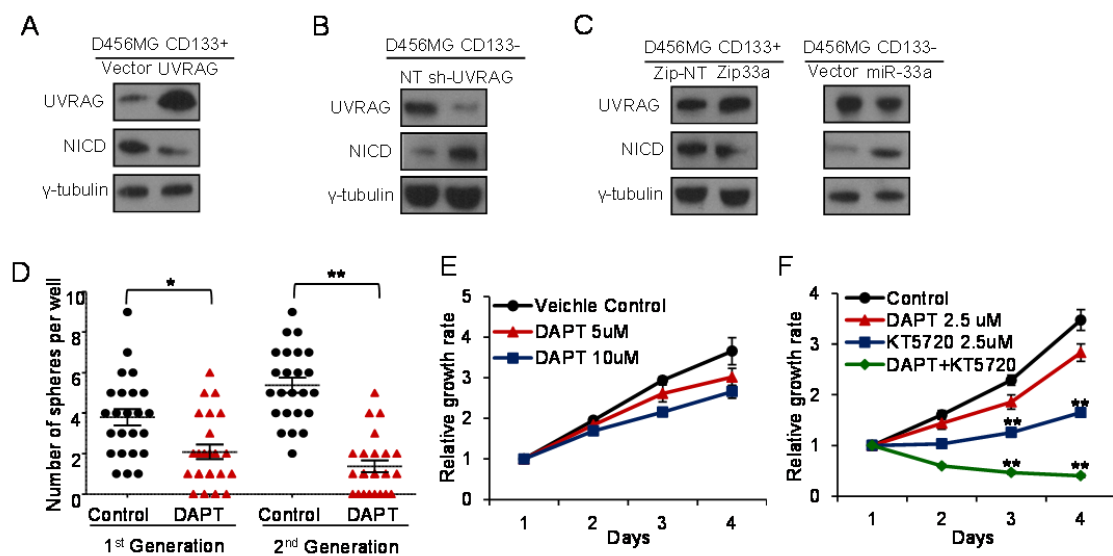


Figure 34: UVRAG regulates GIC self-renewal through Notch pathway.

(A, B) Immunoblots were performed to show Notch intracellular domain (NICD) levels in D456MG cells with UVRAG overexpression or knockdown. (C) Immunoblots were performed to show NICD levels in D456MG cells with miR-33a suppression or overexpression. (D) Neurosphere formation assays were performed in D456MG GICs incubated with 10 μ M DAPT or vehicle control. 50 cells were plated in each well of 24-well plates and number of spheres counted 7 days later. (E) Growth rate of D456MG GICs incubated with 0 μ M, 5 μ M and 10 μ M DAPT was measured by cell titer assay. (F) Growth rate of D456MG GICs incubated with vehicle control, 2.5 μ M DAPT, 2.5 μ M KT5720, or the combination of these two inhibitors was measured by cell titer assay. (In Figure 34D, results are reported as the mean \pm standard deviation of the mean; *, $p < 0.05$; **, $p < 0.01$ compared to control group.)

Together these results strongly suggest that the two independent pathways, PKA and Notch, act cooperatively as effectors of the master determinant miR-33a to positively regulate the biological properties of the GICs.

3.2.7 Targeting miR-33a by a LNA inhibitor suppressed tumor formation in vivo

Since our functional assays have demonstrated the indispensability of miR-33a in maintaining the biological properties of GICs and GIC-derived GBM progression, we tested whether blocking miR-33a activity could have potential therapeutic value. To achieve this goal, we employed modified small RNA inhibitor (Locked Nucleic Acid, LNA) of miR-33a to treat nude mice bearing subcutaneous glioma xenograft. Following a regiment of administering the inhibitor every other day for up to 30-35 days, the mice were sacrificed and tumors removed for analysis. As displayed in Figure 35, in comparison to the control groups, treatment with the miR-33a-LNA caused significant decreases in the growth rates and weights of tumors inoculated with GICs derived from two xenografted glioma lines. The results of these proof-of-concept experiments lend further support to our conclusion that miR-33a is critical for GBM tumor progression and targeting miR-33a using microRNA-antagonizing reagents could be a potentially effective therapeutic against GBM in the future.

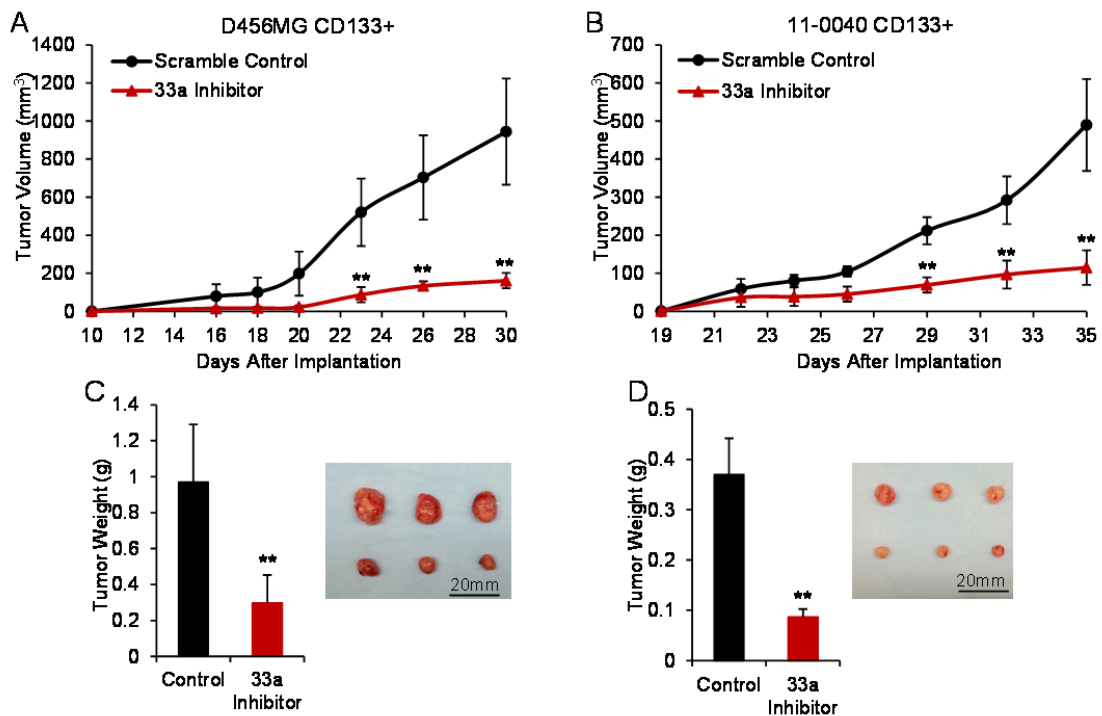


Figure 35: Treatment with a miR-33a LNA inhibitor suppressed tumor growth in vivo. (A, B) 100,000 D456MG or 11-0040 glioma cells were implanted subcutaneously into nude mice. Treatment was started 10 days and 19 days after implantation of the two tumor lines, respectively. 5 μ g LNA scramble control or miR-33a inhibitor was injected intratumorally into each subcutaneous tumor every other day. Tumor volumes were measured by a Vernier Caliper in the indicated days. (C, D) Subcutaneous tumors derived from D456MG and 11-0040 glioma cells in the control and miR-33a LNA inhibitor treated group were weighted immediately after tumors were harvested. Pictures of subcutaneous tumors were displayed. (**, $p < 0.01$ compared to control group.)

3.3 Material and Methods

3.3.1 Isolation of GICs and Non-GICs from patient specimen and mice xenografts

Patient specimens were collected from Duke Brain Tumor Center during 2011 to 2012. Patients provided informed consent under a protocol approved by the Duke University Institutional Review Board. Fresh patient specimens were dissociated by

Papain Dissociation System (Worthington Biochemical) according to the manufacturer's instructions. GICs were enriched by culturing cells in Neurobasal media (Invitrogen) supplemented with B27 without Vitamin A (Invitrogen), L-glutamine (Invitrogen), sodium pyruvate (Invitrogen), 10 ng/ml bFGF, and 10 ng/ml EGF (Millipore); non-GICs cells were cultured in Improved MEM Zinc Option (Invitrogen) with 10% FBS. Human D456MG cell line or primary patient specimens were passaged short term in immune-compromised athymic BALB/c nu/nu mice as subcutaneous xenografts in accordance with a Duke University Institutional Animal Care and Use Committee approved protocol and cells were yield by dissociation of xenografts as described above. To enrich GICs by CD133, cells were separated by microbead-conjugated CD133 antibodies and magnetic columns (Miltenyi Biotec). CD133-positive cells were designated as GICs and cultured in Neurobasal media described above; CD133-negative cells were designated as non-GICs and cultured in Improved MEM Zinc Option with 10% FBS. Before experiments non-GICs were cultured in Neurobasal media for at least 12 hours so experiments were performed in identical media.

3.3.2 miRNA Profiling

Total RNA was prepared using the mirVana™ miRNA Isolation Kit (Ambion). And miRNA was reverse transcribed into cDNA by RT2 miRNA First Strand Kit (Qiagen) and profiling was performed using RT2 miRNA PCR Array (Qiagen), which simultaneously profiled 88 different human miRNAs with potential roles in self-renewal

and differentiation. Human small nuclear U6 RNA was amplified as a normalization control. The profiling and analysis was performed using a Mastercycler® Realplex system (Eppendorf).

3.3.3 Plasmids

miR-33a sponge containing five repeats of anti-sense miR-33a (TGCAAT GCAACTACAATGCAC) was synthesized by GenScript and cloned into pWPXLD vector (Addgene plasmid 12258) . Zip-NT and Zip-33a plasmids were purchased from System Biosciences. Primary miR-33a was cloned into pWPXLD vector to overexpress miR-33a. PDE8A and UVRAG cDNA were cloned into pLenti vector (Addgene plasmid 19068) (Campeau et al., 2009) to overexpress these two genes. All these vectors were co-transfected with the packaging vectors psPAX2 and pCI-VSVG into 293T cells by Lipofectamine 2000 (Invitrogen) to produce virus. Virus-infected GICs or differentiated glioma cells were selected by GFP marker or puromycin (1ug/ml) according to the plasmids used for infection.

3.3.4 Cell Culture

GICs were cultured in Neurobasal media (Invitrogen) supplemented with B27 without Vitamin A (Invitrogen), L-glutamine (Invitrogen), sodium pyruvate (Invitrogen), 10 ng/ml bFGF, and 10 ng/ml EGF (Millipore); differentiated cells were cultured in Improved MEM Zinc Option (Invitrogen) with 10% FBS. 293T cells were

cultured in DMEM (Mediatech) with 10% FBS. All cells were cultured in a 5% CO₂ incubator at 37°C.

3.3.5 Neurosphere Formation Assay

GICs or non-GICs with indicated modification or treatment were plated in 24-well plates at indicated cell number per well by flow cytometry with 1ml Neurobasal media supplemented with B27 without Vitamin A, L-glutamine, sodium pyruvate, 10 ng/ml bFGF, and 10 ng/ml EGF. After 7-10 days, the number of neurospheres in each well was quantified. Then spheres were dissociated to single cells and plated again in 24-well plates at indicated cell number per well by flow cytometry to form 2nd generation of neurospheres.

3.3.6 Cell Viability Assay

Cells with indicated modification or treatment were plated in white with clear bottom 96-well plates (Costar) at 2000 cells per well. Plates were examined every 24 hours by Cell Titer-Glo® Luminescent Cell Viability Assay kit (Promega). Results are reported from at least triplicate samples as the mean ± standard deviation.

3.3.7 Cell Proliferation Assay

Proliferation rates were determined using Click-iT® EdU Alexa Fluor® 647 Flow Cytometry Assay Kit (Invitrogen) according to the manufacturer's instructions. Briefly, cells were incubated with 10µM EdU for two hours, fixed and processed. Analyses were

done using flow cytometry. Results are reported from at least triplicate samples as the mean \pm standard deviation.

3.3.8 Quantitative Real-Time PCR

Total RNA was prepared using the mirVanaTM miRNA isolation Kit (Ambion). To measure messenger RNA, total RNA was reverse transcribed into cDNA using iScript cDNA synthesis kit (BioRad) and mRNA levels were measured using specific primers (sequences were shown in Table 4) with SYBR Green (Qiagen) and a Mastercycler[®] Realplex system (Eppendorf). To measure miRNA, total RNA was reverse transcribed into cDNA by miScript RT Kit (Qiagen). Specific miRNA levels were measured by miScript primers (Qiagen) with the miScript SYBR Green PCR Kit (Qiagen).

Table 4: Primer sequences for qRT-PCR

<i>Gene</i>	Forward primer	Reverse primer
Beta-actin	CATCCACGAAACTACCTTCAACTCC	GAGCCGCCGATCCACACG
Lin28A	TGTAAGTGGTTCAACGTGCG	CCTCACCTCCTTCAAGCTC
Oct-4	CATAGTCGCTGCTTGATCGCTTG	GAGAACCGAGTGAGAGGCAACC
Nanog	GATTTGTGGCCTGAAGAAA	TTGGGACTGGTGAAGAATC
UVRAG	TCCAAAAGGAGGGGAGAAGT	TGAAGTTTTTCAGGTTGGGAA
PDE8A	CCTCTTGGAGTCGGAGCTT	CCCTGCAGAATCCATTACATT
Pim1	CGGGAAGCTGGAGACAGAAG	CCCAGCAAATAGCAGCCTTT
ABCA1	GACGCAAACACAAAAGTGGA	AACAAGCCATGTTCCCTCAG
Cpt1a	TGCTTTACAGGCGCAAAGT	GCAGATGTGTCAGGACCGAGT
PRKAA1	TCCTACCACATCAAGGCTCC	TACATTCTGGGTGACACGCT
CROT	TGTTACCACAGGGATACAAGCCT	TACCTTGGCCTCCCACCGTGCTAA
IRS1	GCTCAACTGGACATCACAGC	AATGGATGCATCGTACCATCT
CDK6	CTGAATGCTCTTGCTCCTTT	AAAGTTTTGGTGGTCCTTGA
IRS2	ACCTCAGTTCAAGGTAAAGCCGGA	AGGTACCTGCACTGGAATCCAACA
ABCG1	CAGGAAGATTAGACTGTGG	GAAAGGGGAATGGAGAGAAGA
CCND1	ACGAAGGTCTGCGCGTGTT	CCGCTGGCCATGAACTACCT

3.3.9 Intracranial tumor assay

GICs with indicated cell number were implanted into the left or right frontal lobes of athymic BALB/c nu/nu mice under a Duke University Institutional Animal Care and Use Committee approved protocol. Mice were maintained for 120 days or until the development of neurologic symptoms. Brains of euthanized mice were collected, fixed in formalin, paraffin embedded, and sectioned for H&E staining.

3.3.10 Isolation of RISC-associated RNA

Following a previously published procedure (Chi et al., 2009). Ten million 11-0040 CD133-negative cells with miR-33a overexpression or vector control were lysed in 750 μ l 1xPXL buffer (1xPBS with 0.1% SDS, 0.5% Sodium deoxycholate and 0.5% NP-40 substitute) with proteinase inhibitor (Sigma, P2714) and 0.3U/ μ l SUPERase•In™ RNase Inhibitor (Life Technologies). Lysates were cleared by centrifugation at 13,000rpm for 15 minutes. For each sample, 50 μ l Dynabeads® Protein A (Invitrogen) was incubate with 15 μ g Rabbit anti-mouse IgG (Jackson Immunoresearch) for 45 min at room temperature, then washed with 500 μ l 1xPBS for 3 times. Then 15 μ l Anti-pan Ago, clone 2A8 antibody (Millipore) or same amount of mouse IgG (Jackson ImmunoResearch) was added to the beads for two hours at 4°C. Beads were washed twice with 500 μ l 1xPXL and cell lysate were added and incubated for another two hours at 4°C. All IP samples were washed three times with 500 μ l 1xPXL buffer. The immunoprecipitated RNA was released by proteinase K digestion and extracted by phenol/chloroform/isopropyl alcohol. RNA was pelleted by ethanol precipitation with glycogen, resolved and treated with DNase I (NEB).

3.3.11 Immunoblots and Antibodies

Quantified protein lysates were resolved on Novex SDS-PAGE (Invitrogen), transferred onto PVDF membrane (Millipore, Billerica, MA) and probed with rabbit anti-human PDE8A (1:1000; Abcam), rabbit anti-human UVRAG (1:500; Cell Signaling),

rabbit anti-human p-CREB(1:1000; Cell Signaling), rabbit anti-human CREB (1:1000; Cell Signaling), rabbit anti-human NICD (1:1000; Cell Signaling) and mouse anti-human Gamma-tubulin (1:10000; Sigma) followed by incubation with secondary HRP-conjugated antibodies (1:5000; Invitrogen).

3.3.12 Luciferase Reporter Assay

3'UTR of PDE8A (916bp, Forward primer: GACGCTAGCTGGGAGACACCACCCAGAGCCC; Reverse primer: GACGTCGACTGTTAAGTCCTAAC TTTTCTTT) and UVRAG (1060bp, Forward primer: GACGCTAGCGTTCCATCTCTTCTAAC CAGCC; Reverse primer: GACGTCGACCCACCCACACTGACTCCAAAAT) containing the predicted binding sites of miR-33a was cloned into NheI and SalI sites of a firefly luciferase reporter of pmirGLO (Promega). For the luciferase assay, 293T cells were co-transfected with 0.1 µg of firefly luciferase constructs and 0 µg, 0.5 µg or 1µg of miR-33a over-expressing plasmid respectively with 1 µg, 0.5 µg and 0 µg empty vector plasmid. And 50ng pRL-TK Renilla luciferase plasmid (Promega) was co-transfected as an internal control. Two days after transfection, firefly and Renilla luciferase activities were measured using the Dual-Luciferase Reporter Assay (Promega). The results were normalized as relative luciferase activity (firefly luciferase/Renilla luciferase) and reported from at least triplicate samples as the mean ± standard deviation.

3.3.13 Lentiviral mediated shRNA targeting

Lentiviral shRNA clones (Sigma Mission RNAi) targeting PDE8A, UVRAG and scramble control (SHC002) were purchased from Sigma. Detailed information of shRNA constructs are provided in Table 5. These vectors were co-transfected with the packaging vectors psPAX2 and pCI-VSVG into 293T cells by Lipofectamine 2000 (Invitrogen) to produce virus.

Table 5: Information of shRNA clones targeting PDE8A and UVRAG

Name of constructs	TRC number	Clone ID	Sequence
sh-PDE8A	TRCN0000301061	NM_002605.2-1335s21c1	CCGGCCGGATACATTCCATGA CAATCTCGAGATTGTCATGGA ATGTATCCGGTTTTTG
Sh-UVRAG	TRCN0000368916	NM_003369.3-2403s21c1	CCGGACTTAACCCTTTGTGAT AATGCTCGAGCATTATCACAA AGGGTTAAGTTTTTG

3.3.14 LNA miR-33a inhibitor treatment

LNA miR-33a inhibitor (TGCAACTACAATGCA) and a LNA scramble control (ACGTCTATACGCCCA) were synthesized by Exiqon. Subcutaneous transplantation of glioma cells into athymic BALB/c nu/nu mice was performed in accordance with a Duke University Institutional Animal Care and Use Committee approved protocol. After subcutaneous tumors were visible by naked eye, mice were randomized into 2 groups for treatment: scramble control and miR-33a inhibitor. Mice were treated with 10mg/kg LNA oligonucleotide packaged with MaxSuppressor™ In vivo RNA-LANCER II (Bioo Scientific) intratumorally every two days. At the same time tumor sizes were measured every two or three days by calipers, and tumor volumes were calculated as Volume

(mm³) = L × W² × 0.5 until tumors were harvested and weighted immediately after sacrificing the mice.

3.3.15 Statistical Analysis

Results are reported as the mean ± standard deviation if not specifically indicated. Significance was tested by two-way student t-test using GraphPad Prism software. Significance of Kaplan Meier curves was tested by Log-rank (Mantel-Cox) test using GraphPad Prism software.

3.4 Discussion

3.4.1 A microRNA acting as a “master determinant” of glioma cell identity

Almost a decade has passed since the discovery of GICs or glioma stem cells among the heterogeneous population of tumor cells within the GBM tumor mass using the cell surface marker CD133. Subsequently it became clear that glioma cells without the expression of CD133 could also possess the same properties defined functionally to be associated with GICs, as GICs could be enriched via culturing the glioma cells dispersed from tumor mass under special conditions. Although lingering doubts persist regarding the importance or even existence of GICs in the context of GBM, extensive research has been done to demonstrate their critical roles in GBM initiation, progression, and recurrence associated with resistance to radio- and chemotherapy. However, almost all of those studies have centered on the biological properties of the GICs, without

providing much information on the features of their counterparts within the tumor mass, namely those non-GICs, probably due to the technical difficulty in separating all the GICs from the rest of tumor cell population. To fill this significant gap in our knowledge on the molecular basis that distinguishes GICs from non-GICs, we have in the present study focused on the identification and functional characterization of the signaling network that controls the identity of GICs. To this end, we have generated compelling evidence to support the notion that a single microRNA, miR-33a, sits at the center of the signaling network since changes in its expression pattern could drastically alter the biological properties of GICs and non-GICs. The higher level of miR-33a expression in GICs appears to be required to maintain the primary biological features of those cells, including self-renewal, stemness and tumor initiation *in vivo*, likely through its ability to induce pluripotent transcription factors Lin28, Oct4 and Nanog. In other words, the pluripotent-like characteristics displayed by GICs could therefore be at least partially attributed to the up-regulation of miR-33a. Moreover, we have provided evidence that miR-33a possesses the capability to reprogram non-GICs with differentiated features to resemble GIC-like status. Although miRNAs have been found to regulate many biological processes, the power of a single miRNA to control the fate or identity of glioma cells is almost unprecedented, as we could find only one example in the literature that the miR-302/367 cluster could reprogram fibroblasts into iPS cells (Anokye-Danso et al., 2011). In a broad sense, miR-33a together with the miR-302/367

cluster appear to belong to an elite group of miRNAs that can function as “master determinant” for controlling signaling network associated with determination of cell fate/identity.

3.4.2 The requirement of activities from two pathways to maintain the properties of GICs

Because of their potential to target multiple genes, miRNAs are believed to exert their regulatory effects on specific biological processes through fine-tuning the activities of multiple signaling pathways or network. In this case, it was not surprising that we have identified at least two downstream effectors, PDE8A and UVRAG, that both serve as direct targets for miR-33a to regulate the activities of two major signaling pathways in GICs. While the Notch pathway has been reported to be important for GIC maintenance and tumor initiation, our finding is the first demonstration on the critical role for UVRAG in suppressing the self-renewal program of GICs as an antagonist of Notch through its regulation of Notch endocytosis. Moreover, this finding has also provided an alternative explanation for UVRAG to be defined as a tumor suppressor in the context of cancer, since we did not observe any changes in the autophagy activity in glioma cells when UVRAG expression was altered (data not shown). In contrast to the Notch pathway, virtually nothing is known about the function of cAMP/PKA pathway in cancer stem cell regulation until we revealed here the critical role of PDE8A as a potent negative regulator of the biological properties of GICs. Although we have shown that inhibiting PDE8A expression by miR-33a significantly enhanced PKA activity, as

measured by the phosphorylation of its known substrate CREB transcription factor, the exact activities of the cAMP/PKA at the mechanistic level in regulating GIC function remain to be further investigated.

The findings that miR-33a represses both PDE8A and UVRAG to enhance the activities of the cAMP/PKA and Notch pathways exemplify how microRNAs, which often have only mild to modest repressive effect on single target genes, could produce dramatic biological outcomes. The widespread distribution of their targeting sequences throughout the genome has predetermined the unique mechanism of their working mode, which is to orchestrate modest changes in the expression pattern of groups of genes to produce convergent effects from multiple pathways or signaling network. This notion is clearly demonstrated by the additive effects of the combined actions of inhibitors for both PKA and Notch pathways in blocking the growth of GICs.

3.4.3 A potential therapeutic avenue for GBM

A rapidly growing body of evidence has shown miRNAs as potential targets for cancer therapy. For example, overexpression of miR-26 by adeno-associated virus in a MYC-driven liver cancer model can attenuate tumor formation (Kota et al., 2009); inhibition of miR-10b by delivery of miRNA antagonists does not block primary tumor growth but can attenuate breast cancer metastasis in animal models (Ma et al., 2010a). The molecular nature of microRNA offers extraordinary target specificity for miRNA-based therapeutic development. Chemically locked miRNA mimetics, by avoiding the

risk of introducing foreign DNA molecules into the body, provide extra safety and stability in vivo when developed as potential anti-cancer drugs. In our study, LNA inhibitor of miR-33a was able to block tumor progression in a xenograft model, providing a promising approach to combat malignant glioma, particularly those driven by GICs. Although systemic delivery of LNA inhibitors into the brain crossing the blood-brain barrier remains to be challenging, the striking inhibitory effect of miR-33a antagonist on the growth of subcutaneous tumor strongly suggests that further efforts toward development of anti-miR-33a-based therapeutics is fully warranted.

4. Conclusions and Future Directions

4.1 Conclusion

Recent study of TICs within glioblastoma has led to the characterization of this distinct neoplastic subpopulation. These GICs display malignant characteristics, including persistent self-renewal, sustained proliferation, resistance to radio- and chemotherapy, and capacity to potently initiate tumors in xenograft transplantation.

My thesis study first investigated the role of IL6-Stat3 pathway in supporting some of these pivotal GIC-specific behaviors. My data demonstrated an important role for IL6-Stat3 signaling in GIC growth and survival. Furthermore, targeting of IL6 with antibody increased tumor latency in mice bearing human glioma xenografts, suggesting that IL6 is a novel GIC directed therapeutic target.

In the second part of my thesis, I screened 88 miRNAs and focused on miR-33a to explore its function as an onco-mir in GICs. I identified microRNA-33a as a master determinant whose expression is dispensable for GIC self-renewal and the functional differences between GIC and non-GICs. Antagonizing miR-33a in GICs led to reduced self-renewal and tumor progression in immune-compromised mice, whereas overexpression of miR-33a in non-GICs rendered them to display features associated with GICs. Mechanistically, miR-33a acts to confer the biological property of GICs via enhancing the activities of cAMP/PKA pathway and Notch signaling by targeting negative regulators of these two pathways. Together these findings reveal a miR-33a-

centered signaling network that dictates the identity/activity of GICs and consequently serves as a therapeutic target for the treatment of GBM.

4.2 Future Direction

I focused my studies on the distinctive properties of GICs and developed strategies to target this specific population for future therapeutic application. While anti-GIC therapies might ultimately become a critical component of therapeutic regimens for malignant brain tumors, it is not realistic to expect that mono-therapy targeting GICs will effectively treat the tumor as a whole. Thus combination of anti-GIC strategies with approaches that target the tumor bulk and also the tumor microenvironment will be the future direction for GBM treatment. My Future investigations of anti-IL6/Stat3 and anti-miR-33a in the treatment of GIC populations will focus on combining these GIC-specific strategies with other established treatment such as standard radio- and chemotherapy that might potentially provide additive or synergistic therapeutic benefits.

Currently, systematic delivery of drugs to cross brain-blood barrier is still challenging. In preclinical studies, we plan to further evaluate the effect of miR-33a inhibitors in intracranial xenograft tumors by directly introducing the drug into CNS system. For future application on patients, novel modifications on small RNA inhibitors need to be made to cross the brain-blood barrier, or drugs that can temporally open Brian-Blood barrier should be delivered in coordinate with treatments of GBM.

In summary, I hope my thesis work not only contribute to the knowledge of cancer biology, but also inspire the development of therapeutic applications for future GBM treatment.

Appendix

In addition to the work described in Chapters 1-4, involving the identification of critical biological effectors in Glioma Initiating Cells, I also completed an additional study with collaboration with Valerie F. Curtis, a former student in my laboratory, which is under revision of the journal of *PLoS One*. I contributed to a large part of study in the glioblastoma section.

Infiltration of myeloid cells in the tumor microenvironment is often associated with enhanced angiogenesis and tumor progression, resulting in poor prognosis in many types of cancer. The polypeptide chemokine PK2 (Bv8) has been shown to regulate myeloid cell mobilization from the bone marrow, leading to activation of the angiogenic process, as well as accumulation of macrophages and neutrophils in the tumor site. Neutralizing antibodies against PK2 were shown to display potent anti-tumor efficacy, illustrating the potential of PK2-antagonists as therapeutic agents for the treatment of cancer. In this study we demonstrate the anti-tumor activity of a small molecule PK2 antagonist, PKRA7, in the contexts of glioblastoma and pancreatic cancer xenograft tumor models. For the highly vascularized glioblastoma, PKRA7 decreased blood vessel density while increased necrotic areas in the tumor mass. Consistent with the anti-angiogenic activity of PKRA7 in vivo, this compound effectively reduced PK2-induced microvascular endothelial cell branching in vitro. For the poorly vascularized pancreatic cancer, the primary anti-tumor effect of PKRA7 appears to be mediated by the blockage

of myeloid cell migration/infiltration. At the molecular level, PKRA7 inhibits PK2-induced expression of certain pro-migratory chemokines and chemokine receptors in macrophages. Combining PKRA7 treatment with standard chemotherapeutic agents resulted in enhanced effects in xenograft models for both types of tumor. Taken together, our results indicate that the anti-tumor activity of PKRA7 can be mediated by two distinct mechanisms that are relevant to the pathological features of the specific type of cancer and this small molecule PK2 antagonist holds the promise to be further developed into an effective agent for combinational cancer therapy.

References

- Al-Hajj, M., Wicha, M.S., Benito-Hernandez, A., Morrison, S.J., and Clarke, M.F. (2003). Prospective identification of tumorigenic breast cancer cells. *Proc Natl Acad Sci U S A* 100, 3983-3988.
- Ancrile, B., Lim, K.H., and Counter, C.M. (2007). Oncogenic Ras-induced secretion of IL6 is required for tumorigenesis. *Genes Dev* 21, 1714-1719.
- Anokye-Danso, F., Trivedi, C.M., Juhr, D., Gupta, M., Cui, Z., Tian, Y., Zhang, Y., Yang, W., Gruber, P.J., Epstein, J.A., et al. (2011). Highly efficient miRNA-mediated reprogramming of mouse and human somatic cells to pluripotency. *Cell Stem Cell* 8, 376-388.
- Baek, D., Villen, J., Shin, C., Camargo, F.D., Gygi, S.P., and Bartel, D.P. (2008). The impact of microRNAs on protein output. *Nature* 455, 64-71.
- Bao, S., Wu, Q., Li, Z., Sathornsumetee, S., Wang, H., McLendon, R.E., Hjelmeland, A.B., and Rich, J.N. (2008). Targeting cancer stem cells through L1CAM suppresses glioma growth. *Cancer Res* 68, 6043-6048.
- Bao, S., Wu, Q., McLendon, R.E., Hao, Y., Shi, Q., Hjelmeland, A.B., Dewhirst, M.W., Bigner, D.D., and Rich, J.N. (2006a). Glioma stem cells promote radioresistance by preferential activation of the DNA damage response. *Nature* 444, 756-760.
- Bao, S., Wu, Q., Sathornsumetee, S., Hao, Y., Li, Z., Hjelmeland, A.B., Shi, Q., McLendon, R.E., Bigner, D.D., and Rich, J.N. (2006b). Stem cell-like glioma cells promote tumor angiogenesis through vascular endothelial growth factor. *Cancer Res* 66, 7843-7848.
- Bonnet, D., and Dick, J.E. (1997). Human acute myeloid leukemia is organized as a hierarchy that originates from a primitive hematopoietic cell. *Nat Med* 3, 730-737.
- Bushati, N., and Cohen, S.M. (2007). microRNA functions. *Annu Rev Cell Dev Biol* 23, 175-205.
- Campeau, E., Ruhl, V.E., Rodier, F., Smith, C.L., Rahmberg, B.L., Fuss, J.O., Campisi, J., Yaswen, P., Cooper, P.K., and Kaufman, P.D. (2009). A versatile viral system for expression and depletion of proteins in mammalian cells. *PLoS One* 4, e6529.
- CBTRUS (2005). Statistical Report: Primary Brain Tumors in the United States, 1998-2002. Published by the Central Brain Tumor Registry of the United States.

- Chamberlain, M.C. (2006). Treatment options for glioblastoma. *Neurosurg Focus* 20, E19.
- Chan, X.H., Nama, S., Gopal, F., Rizk, P., Ramasamy, S., Sundaram, G., Ow, G.S., Vladimirovna, I.A., Tanavde, V., Haybaeck, J., et al. (2012). Targeting Glioma Stem Cells by Functional Inhibition of a Prosurvival OncomiR-138 in Malignant Gliomas. *Cell Rep*.
- Chen, R., Nishimura, M.C., Bumbaca, S.M., Kharbanda, S., Forrest, W.F., Kasman, I.M., Greve, J.M., Soriano, R.H., Gilmour, L.L., Rivers, C.S., et al. (2010). A hierarchy of self-renewing tumor-initiating cell types in glioblastoma. *Cancer Cell* 17, 362-375.
- Chi, S.W., Zang, J.B., Mele, A., and Darnell, R.B. (2009). Argonaute HITS-CLIP decodes microRNA-mRNA interaction maps. *Nature* 460, 479-486.
- Choi, C., Gillespie, G.Y., Van Wagoner, N.J., and Benveniste, E.N. (2002). Fas engagement increases expression of interleukin-6 in human glioma cells. *J Neurooncol* 56, 13-19.
- Cohen, M.H., Shen, Y.L., Keegan, P., and Pazdur, R. (2009). FDA drug approval summary: bevacizumab (Avastin) as treatment of recurrent glioblastoma multiforme. *Oncologist* 14, 1131-1138.
- Conze, D., Weiss, L., Regen, P.S., Bhushan, A., Weaver, D., Johnson, P., and Rincon, M. (2001). Autocrine production of interleukin 6 causes multidrug resistance in breast cancer cells. *Cancer Res* 61, 8851-8858.
- Curley, M.D., Therrien, V.A., Cummings, C.L., Sergent, P.A., Koulouris, C.R., Friel, A.M., Roberts, D.J., Seiden, M.V., Scadden, D.T., Rueda, B.R., et al. (2009). CD133 expression defines a tumor initiating cell population in primary human ovarian cancer. *Stem Cells* 27, 2875-2883.
- Dalerba, P., Dylla, S.J., Park, I.K., Liu, R., Wang, X., Cho, R.W., Hoey, T., Gurney, A., Huang, E.H., Simeone, D.M., et al. (2007). Phenotypic characterization of human colorectal cancer stem cells. *Proc Natl Acad Sci U S A* 104, 10158-10163.
- Davalos, A., Goedeke, L., Smibert, P., Ramirez, C.M., Warriar, N.P., Andreo, U., Cirera-Salinas, D., Rayner, K., Suresh, U., Pastor-Pareja, J.C., et al. (2011). miR-33a/b contribute to the regulation of fatty acid metabolism and insulin signaling. *Proc Natl Acad Sci U S A* 108, 9232-9237.
- Dick, J.E. (2008). Stem cell concepts renew cancer research. *Blood* 112, 4793-4807.

- Farazi, T.A., Spitzer, J.I., Morozov, P., and Tuschl, T. (2011). miRNAs in human cancer. *J Pathol* 223, 102-115.
- Fidler, I.J., and Hart, I.R. (1982). Biological diversity in metastatic neoplasms: origins and implications. *Science* 217, 998-1003.
- Fidler, I.J., and Kripke, M.L. (1977). Metastasis results from preexisting variant cells within a malignant tumor. *Science* 197, 893-895.
- Fisher, D.A., Smith, J.F., Pillar, J.S., St Denis, S.H., and Cheng, J.B. (1998). Isolation and characterization of PDE8A, a novel human cAMP-specific phosphodiesterase. *Biochem Biophys Res Commun* 246, 570-577.
- Furnari, F.B., Fenton, T., Bachoo, R.M., Mukasa, A., Stommel, J.M., Stegh, A., Hahn, W.C., Ligon, K.L., Louis, D.N., Brennan, C., et al. (2007). Malignant astrocytic glioma: genetics, biology, and paths to treatment. *Genes Dev* 21, 2683-2710.
- Gerin, I., Clerbaux, L.A., Haumont, O., Lanthier, N., Das, A.K., Burant, C.F., Leclercq, I.A., MacDougald, O.A., and Bommer, G.T. (2010). Expression of miR-33 from an SREBP2 intron inhibits cholesterol export and fatty acid oxidation. *J Biol Chem* 285, 33652-33661.
- Harris, A.L. (2002). Hypoxia--a key regulatory factor in tumour growth. *Nat Rev Cancer* 2, 38-47.
- Heddleston, J.M., Li, Z., McLendon, R.E., Hjelmeland, A.B., and Rich, J.N. (2009). The hypoxic microenvironment maintains glioblastoma stem cells and promotes reprogramming towards a cancer stem cell phenotype. *Cell Cycle* 8, 3274-3284.
- Heinrich, P.C., Behrmann, I., Haan, S., Hermanns, H.M., Muller-Newen, G., and Schaper, F. (2003). Principles of interleukin (IL)-6-type cytokine signalling and its regulation. *Biochem J* 374, 1-20.
- Hodge, D.R., Hurt, E.M., and Farrar, W.L. (2005). The role of IL-6 and STAT3 in inflammation and cancer. *Eur J Cancer* 41, 2502-2512.
- Hwang-Verslues, W.W., Chang, P.H., Wei, P.C., Yang, C.Y., Huang, C.K., Kuo, W.H., Shew, J.Y., Chang, K.J., Lee, E.Y., and Lee, W.H. (2011). miR-495 is upregulated by E12/E47 in breast cancer stem cells, and promotes oncogenesis and hypoxia resistance via downregulation of E-cadherin and REDD1. *Oncogene* 30, 2463-2474.

- Ishioka, S., van Haaften-Day, C., Sagae, S., Kudo, R., and Hacker, N.F. (1999). Interleukin-6 (IL-6) does not change the expression of Bcl-2 protein in the prevention of cisplatin-induced apoptosis in ovarian cancer cell lines. *J Obstet Gynaecol Res* 25, 23-27.
- Jazbutyte, V., and Thum, T. (2010). MicroRNA-21: from cancer to cardiovascular disease. *Curr Drug Targets* 11, 926-935.
- Kim, L., and Glantz, M. (2006). Chemotherapeutic options for primary brain tumors. *Curr Treat Options Oncol* 7, 467-478.
- Kishimoto, T. (2005). Interleukin-6: from basic science to medicine--40 years in immunology. *Annu Rev Immunol* 23, 1-21.
- Kleinsmith, L.J., and Pierce, G.B., Jr. (1964). Multipotentiality of Single Embryonal Carcinoma Cells. *Cancer Res* 24, 1544-1551.
- Knaevelsrud, H., Ahlquist, T., Merok, M.A., Nesbakken, A., Stenmark, H., Lothe, R.A., and Simonsen, A. (2010). UVRAG mutations associated with microsatellite unstable colon cancer do not affect autophagy. *Autophagy* 6, 863-870.
- Kohler, B.A., Ward, E., McCarthy, B.J., Schymura, M.J., Ries, L.A., Ehemann, C., Jemal, A., Anderson, R.N., Ajani, U.A., and Edwards, B.K. (2011). Annual report to the nation on the status of cancer, 1975-2007, featuring tumors of the brain and other nervous system. *J Natl Cancer Inst* 103, 714-736.
- Konnikova, L., Kotecki, M., Kruger, M.M., and Cochran, B.H. (2003). Knockdown of STAT3 expression by RNAi induces apoptosis in astrocytoma cells. *BMC Cancer* 3, 23.
- Kota, J., Chivukula, R.R., O'Donnell, K.A., Wentzel, E.A., Montgomery, C.L., Hwang, H.W., Chang, T.C., Vivekanandan, P., Torbenson, M., Clark, K.R., et al. (2009). Therapeutic microRNA delivery suppresses tumorigenesis in a murine liver cancer model. *Cell* 137, 1005-1017.
- Lee, G., Liang, C., Park, G., Jang, C., Jung, J.U., and Chung, J. (2011). UVRAG is required for organ rotation by regulating Notch endocytosis in *Drosophila*. *Dev Biol* 356, 588-597.
- Lee, R.C., Feinbaum, R.L., and Ambros, V. (1993). The *C. elegans* heterochronic gene *lin-4* encodes small RNAs with antisense complementarity to *lin-14*. *Cell* 75, 843-854.
- Li, C., Heidt, D.G., Dalerba, P., Burant, C.F., Zhang, L., Adsay, V., Wicha, M., Clarke, M.F., and Simeone, D.M. (2007). Identification of pancreatic cancer stem cells. *Cancer Res* 67, 1030-1037.

- Li, Z., Bao, S., Wu, Q., Wang, H., Eyler, C., Sathornsumetee, S., Shi, Q., Cao, Y., Lathia, J., McLendon, R.E., et al. (2009). Hypoxia-inducible factors regulate tumorigenic capacity of glioma stem cells. *Cancer Cell* 15, 501-513.
- Liang, C., Feng, P., Ku, B., Dotan, I., Canaani, D., Oh, B.H., and Jung, J.U. (2006). Autophagic and tumour suppressor activity of a novel Beclin1-binding protein UVRAG. *Nat Cell Biol* 8, 688-699.
- Liang, C., Feng, P., Ku, B., Oh, B.H., and Jung, J.U. (2007). UVRAG: a new player in autophagy and tumor cell growth. *Autophagy* 3, 69-71.
- Liu, G., Yuan, X., Zeng, Z., Tunici, P., Ng, H., Abdulkadir, I.R., Lu, L., Irvin, D., Black, K.L., and Yu, J.S. (2006). Analysis of gene expression and chemoresistance of CD133+ cancer stem cells in glioblastoma. *Mol Cancer* 5, 67.
- Loeffler, S., Fayard, B., Weis, J., and Weissenberger, J. (2005). Interleukin-6 induces transcriptional activation of vascular endothelial growth factor (VEGF) in astrocytes in vivo and regulates VEGF promoter activity in glioblastoma cells via direct interaction between STAT3 and Sp1. *Int J Cancer* 115, 202-213.
- Ma, L., Reinhardt, F., Pan, E., Soutschek, J., Bhat, B., Marcusson, E.G., Teruya-Feldstein, J., Bell, G.W., and Weinberg, R.A. (2010a). Therapeutic silencing of miR-10b inhibits metastasis in a mouse mammary tumor model. *Nat Biotechnol* 28, 341-347.
- Ma, S., Tang, K.H., Chan, Y.P., Lee, T.K., Kwan, P.S., Castilho, A., Ng, I., Man, K., Wong, N., To, K.F., et al. (2010b). miR-130b Promotes CD133(+) liver tumor-initiating cell growth and self-renewal via tumor protein 53-induced nuclear protein 1. *Cell Stem Cell* 7, 694-707.
- Magee, J.A., Piskounova, E., and Morrison, S.J. (2012). Cancer stem cells: impact, heterogeneity, and uncertainty. *Cancer Cell* 21, 283-296.
- Mani, S.A., Guo, W., Liao, M.J., Eaton, E.N., Ayyanan, A., Zhou, A.Y., Brooks, M., Reinhard, F., Zhang, C.C., Shipitsin, M., et al. (2008). The epithelial-mesenchymal transition generates cells with properties of stem cells. *Cell* 133, 704-715.
- Matsuda, T., Nakamura, T., Nakao, K., Arai, T., Katsuki, M., Heike, T., and Yokota, T. (1999). STAT3 activation is sufficient to maintain an undifferentiated state of mouse embryonic stem cells. *EMBO J* 18, 4261-4269.
- Meltzer, P.S. (2005). Cancer genomics: small RNAs with big impacts. *Nature* 435, 745-746.

- Mendell, J.T. (2008). miRiad roles for the miR-17-92 cluster in development and disease. *Cell* 133, 217-222.
- Mizrak, D., Brittan, M., and Alison, M.R. (2008). CD133: molecule of the moment. *J Pathol* 214, 3-9.
- Morel, A.P., Lievre, M., Thomas, C., Hinkal, G., Ansieau, S., and Puisieux, A. (2008). Generation of breast cancer stem cells through epithelial-mesenchymal transition. *PLoS One* 3, e2888.
- Niwa, H., Burdon, T., Chambers, I., and Smith, A. (1998). Self-renewal of pluripotent embryonic stem cells is mediated via activation of STAT3. *Genes Dev* 12, 2048-2060.
- O'Brien, C.A., Pollett, A., Gallinger, S., and Dick, J.E. (2007). A human colon cancer cell capable of initiating tumour growth in immunodeficient mice. *Nature* 445, 106-110.
- Piccirillo, S.G., Reynolds, B.A., Zanetti, N., Lamorte, G., Binda, E., Broggi, G., Brem, H., Olivi, A., Dimeco, F., and Vescovi, A.L. (2006). Bone morphogenetic proteins inhibit the tumorigenic potential of human brain tumour-initiating cells. *Nature* 444, 761-765.
- Poliseno, L., Salmena, L., Riccardi, L., Fornari, A., Song, M.S., Hobbs, R.M., Sportoletti, P., Varmeh, S., Egia, A., Fedele, G., et al. (2010). Identification of the miR-106b-25 microRNA cluster as a proto-oncogenic PTEN-targeting intron that cooperates with its host gene MCM7 in transformation. *Sci Signal* 3, ra29.
- Rahaman, S.O., Harbor, P.C., Chernova, O., Barnett, G.H., Vogelbaum, M.A., and Haque, S.J. (2002). Inhibition of constitutively active Stat3 suppresses proliferation and induces apoptosis in glioblastoma multiforme cells. *Oncogene* 21, 8404-8413.
- Rayner, K.J., Suarez, Y., Davalos, A., Parathath, S., Fitzgerald, M.L., Tamehiro, N., Fisher, E.A., Moore, K.J., and Fernandez-Hernando, C. (2010). MiR-33 contributes to the regulation of cholesterol homeostasis. *Science* 328, 1570-1573.
- Reinhart, B.J., Slack, F.J., Basson, M., Pasquinelli, A.E., Bettinger, J.C., Rougvié, A.E., Horvitz, H.R., and Ruvkun, G. (2000). The 21-nucleotide let-7 RNA regulates developmental timing in *Caenorhabditis elegans*. *Nature* 403, 901-906.
- Reya, T., Morrison, S.J., Clarke, M.F., and Weissman, I.L. (2001). Stem cells, cancer, and cancer stem cells. *Nature* 414, 105-111.

- Ricci-Vitiani, L., Lombardi, D.G., Pilozzi, E., Biffoni, M., Todaro, M., Peschle, C., and De Maria, R. (2007). Identification and expansion of human colon-cancer-initiating cells. *Nature* 445, 111-115.
- Sands, W.A., and Palmer, T.M. (2008). Regulating gene transcription in response to cyclic AMP elevation. *Cell Signal* 20, 460-466.
- Sansone, P., Storci, G., Tavolari, S., Guarnieri, T., Giovannini, C., Taffurelli, M., Ceccarelli, C., Santini, D., Paterini, P., Marcu, K.B., et al. (2007). IL-6 triggers malignant features in mammospheres from human ductal breast carcinoma and normal mammary gland. *J Clin Invest* 117, 3988-4002.
- Scheel, C., Eaton, E.N., Li, S.H., Chaffer, C.L., Reinhardt, F., Kah, K.J., Bell, G., Guo, W., Rubin, J., Richardson, A.L., et al. (2011). Paracrine and autocrine signals induce and maintain mesenchymal and stem cell states in the breast. *Cell* 145, 926-940.
- Schraivogel, D., Weinmann, L., Beier, D., Tabatabai, G., Eichner, A., Zhu, J.Y., Anton, M., Sixt, M., Weller, M., Beier, C.P., et al. (2011). CAMTA1 is a novel tumour suppressor regulated by miR-9/9* in glioblastoma stem cells. *EMBO J* 30, 4309-4322.
- Schust, J., Sperl, B., Hollis, A., Mayer, T.U., and Berg, T. (2006). Stattic: a small-molecule inhibitor of STAT3 activation and dimerization. *Chem Biol* 13, 1235-1242.
- Sehgal, P.B., and Tamm, I. (1991). Interleukin-6 enhances motility of breast carcinoma cells. *EXS* 59, 178-193.
- Selmaj, K.W., Farooq, M., Norton, W.T., Raine, C.S., and Brosnan, C.F. (1990). Proliferation of astrocytes in vitro in response to cytokines. A primary role for tumor necrosis factor. *J Immunol* 144, 129-135.
- Shackleton, M., Quintana, E., Fearon, E.R., and Morrison, S.J. (2009). Heterogeneity in cancer: cancer stem cells versus clonal evolution. *Cell* 138, 822-829.
- Shu, Q., Wong, K.K., Su, J.M., Adesina, A.M., Yu, L.T., Tsang, Y.T., Antalffy, B.C., Baxter, P., Perlaky, L., Yang, J., et al. (2008). Direct orthotopic transplantation of fresh surgical specimen preserves CD133+ tumor cells in clinically relevant mouse models of medulloblastoma and glioma. *Stem Cells* 26, 1414-1424.
- Silber, J., Lim, D.A., Petritsch, C., Persson, A.I., Maunakea, A.K., Yu, M., Vandenberg, S.R., Ginzinger, D.G., James, C.D., Costello, J.F., et al. (2008). miR-124 and miR-137 inhibit proliferation of glioblastoma multiforme cells and induce differentiation of brain tumor stem cells. *BMC Med* 6, 14.

- Singh, S.K., Hawkins, C., Clarke, I.D., Squire, J.A., Bayani, J., Hide, T., Henkelman, R.M., Cusimano, M.D., and Dirks, P.B. (2004). Identification of human brain tumour initiating cells. *Nature* 432, 396-401.
- Skalhegg, B.S., and Tasken, K. (1997). Specificity in the cAMP/PKA signaling pathway. differential expression, regulation, and subcellular localization of subunits of PKA. *Front Biosci* 2, d331-342.
- Stewart, J.M., Shaw, P.A., Gedye, C., Bernardini, M.Q., Neel, B.G., and Ailles, L.E. (2011). Phenotypic heterogeneity and instability of human ovarian tumor-initiating cells. *Proc Natl Acad Sci U S A* 108, 6468-6473.
- Stupp, R., Mason, W.P., van den Bent, M.J., Weller, M., Fisher, B., Taphoorn, M.J., Belanger, K., Brandes, A.A., Marosi, C., Bogdahn, U., et al. (2005). Radiotherapy plus concomitant and adjuvant temozolomide for glioblastoma. *N Engl J Med* 352, 987-996.
- Su, Y., Li, G., Zhang, X., Gu, J., Zhang, C., Tian, Z., and Zhang, J. (2008). JSI-124 inhibits glioblastoma multiforme cell proliferation through G(2)/M cell cycle arrest and apoptosis augment. *Cancer Biol Ther* 7, 1243-1249.
- Takahashi, K., Tanabe, K., Ohnuki, M., Narita, M., Ichisaka, T., Tomoda, K., and Yamanaka, S. (2007). Induction of pluripotent stem cells from adult human fibroblasts by defined factors. *Cell* 131, 861-872.
- Tchirkov, A., Khalil, T., Chautard, E., Mokhtari, K., Veronese, L., Irthum, B., Vago, P., Kemeny, J.L., and Verrelle, P. (2007). Interleukin-6 gene amplification and shortened survival in glioblastoma patients. *Br J Cancer* 96, 474-476.
- Trikha, M., Corringham, R., Klein, B., and Rossi, J.F. (2003). Targeted anti-interleukin-6 monoclonal antibody therapy for cancer: a review of the rationale and clinical evidence. *Clin Cancer Res* 9, 4653-4665.
- Vredenburgh, J.J., Desjardins, A., Herndon, J.E., 2nd, Marcello, J., Reardon, D.A., Quinn, J.A., Rich, J.N., Sathornsumetee, S., Gururangan, S., Sampson, J., et al. (2007). Bevacizumab plus irinotecan in recurrent glioblastoma multiforme. *J Clin Oncol* 25, 4722-4729.
- Wang, H., Zhang, W., Huang, H.J., Liao, W.S., and Fuller, G.N. (2004). Analysis of the activation status of Akt, NFkappaB, and Stat3 in human diffuse gliomas. *Lab Invest* 84, 941-951.

Wang, J., Wakeman, T.P., Lathia, J.D., Hjelmeland, A.B., Wang, X.F., White, R.R., Rich, J.N., and Sullenger, B.A. (2010). Notch promotes radioresistance of glioma stem cells. *Stem Cells* 28, 17-28.

Weissenberger, J., Loeffler, S., Kappeler, A., Kopf, M., Lukes, A., Afanasieva, T.A., Aguzzi, A., and Weis, J. (2004). IL-6 is required for glioma development in a mouse model. *Oncogene* 23, 3308-3316.

Yuan, X., Curtin, J., Xiong, Y., Liu, G., Waschmann-Hogiu, S., Farkas, D.L., Black, K.L., and Yu, J.S. (2004). Isolation of cancer stem cells from adult glioblastoma multiforme. *Oncogene* 23, 9392-9400.

Zhao, Z., Oh, S., Li, D., Ni, D., Pirooz, S.D., Lee, J.H., Yang, S., Lee, J.Y., Ghosalli, I., Costanzo, V., et al. (2012). A dual role for UVRAG in maintaining chromosomal stability independent of autophagy. *Dev Cell* 22, 1001-1016.

Biography

HUI WANG

Born June 13, 1984 in Shanxi Province, China

EDUCATION

Duke University, Durham, NC
Ph.D. in Pharmacology

Expected Dec 2012

Tsinghua University, Beijing, China
B.S. in Biological Science

Jul 2006

PUBLICATION

Cao Y, Lathia JD, Eyler CE, Wu Q, Li Z, **Wang H**, McLendon RE, Hjelmeland AB, Rich JN. Erythropoietin Receptor Signaling through STAT3 Is Required for Glioma Stem Cell Maintenance. *Genes & Cancer*. 2010 Jan; 1(1): 50-61.

Wang H, Lathia JD, Wu Q, Wang J, Li Z, Heddleston JM, Eyler CE, Elderbroom J, Gallagher J, Schuschu J, MacSwords J, Cao Y, McLendon RE, Wang XF, Hjelmeland AB, Rich JN. Targeting Interleukin 6 Signaling Suppresses Glioma Stem Cell Survival and Tumor Growth. *Stem Cells*. 2009 Oct; 27(10): 2393-404.

Li Z, **Wang H**, Eyler CE, Hjelmeland AB, Rich JN. Turning Cancer Stem Cells Inside-out: an Exploration of Glioma Stem Cell Signaling Pathways. *J Biol Chem*. 2009 Jun; 284(25): 16705-9.

Li Z, Bao S, Wu Q, **Wang H**, Eyler C, Sathornsumetee S, Shi Q, Cao Y, Lathia J, McLendon RE, Hjelmeland AB, Rich JN. Hypoxia-Inducible Factors Regulate Tumorigenic Capacity of Glioma Stem Cells. *Cancer Cell*. 2009 Jun; 15(6): 501-13.

Wang J, **Wang H**, Li Z, Wu Q, Lathia JD, McLendon RE, Hjelmeland AB, Rich JN. c-Myc is Required for Maintenance of Glioma Cancer Stem Cells. *PLoS One*. 2008 Nov; 3(11): e3769.

Bao S, Wu Q, Li Z, Sathornsumetee S, **Wang H**, McLendon RE, Hjelmeland AB, Rich JN. Targeting Cancer Stem Cells through L1CAM Suppresses Glioma Growth. *Cancer Res*. 2008 Aug; 68(15): 6043-8.

Shi W, **Wang H**, Pan G, Geng Y, Guo Y, Pei D. Regulation of the Pluripotency Marker Rex-1 by Nanog and Sox2. *J Biol Chem*. 2006 Aug; 281(33): 23319-25.

MANUSCRIPTS IN PROGRESS

Wang H, Sun T, Rao YH, Hu J, McLendon RE, Friedman AH, Keir ST, Bigner DD, Li QJ, Wang XF. Acting as a Master Determinant, miR-33a Confers Biological Properties of Glioma Initiating Cells via Modulation of the cAMP/PKA and Notch Signaling Pathways. Manuscript submitted to *Cell*.

Curtis VF, **Wang H**, Yang PY, McLendon RE, Zhou QY, Wang XF. A Synthetic Bv8/PK2 Antagonist Suppresses Tumorigenic Processes via Distinct Mechanisms: Inhibiting Angiogenesis in Glioma and Blocking Myeloid Cell Infiltration in Pancreatic Cancer. *PLoS ONE*. Under revision.

HONORS/AWARDS

Chinese Government Award for Outstanding Self-Financed Students Abroad Jun 2011
\$5000 • China Scholarship Council, Beijing, China

Student Travel Award Apr 2011
\$500 • Duke University, Graduate School, Durham, NC

Student Travel Award Oct 2009
\$500 • Duke University, Graduate School, Durham, NC